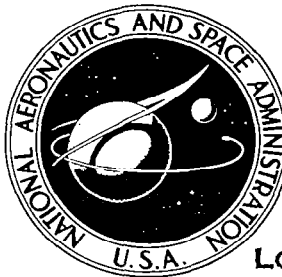
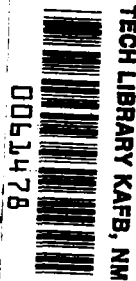


**NASA CONTRACTOR
REPORT**

NASA CR-2695



NASA CR-



TECH LIBRARY KAFB, NM

LOAN COPY: RETURN TO
AFWL TECHNICAL LIBRARY
KIRTLAND AFB, N. M.

**CALCULATION OF SUBSONIC AND SUPERSONIC
STEADY AND UNSTEADY AERODYNAMIC FORCES
USING VELOCITY POTENTIAL
AERODYNAMIC ELEMENTS**

John Kenneth Haviland and Young Sik Yoo

Prepared by
UNIVERSITY OF VIRGINIA
Charlottesville, Va. 22901
for Langley Research Center



NATIONAL AERONAUTICS AND SPACE ADMINISTRATION • WASHINGTON, D. C. • JULY 1976



0061478

1. Report No. NASA CR-2695		2. Government Accession No.		3. Recipient's Catalog No.	
4. Title and Subtitle CALCULATION OF SUBSONIC AND SUPERSONIC STEADY AND UNSTEADY AERODYNAMIC FORCES USING VELOCITY POTENTIAL AERODYNAMIC ELEMENTS				5. Report Date JULY 1976	
				6. Performing Organization Code	
7. Author(s) Dr. John Kenneth Haviland and Dr. Young Sik Yoo				8. Performing Organization Report No. ESS-4099-112-75	
9. Performing Organization Name and Address Department of Engineering Science and Systems University of Virginia Charlottesville, Virginia 22901				10. Work Unit No.	
				11. Contract or Grant No. NGL 47-005-098	
12. Sponsoring Agency Name and Address National Aeronautics and Space Administration Washington, DC 20546				13. Type of Report and Period Covered Contractor Report	
				14. Sponsoring Agency Code	
15. Supplementary Notes Final Report Dr. E. Carson Yates, Jr. was technical monitor for the grant.					
16. Abstract Expressions for calculation of subsonic and supersonic, steady and unsteady aerodynamic forces are derived, using the concept of aerodynamic elements applied to the downwash-velocity potential method (also called the integrated potential method). Aerodynamic elements can be of arbitrary out-of-plane polygon shape, although numerical calculations are restricted to rectangular elements, and to the steady state case in the supersonic examples. Agreement with other published results is generally satisfactory for the in-plane cases, although the results for swept wings at high subsonic Mach numbers indicate room for improvement. It is suggested that the use of conforming, in place of rectangular elements, would give better results, though this remains to be demonstrated. Agreement with published results for subsonic oscillating T-tails is fair, but results do not converge as the number of collocation points is increased. This appears to be due to the form of expression used in the calculations. The final form of expression developed, however, should converge, although this also remains to be demonstrated. The methods derived in this report are expected to facilitate automated flutter analysis on the computer. In particular, the aerodynamic element concept is consistent with finite element methods already used for structural analysis. Also, the method is universal for the complete Mach number range, and, finally, the calculations can be arranged so that they do not have to be repeated completely for every reduced frequency.					
17. Key Words (Suggested by Author(s)) Potential Flow Lifting Surface Theory Unsteady Flow Aircraft Aerodynamics				18. Distribution Statement Unclassified - Unlimited Star Category: 02	
19. Security Classif. (of this report) Unclassified		20. Security Classif. (of this page) Unclassified		21. No. of Pages 190	
				22. Price* \$7.00	

TABLE OF CONTENTS

	Page
LIST OF TABLES	vii
LIST OF FIGURES	viii
LIST OF SYMBOLS	xi
INTRODUCTION	1
THEORETICAL DEVELOPMENT	6
Statement of Problem	6
Coordinate System	6
Governing Differential Equation	6
Integral Equation	8
Expression for Green's function	9
Expression for K_ϕ	10
METHOD OF SOLUTION	12
Introduction	12
Integration of Discrete Elements	12
Aerodynamic Elements	13
Basic form	13
Subsonic aerodynamic elements	15
Midpoint constant potential (MPCP) rectangular elements	16
Zero order constant potential (ZOCP) rectangular elements	16
First order constant potential (FOCP) rectangular elements	17
First order zero pressure (FOZP) rectangular elements	19

	Page
Supersonic aerodynamic elements	19
In-plane steady supersonic (IPSS) rectangular elements	22
Calculation of Aerodynamic Forces	27
Basic approach	27
Generalized forces	28
Flutter airforce matrix for constant potential case	29
Flutter airforce matrix for zero pressure case	30
COMPUTED RESULTS AND DISCUSSIONS	31
Computer Program	31
Scope of Computations	32
Discretization of Surfaces	32
Results and Discussions	41
Case 1: convergence of the results with the wake length	41
Case 2: rectangular wing pitching about midchord	41
Case 3: lift distribution of a rectangular wing; subsonic steady	51
Case 4: tapered and swept wings; subsonic steady	51
Case 5: swept wing with control surface - subsonic unsteady	63
Case 6: T-tails - subsonic unsteady	71
Case 7: rectangular wings - supersonic steady	76
Computation Time	81

	Page
PROPOSED EXTENDED METHOD OF ANALYSIS	81
Statement of Problem	81
Coordinate System	81
Governing Differential Equation	81
Integral Equation	81
Expression for Green's function	82
Expression for K_ϕ	82
Method of Solution	83
Integration by Discrete Elements	83
Aerodynamic Elements	83
Basic form	83
Subsonic aerodynamic elements	85
Minimum first order expansion-subsonic	85
Supersonic aerodynamic elements	87
Minimum first order expansion-supersonic	87
Evaluation of Integrals by Contour Integration	88
Case I. no Mach cone intersection	93
"F" integrals of the first kind	93
"F" integrals of the second kind	95
Case II with Mach cone intersection	96
"F" integrals of the first kind with Mach cone intersection	99
"F" integrals of the second kind with Mach cone intersection	100
"K" integrals of first and second kind	100
Additional Supersonic Terms	102
Numerical Problems In Computation	102

	<u>Page</u>
Comparison of Extended Method with Previous Results	103
Computer Program	107
Missing Term	108
Summary of Extended Method	108
CONCLUDING REMARKS	110
RECOMMENDATIONS	113
REFERENCES	114
APPENDIX A	117
APPENDIX B	175
APPENDIX C	176

LIST OF TABLES

I	Calculations Performed	38
II	Convergence of Calculated Results for Aspect Ratio Two Rectangular Wing, Oscillating about Midchord at Reduced Frequency of 0.5 and Mach Number 0.9, as Ratio Wake Length/Chord is changed	41
III	Sectional Lift Slope and Aerodynamic Centers, Total Lift and Moment for Aspect Ratio 8 Rectangular Wing with the Variations in Station Spacing. Mach Number = 0, $K_r = 0$, $\alpha = 1.0$	56
IV	Tapered Wing at 11.4° Angle of Attack	61
V	Uncambered Swept Wing	62
VI	Lift and Moment Derivatives for Aspect Ratio Two Swept Wing with Partial-Span Flaps (Leading Edge Sweep Angle = 60° , Taper Ratio = .2376) Rotating about Root Midchord ($K_r = .5$)	69
VII	Comparison of Side Force and Moment Derivatives for Rectangular T-tail Oscillating in Yaw about the Fin Midchord	72
VIII	Comparison of Aerodynamic Coefficients for Stark's T-tail (Mach No. = .8)	73
IX	Comparison of Various Aerodynamic Elements for Stark's T-tail ($N_{RP} = 18$, $K_r = .2$)	75
X	Comparison of Lift and Pitching Moment Derivatives (About Leading Edge) in Steady Supersonic Flows.	78
XI	Comparison of Lift and Pitching Moment Derivatives (About Midchord) for Rectangular Wings in Steady Supersonic Flow, Mach No. = 1.3	80
A-1	Composition of A Vector	123

LIST OF FIGURES

Figure	Page
1 Coordinate Systems	7
2 Designation of Elements for Wing and Wake	14
3 Constant Potential Elements	18
4 Zero Pressure Elements	20
5 Paths of Integration for Complete and Partial Rectangular Elements Inside Aft Mach Lines	25
6 Rectangular Wing A.R. = 2 (Planform No. 1)	33
7 Rectangular Wing A.R. = 8 (Planform No. 2)	33
8 Tapered Wing A.R. = 5.0 (Planform No. 3)	34
9 Swept Wing A.R. = 5.0 (Planform No. 4)	34
10 Swept Wing with Partial-Span Flaps A.R. = 2 (Planform No. 5)	35
11 Rectangular T-tail (Planform No. 6)	36
12 Stark's T-tail (Planform No. 7)	36
13 Rectangular Wings for Supersonic Calculations (Planform No. 8)	37
14 Comparison of Four-by-Four Arrays. Present Method and Hedman's	40
15 Lift Derivative (Real Part) for Aspect Ratio Two Rectangular Wing Rotating about Mid-Chord at Zero Mach Number	43
16 Lift Derivative (Imaginary Part) for Aspect Ratio Two Rectangular Wing Rotating about Mid-Chord at Zero Mach Number	44
17 Moment Derivative (Real Part) for Aspect Ratio Two Rectangular Wing Rotating about Mid-Chord at Zero Mach Number	45
18 Moment Derivative (Imaginary Part) for Aspect Ratio Two Rectangular Wing Rotating about Mid-Chord at Zero Mach Number	46

	<u>Page</u>
19 Moment Derivative (Real Part) for Aspect Ratio Two Rectangular Wing Rotating about Mid-Chord at Mach Number 0.8	47
20 Moment Derivative (Imaginary Part) for Aspect Ratio Two Rectangular Wing Rotating about Mid-Chord at Mach Number 0.8	48
21 Moment Derivative (Real Part) for Aspect Ratio Two Rectangular Wing Rotating about Mid-Chord at Mach Number 0.9	49
22 Moment Derivative (Imaginary Part) for Aspect Ratio Two Rectangular Wing Rotating about Mid-Chord at Mach Number 0.9 . .	50
23 Planform for Aspect Ratio 8 Rectangular Wing with 8 x 8 Arrays of Points, Evenly Spaced	52
24 Planform for an Aspect Ratio 8 Rectangular Wing with 8 x 8 Arrays of Elements and Strip Width Reduced Towards Tip	53
25 Comparison of Section Lift Slope for Aspect Ratio 8 Rectangular Wing, Mach No.=0, $k = 0$	54
26 Comparison of Aerodynamic Center for Aspect Ratio 8 Rectangular Wing, Mach No.=0, $k = 0$	55
27 Arrangement of Aerodynamic Elements for Aspect Ratio 5 Tapered Wing (Taper Ratio = 0.5, Leading Edge Sweep Angle = 3.817° , Trailing Edge Sweep Angle = 11.308°)	57
28 Arrangement of Aerodynamic Elements for Aspect Ratio 5 Swept Wing (Sweep Angle = 15°)	58
29 Spanwise Lift Distribution for Tapered Wing at 11.4° Angle of Attack	58
30 Spanwise Distribution of Chordwise Location of Center of Pressure for the Tapered Wing at 11.4° Angle of Attack	60
31 Arrangement of Aerodynamic Elements for a Swept Wing with Partial-Span Control Surface	64
32 Arrangement with Evenly Spaced Strip Width for Aspect Ratio Two Swept Wing (Leading Edge Sweep Angle 60° , Taper Ratio = .2376). .	65
33 Arrangement with Reduced Strip Width Towards Tip for Aspect Ratio Two Swept Wing (Leading Edge Sweep Angle = 60° , Taper Ratio = .2376)	66
34 Pitching Moment Coefficient for a Tapered Swept Wing Oscillating in Pitch	67
35 Flap Moment Coefficient Due to Control Surface Rotation, $K_r = .5$	68

36	Arrangement of Aerodynamic Elements for Aspect Ratio Two Rectangular Wing for Steady Supersonic Calculations	77
37	Contour Integral	90
38	Case of Positive X' in Forward Mach Cone	94
39	Intersection with Forward Mach Cone	97
40	Derivation of I'_0 for Rectangle	106
41	Aerodynamic Forces	109
A-1	Flow Diagram	120
A-2	Symmetry Conditions	125
A-3	Examples of Configurations	126
A-4	Rectangular Wing of Aspect Ratio Two, Pitching about Midchord	140
A-5	Chordwise Strip Arrangement for a Swept Wing with Partial-Span Flaps	145

LIST OF SYMBOLS

$$a^2 = M^2 - 1$$

$A_{k,l}$	Aerodynamic influence matrix
$A(l)$	Area of element l
b	Half chord
b	Fin height
b	Semi span
BMCP	Bending moment center of pressure
c	Local speed of sound
c	Chord
C_{REF}	Reference length (see Fig. 11)
C_{BM}	Total bending moment coefficient
$C_{i,j}$	Flutter airforce matrix
C_l	Sectional lift coefficient, $\frac{Lift}{\frac{1}{2} \rho V^2 c}$
$C_{l\alpha}$	Sectional lift slope
C_L	Total lift coefficient, $\frac{Lift}{\frac{1}{2} \rho V^2 S}$
$C_{L\alpha}$	Total lift slope
C_m	Sectional moment coefficient, $\frac{Moment}{\frac{1}{2} \rho V^2 c^2}$
$C_{m\alpha}$	Sectional moment slope
C_M	Pitching moment coefficient, $\frac{Moment}{\frac{1}{2} \rho V^2 S c}$
$C_{M\alpha}$	Total moment slope
C_{PM}	Total pitching moment coefficient
$C_{N,\psi}$	Moment derivative
$C_{Y,\psi}$	Side force derivative
d	Modal deflection

E	See Eq. (113)
f	Shape factor
F	Wake length/chord
F	Integral. See Eqs.(106) (107)
F	Force
F	Cutoff Function. See Eq. (80)
F_{SS}, F_{US}	See Eqs. (27), (33) and (45)
F_Y	Side force
g	Angle between local normal n and z-axis
G	Green's function
h	Amplitude of local displacement
I	Integral. See Eqs.(93) to (96), (100) to (103)
J	Integral. See Eqs. (104), (105)
k	"receiving" or collocation point
k_ϕ	See Eq.(16)
k_1, k_2	See Eq.(20), (21)
k_{IR}, k_{IA}	See Eqs. (38), (39)
K	See Eq.(61)
K_r, k	Reduced frequency, $\frac{\omega b}{V}$ or $\frac{\omega c}{2V}$
k_{SS}	See Eqs.(26), (44), (56), and (57)
k_{US}	See Eq.(32)
K_ϕ	See Eq.(5)
K_1	See Eq.(9)
K_2	See Eq.(11)
l, l^*	"sending" point on wing, wake
L	Lift
L	See Eq.(22) and (40)

M	Mach number
M, M_ψ	Pitching moment
$N = N(k) = v - v(k)$	
N_{RP}	Number of reference point
p	Amplitude of pressure perturbation
P	See Eq. (50)
PMCP	Pitching moment center of pressure
q	Dynamic pressure
\bar{q}_i	Generalized coordinate
Q	See Eq. (50)
\tilde{Q}	Generalized force
$Q_{m,n}$	Generalized aerodynamic force coefficient
\mathbf{r}	Coordinate vector of "receiving" or "downwash"
$R^2 = (x'-\xi)^2 + \beta^2(y-\eta)^2 + \beta^2(z-\xi)^2$	
S	Surface of integration
$S = S(k) = \sigma - \sigma(k)$	
S =	Wing area
S_{FIN}	Fin area
t	Time
T_1	See Eq.(8)
T_2	See Eq.(10)
U(x)	Step function
V	Steady flow velocity
w	Normal velocity
x, s, n	Cartesian coordinates attached to wing moving in negative x direction
x', y, z	Cartesian coordinates (fixed relative to the fluid at infinity) used to locate "receiving" or "downwash" point

X', Y'	Wing plan coordinates. Figs. 29 and 30
x', s'	Transformed coordinates, Eq. (114), (115)
$X = X(k) = \xi - \xi(k)$	
y	Spanwise station
α	Amplitude of local angle of attack
$\beta^2 = 1 - M^2$	
γ	Angle between local normal v and z -axis
$\delta(x)$	Dirac delta function
η	Dimensionless spanwise station
ξ, σ, v	Cartesian local coordinates used to designate "sending point"
ξ', η, ζ	Cartesian coordinates used to locate "sending point"
ρ	Fluid density
\mathcal{P}	Coordinate vector of "sending", "potential perturbation" or "dummy point."
τ_A	Time of transit of "advanced wave"
τ_R	Time of transit of "retarded wave"
ϕ	Amplitude of velocity potential perturbation
Φ	Velocity potential
ΔP	Pressure differential
$\Delta \phi$	Velocity potential differential
ω	Radial frequency

INTRODUCTION

Three-dimensional flutter solutions in subsonic and supersonic flows are an essential part of automated structural design. The methods that have been developed for subsonic flow are based on the numerical solution of the singular integral equation relating the pressure loading (or any other related quantity) to the downwash induced by the motion of the surface. The commonly used method is to treat the pressure as a series of preselected loading functions with unknown coefficients which are to be determined by satisfying the boundary conditions. In supersonic flows, the most frequently used method is to solve for the velocity potential directly in terms of distributed sources over the surface, although the integral equation approach has also been used. There is a need for a new method for both subsonic and supersonic speeds which is more oriented towards inclusion in a computer system (such as is used in automated design).

The objectives of this work include the development of a method based on the aerodynamic element concept which is to be used over the subsonic and supersonic Mach number range and the determination of aerodynamic forces on oscillating surfaces which are compatible with the structural breakdown.

There are three principal features in the current developmental work. Firstly, the concept of aerodynamic elements is adapted to unsteady aerodynamics. Secondly, the downwash-velocity potential method is used (also referred to as the integrated potential method) which results in simpler expressions than those resulting from the normally used downwash-pressure formulation. Lastly, the method developed is applicable to both subsonic and supersonic speeds.

In this report, a numerical method is formulated for calculating the aerodynamic matrix and generalized airforce matrix for both planar and non-planar wings of arbitrary planforms in steady and unsteady subsonic and supersonic flows.

The method uses the concept of "aerodynamic elements" and the downwash-velocity potential relationship (in preference to the downwash-pressure

relationship more commonly used by others). The downwash-velocity potential method, using this aerodynamic element concept, was applied to lifting surfaces at steady angles of attack in a Note (Ref. 1) by Haviland. In this case, the method was applied to a very simple steady-state rectangular wing model in subsonic flow. It was shown that a wake strip could be constructed using the same elements and that it could be terminated a few chord lengths from the wing. The arrangement of surface elements was selected in an attempt to simulate the nested horse-shoe vortices used by Hedman (Ref. 2). Exact agreement with the latter method was demonstrated. The work reported here is an extension of this method applied to the oscillating case in subsonic and supersonic flows. The application of the present method to an oscillating rectangular wing in subsonic flows has already been reported in reference 3.

The idea of using arbitrary surface elements in the steady case has been advanced by Woodward (ref. 4) and by Rubbert and Saaris (ref. 5). In these cases, researchers intended to represent curved surfaces, fillets, and arbitrary planforms in an optimum manner. The use of closed vortex loops surrounding surfaces of uniform potential by Rubbert and Saaris is of special interest here since it is the steady-state limit of the velocity potential method described in this report. Unfortunately, the concept of vortex lines has not proved to be useful for unsteady compressible flows. However, by specifying velocity potential distributions over the surface elements (without wake effects) and adding velocity potential distributions in the wake separately as functions of the trailing edge values, the computations are simplified considerably over those resulting from methods using the downwash-pressure methods. Both of these approaches employ doublet distributions to formulate nonhomogeneous integral equations. Examples of the downwash-pressure method (also called the integrated pressure method) include the kernel function method of Watkins, et al. (ref. 6), and the doublet-lattice method of Albano and Rodden (ref. 7). Other researchers, such as Jones (ref. 8), Stark (ref. 9), Houbolt (ref. 10), and Morino and Kuo (ref. 11) in the subsonic case, Rodemich and Andrew (ref. 12) in the transonic case, and Donato and Huhn (ref. 13) in the supersonic case have used the velocity potential. Most formulations of the supersonic problem have used the direct source method, as opposed to the doublet formulation necessary in the subsonic case. However, the downwash-pressure methods have

been employed by Watkins et al. (ref. 14) using the kernel function approach, and an extension of the doublet-lattice method has been suggested by Harder and Rodden (ref. 15). A comprehensive review of the state of art was provided by Landahl and Stark (ref. 16).

The method of solution proposed in this work is to select N_{RP} downwash collocation points at which the complex normal flow velocity components are known in terms of amplitudes and phase of oscillatory motion, and then to select an equal number of velocity potential distributions (each multiplied by an unknown factor which is to be found). In the simplest application, there is a collocation point for each surface element and one for each strip of wake. There is one point corresponding to each velocity potential at the center of a surface element or on the trailing edge.

In the proposed application, one would first specify the surface element geometry, the collocation points, and the unknowns in the velocity potential. One would then select the aerodynamic elements which one feels to be most appropriate and supply the geometric data specified for these. If the computer system provides sufficient flexibility, one would be able to have subroutines in the library which could process the input data so as to solve a given type of problem repeatedly. The basic computer program would compute an aerodynamic influence matrix using subsonic or supersonic aerodynamics (whichever is applicable) and would give complex downwash at the collocation points in terms of the unknowns in the velocity potential. In most cases, the inverse of this matrix would be required which has the nature of an "aerodynamic stiffness matrix" and gives the solution for the unknown velocity potential in terms of the downwashes. The next step depends largely on the particular application. In structural applications, the forces at the structural nodes would be calculated, using subroutines which would supplement the aerodynamic element subroutines. In flutter applications, similar subroutines would be used to calculate the generalized forces. The main objective of this work is to develop an efficient method for calculating the aerodynamic influence matrix. Since most available results from various other methods are given in the form of overall lift and moment derivatives (which can be readily calculated as generalized forces), these were calculated in the present work.

In order to evaluate the effectiveness of the method discussed here, various comparisons were made against results obtained by using other methods found in the literature. At present, the subsonic rectangular elements have been successfully applied not only to steady and to harmonically oscillating rectangular wings but also to swept wings with or without control surfaces and to T-tail configurations. The demonstration of supersonic rectangular elements has been restricted to planar, steady-state rectangular wings of various aspect ratios. This has also been compared with results of previous research.

The mathematical formulation of the problem begins with the well-known three-dimensional linearized potential flow equation in a moving coordinate system. This equation is derivable by a perturbation of the Eulerian momentum equations, the continuity equation, and the equation of state. An alternative way of deriving this equation is by using the Galilean transformation of the acoustical equation. The following assumptions are made:

1. Inviscid flow.
2. Adiabatic flow.
3. Irrotational flow (except for a certain prescribed region downstream of a body).
4. No body forces.
5. Equation of state for perfect gas.

The boundary conditions on a thin aerodynamic surface can be stated as follows:

1. Normal flow velocities at the collocation points (often referred to as the "downwash") are determined by the requirement that flow conforms to upper and lower surfaces.
2. Normal flow velocities are equal on upper and lower surfaces, (i.e., no relative velocities or "breathing" of the two surfaces).
3. Disturbances are felt after their cause. This eliminates parts of the solution and is sometimes derived from the condition that there is no radiation from infinity (Sommerfeld radiation condition).

The wake region streaming behind an aerodynamic surface is a sheet of vortices. It is treated as an additional boundary which can accommodate any normal flow and, therefore, any potential discontinuity but cannot sustain a pressure differential. Beyond this measure, no further steps are taken to assure that the Kutta condition is met (i.e., that the pressure goes to zero at the trailing edge).

The basic equation defines an acoustical perturbation of a uniform flow and is appropriate for subsonic, transonic and supersonic flows. However, no further consideration has been given to the transonic case because it is not appropriate for flows over bodies of finite thickness. Rather, for such cases, it would be necessary to perturb the actual, nonuniform flow over such a body. Experience to date with the comparison of theoretical and experimental flutter results indicates that wings of practical thickness can be treated successfully by uniform flow perturbations except in the transonic speed range.

Further discussion on the derivation of the equation, assumptions, and limitations involved can be found in references 6, 10, 11, and 14.

In the following three sections, the theoretical development is described, a method of solution is discussed applicable to rectangular elements, and computer results are presented. These cover subsonic rectangular elements applied to rectangular and swept wings and to T-tail configurations. In addition, supersonic elements are applied to steady state rectangular wings.

The next section presents a proposed extended method for subsonic and supersonic elements of polygonal plan form. Formally, the new method is based on the development of contour integrals around the elements, as is also used for the steady-state supersonic results. Previously, however, surface integrals had been used for the subsonic case. Similar contour integrals have been used by Jones (ref. 17). It can be readily demonstrated that the new method would give identically the same results as the former for all in-plane calculations.

Although the main effort reported here has been concentrated on obtaining results for comparison with vortex lattice or doublet methods, the need for irregular aerodynamic elements may dictate the development of improved velocity potential distributions in which finite vortices would be eliminated. One method for doing this was described by Mercer et al. (ref. 18). However,

there is some expectation that the polynomial expressions described in the section "Proposed Extended Method of Analysis" may prove adequate for this purpose.

The final sections contain conclusions and recommendations. They are followed by three Appendices, covering the subsonic computer program, standard integrals, and a description of the modifications made to the computer program to enable it to handle the steady-state supersonic calculations.

THEORETICAL DEVELOPMENT

Statement of Problem

The problem of the present investigation is to determine the aerodynamic forces on thin, flat plates undergoing harmonic oscillations in subsonic and supersonic flows.

Coordinate System

The basic coordinate system is x', y, z , or r with a uniform flow velocity V in the positive x -direction as shown in Figure 1. Each surface has its own coordinate system x, s, n , with x parallel to x' , s as the other coordinate in the plane of the surface and n as the local normal. The latter makes an angle g with the z -axis, measured in a right-handed manner about x .

The x', y and z system locates the "receiving point" or "collocation point," sometimes given as the point k . The sending point p is designated by the dummy coordinates ξ', η, ζ and by the local coordinates ξ, σ, v , and is sometimes given as the point l . The angle between the local normal v and the z -axis is γ . Surrounding each point l is an element of surface area sometimes referred to as a "sending region."

Governing Differential Equation

For the propagation of small disturbances that must be satisfied by the velocity potentials, the linearized potential flow equation in the coordinate system shown in Figure 1 may be written in the form:

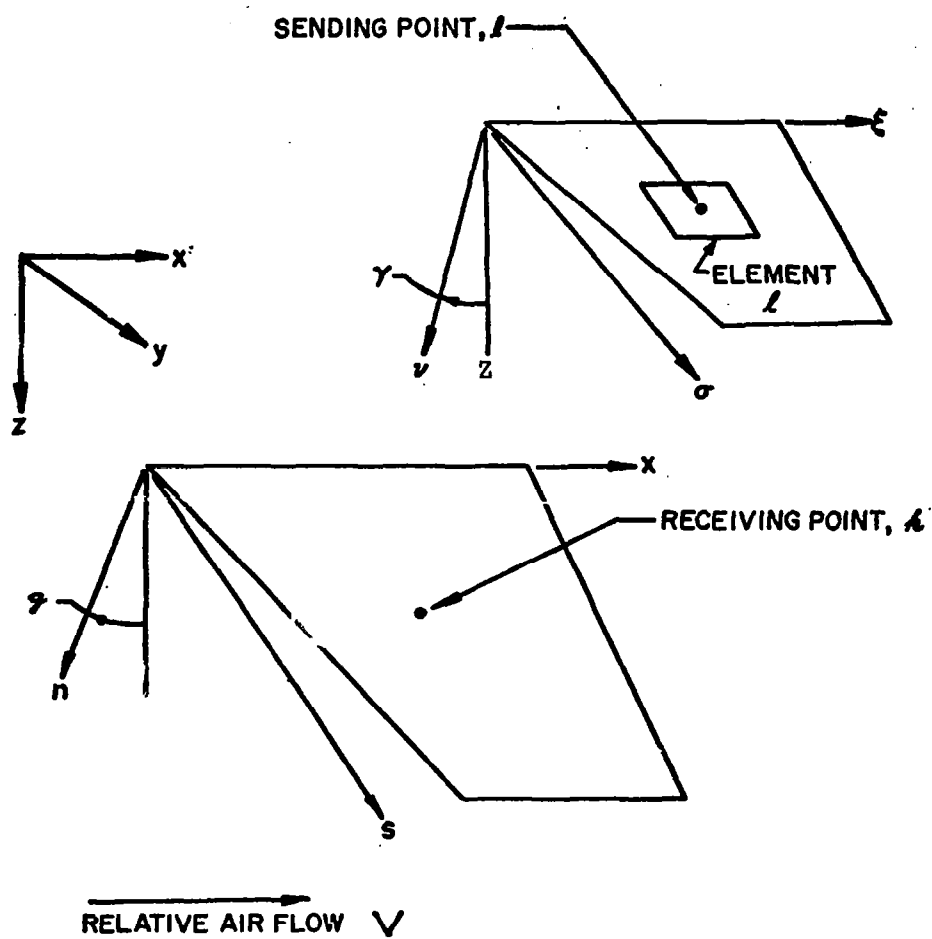


Fig. 1. Coordinate Systems

$$\frac{1}{c^2} \left(\frac{\partial}{\partial t} + V \frac{\partial}{\partial x'} \right)^2 \phi = \frac{\partial^2 \phi}{\partial x'^2} + \frac{\partial^2 \phi}{\partial y^2} + \frac{\partial^2 \phi}{\partial z^2} \quad (1)$$

where V and c are local unperturbed flow velocity and sound velocity, respectively.

For a harmonically oscillating system with ϕ equivalent to $\phi(r)e^{i\omega t}$, Eq. (1) becomes

$$\begin{aligned} \left(-\frac{\omega^2}{c^2} \right) \phi + \left(\frac{2i\omega V}{c^2} \right) \frac{\partial \phi}{\partial x'} + \left(\frac{V^2}{c^2} \right) \frac{\partial^2 \phi}{\partial x'^2} \\ = \frac{\partial^2 \phi}{\partial x'^2} + \frac{\partial^2 \phi}{\partial y^2} + \frac{\partial^2 \phi}{\partial z^2} \end{aligned} \quad (2)$$

Throughout the remainder of the report, the oscillatory case will be considered only, and the symbols for the field quantities will refer to their complex amplitudes, so that, for example, the actual velocity potential is $\phi e^{i\omega t}$. This also applies to pressure p , to density ρ , and to normal velocity w .

Integral Equation

Since it is very unlikely that an exact solution to Eq. (2) can be found, one approach to solving the problem is the transformation of the governing differential equation and its associated boundary condition to an integral equation for which approximate solutions can be found. For compressible flow, the integral equation as derived on the basis of the velocity potential and given for example in reference 13 may be written as

$$\phi(r) = \int_S \Delta \phi(r, \rho) \frac{\partial G(r, \rho)}{\partial v} dS \quad (3)$$

This integral equation relates the velocity potential differential across a thin aerodynamic surface or a wake, $\Delta \phi$, which is taken to be positive if it decreases in the positive v -direction, to the velocity potential in the field.

In Eq. (3), $G(r, \rho)$, represents Green's function which appears here in derivative or "doublet" form. The normal flow velocity $w(r)$, at the

collocation point r where the local normal is n can be obtained by differentiating Eq. (3) with respect to n which results in

$$w(r) = \left. \frac{\partial \phi(r)}{\partial n} \right|_{n \rightarrow 0} = \int_S \Delta \phi(p) K_\phi(r, p) dS \quad (4)$$

where

$$K_\phi(r, p) = \lim_{n, v \rightarrow 0} \frac{\partial^2 G(r, p)}{\partial n \partial v} \quad (5)$$

The surface of integration, S , appearing in Eq. (3) includes the aerodynamic surfaces and their wakes. Elsewhere in the field, $\Delta \phi$ is zero.

Expression for Green's function.— The Green's function, $G(r, p)$, appearing in Eqs. (3) and (5) can be written in a general form:

$$G(r, p) = U(\tau_R) G_R(r, p) + U(\tau_A) G_A(r, p) \quad (6)$$

where

$$G_R(r, p) = -e^{-i\omega\tau_R/4\pi R}$$

$$G_A(r, p) = -e^{-i\omega\tau_A/4\pi R}$$

$$R^2 = (x' - \xi')^2 + \beta^2(y - \eta)^2 + \beta^2(z - \zeta)^2$$

$$\tau_R = \{R - M(x' - \xi')\}/\beta^2 c$$

= Time of transit of "retarded wave"

$$\tau_A = \{-R - M(x' - \xi')\}/\beta^2 c$$

= Time of transit of "advanced wave"

$$\beta = \sqrt{1 - M^2}$$

$$U(\tau_R) = \begin{cases} 1 & \text{if } \tau_R \text{ is real and positive} \\ 0 & \text{otherwise} \end{cases}$$

$$U(\tau_A) = \begin{cases} 1 & \text{if } \tau_A \text{ is real and positive} \\ 0 & \text{otherwise} \end{cases}$$

In the subsonic case, ($M < 1$), τ_A is negative and G consists of only one term, $G_R(r, \rho)$. For supersonic flow, ($M > 1$), both τ_R and τ_A are positive when R is real; therefore, disturbances are restricted to the region of the aft Mach cone from the disturbing point. (This is equivalent of the statement made later that only disturbances in the forward Mach cone from a given receiving point are felt.) Also note that τ_R and τ_A are used in the same sense as in reference 14. In supersonic flow, the retarded wave arrives ahead of the advanced wave.

Expression for K_ϕ

The term K_ϕ defined by Eq. (5) might be termed the "velocity potential kernel function." It can be simplified when the thin surface coordinate system is used because K_ϕ varies with the normal coordinates n and v only through the "acoustical distance" R . Thus noting that

$$\frac{\partial G}{\partial v} = \left(\frac{-R}{\beta^2} \frac{\partial R}{\partial v} \right) \left(\frac{-\beta^2}{R} \frac{\partial G}{\partial R} \right)$$

with a similar relationship existing for the derivative with respect to n , K_ϕ can be written as

$$\begin{aligned} K_\phi(r, \rho) &= \left\{ \frac{\partial}{\partial n} \left(-\frac{R}{\beta^2} \frac{\partial R}{\partial v} \right) \right\} \left(-\frac{\beta^2}{R} \frac{\partial G}{\partial R} \right) \\ &+ \left(-\frac{1}{\beta^2} \frac{\partial R}{\partial v} \right) \left(-\frac{1}{\beta^2} \frac{\partial R}{\partial n} \right) \left\{ -\beta^2 R \frac{\partial}{\partial R} \left(-\frac{\beta^2}{R} \frac{\partial G}{\partial R} \right) \right\} \\ &= T_1(r, \rho) K_1(r, \rho) + T_2(r, \rho) K_2(r, \rho) \end{aligned} \quad (7)$$

After substitution of the Green's function from Eq. (6) the following expressions result:

$$T_1(r, p) = \frac{\partial}{\partial n} \left(-\frac{R}{\beta^2} \frac{\partial R}{\partial v} \right) = \cos(\gamma - \theta) \quad (8)$$

$$K_1(r, p) = -\frac{\beta^2}{R} \frac{\partial G}{\partial R} \quad (9)$$

$$T_2(r, p) = \left(-\frac{1}{\beta^2} \frac{\partial R}{\partial v} \right) \left(-\frac{1}{\beta^2} \frac{\partial R}{\partial n} \right) = \frac{n(p)v(r)}{R^2} \quad (10)$$

$$K_2(r, p) = -\beta^2 R \frac{\partial K_1}{\partial R} \quad (11)$$

In the expression for T_2 , the term $n(p)$ denotes the n -coordinate of the sending point p , and $v(r)$ denotes the v -coordinate of the receiving point r . In actuality, both T_1 and T_2 are equivalent to terms given by Vivian and Andrew (ref. 19). However, the expressions for K_1 and K_2 are different from the corresponding expressions given by these authors, and, in particular, they are only singular when r and p coincide.

The Green's function, G , introduced in Eq. (5), is often referred to as the "free-field Green's function" or as the "fundamental solution." The term Green's function is retained here for brevity and convenience.

The kernel function, K_ϕ , introduced in Eq. (5), relates the unknown velocity potential differential across an aerodynamic surface or its wake to the known normal flow velocity or "downwash." Because of this relationship, the method is called the "Downwash-Velocity Potential Method." Other authors, such as Allen and Sadler (ref. 20), have used the term "Integrated Potential Method."

The alternative methods of Watkins et al (ref. 6) and of Albano and Rodden (ref. 7) lead to kernels which have more complex forms and less tractable singularities. The assumption has been made that the present form results in numerical simplicity; this is, however, a difficult point to substantiate. Certainly, the aerodynamic element concept does not preclude the use of such kernels which would relate the unknown pressure differential to the known normal flow velocity as is noted in the following section. However, the use of global defining functions for the unknown pressures, as introduced by Watkins, et al (ref. 6), would lead to unnecessary complication and would negate the inherent simplicity of the aerodynamic element concept.

METHOD OF SOLUTION

Introduction

The integral equation shown in Eq. (3) is solved using an approximate method. The method assumes that the velocity potential distributions over selected "elements" on the aerodynamic surfaces are expressed in terms of unknown parameters. The velocity potential distribution of each element is determined by satisfying normal velocity boundary conditions at a set of collocation points located over the surface using the relationship given in Eq. (4). The computer program sets up simultaneous equations relating the velocity potentials to the known normal flow velocities at collocation points. Typically, there is one such point to each element. Solution of the simultaneous equations and interpretation of the velocity potential parameters results in the required aerodynamic forces. Since there is a one-to-one correspondence between velocity potential and pressure distribution, any system of calculation based on pressure distribution can be performed in terms of velocity potentials.

Integration by Discrete Elements

In the downwash-integral equation as expressed in Eq. (4), the velocity potential distribution $\Delta\phi(\rho)$ is the only unknown function within the equation. The integration of Eq. (4) is required for each collocation point $k = 1, \dots, N_{RP}$ and can be performed by integrating separately over the appropriate sending regions relating to the unknown velocity potential amplitude coefficients $\Delta\phi_\ell$ ($\ell = 1, \dots, N_{RP}$). Thus, a set of simultaneous equations is formed which can be written as

$$\frac{w_k}{V} = \sum_{\ell=1}^{N_{RP}} A_{k,\ell} \frac{\Delta\phi_\ell}{V} \quad (12)$$

where the matrix $A_{k,\ell}$ is the "aerodynamic influence matrix." The principle concern of this report is the determination of the matrix $A_{k,\ell}$. Once this matrix is known, it is a fairly straightforward procedure to obtain the perturbation velocity potential differentials $\Delta\phi$'s for all the collocation points and to calculate the generalized airforce matrix.

Aerodynamic Elements

In calculating the aerodynamic influence matrix, the concept of "aerodynamic elements" is employed. This means that the user is given a catalog of subprograms capable of handling elements of different shape and different Mach number range. For an experimental program such as reported in this work, this concept also provides a convenient way of evaluating various mathematical formulations of the same problem. The concept is very similar to that used in finite element method in structural analysis in which there is a basic program containing sufficient subprograms to handle a wide variety of structural elements which may be required.

Basic form. - Expressions for the terms of the aerodynamic influence coefficient $A_{k,l}$ given in Eq. (12) can be obtained by breaking the surfaces up into elements (the unknown velocity potential differential $\Delta\phi_l$ being associated with the element l). To facilitate the handling of wake effects and to provide for cases where the velocity potential differential is not constant over an element, it is convenient to define a corresponding point l^* in each wake element l^* . Thus, the velocity potential differential can be written in the form:

$$\Delta\phi(l^*, \xi, \sigma) = \Delta\phi_l f(l^*, \xi, \sigma) \exp[-i\omega[\xi(l^*) - \xi(l)]/V] \quad (13)$$

In the above expression, f is a shape factor. However, even if this is uniform, the exponential term assures that the potential at the point l^* conforms to the expression relating the velocity potential in the wake to the velocity potential near trailing edge. In order to standardize the terminology for on-surface and wake elements, the notations l and l^* are used throughout, but it is to be understood that they become identical for on-surface elements. The system of points and regions is illustrated in Fig. 2. When Eq. (13) is substituted into Eq. (4), and the result is redefined as in Eq. (12), it is found that the aerodynamic influence matrix can be expressed in the form:

$$A_{k,l} = \Sigma(l^*) k_\phi(k, l, l^*) \quad (14)$$

which reduces for on-surface elements to

$$A_{k,l} = k_\phi(k, l, l) \quad (15)$$

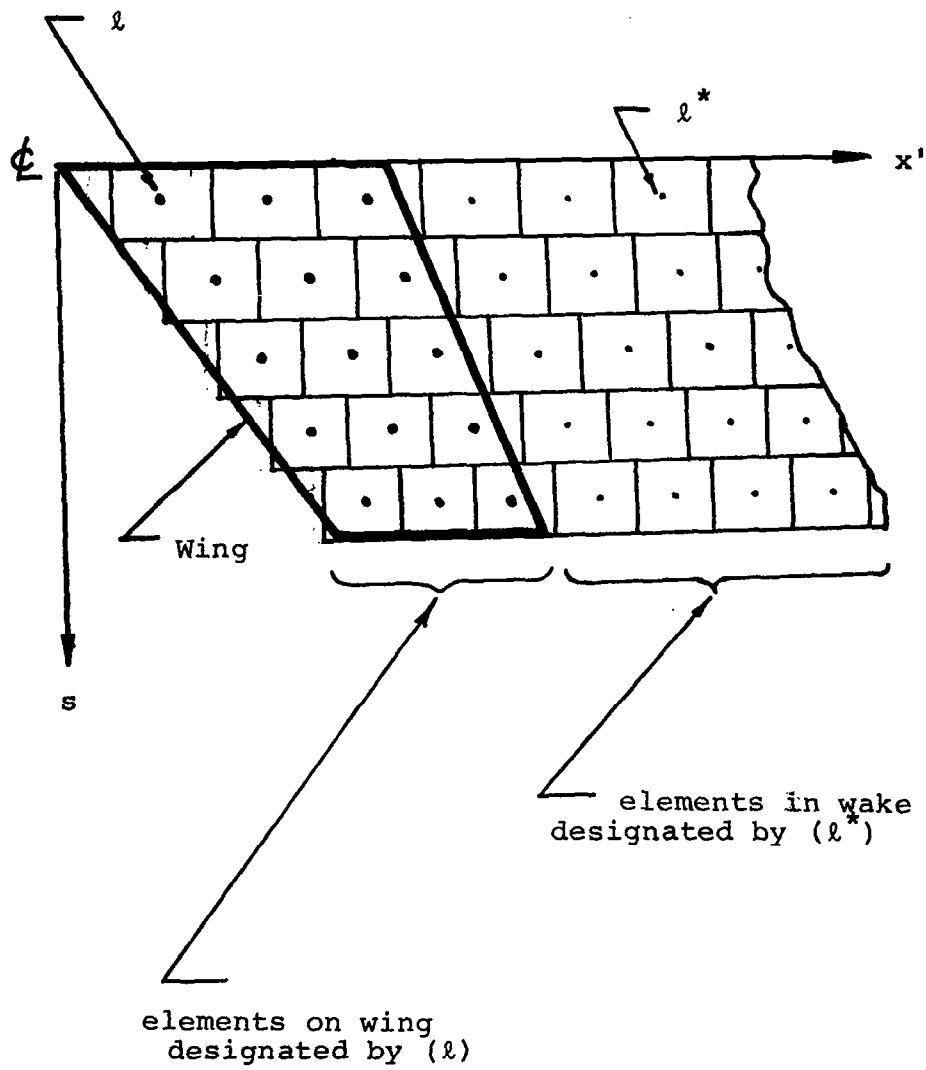


Fig. 2. Designation of elements for Wing and Wake

where

$$k_{\phi}(k, l, l^*) = \iint_{l^*} K_{\phi}(r, \rho) f(l^*, \xi, \sigma) \exp\left\{-\frac{i\omega}{V} [\xi(l^*) - \xi(l)]\right\} d\xi d\sigma \quad (16)$$

In Eq. (16), the area integration is restricted to the element l^* .

Subsonic aerodynamic elements.— Having performed the indicated differentiations in Eqs. (9) and (11), the expressions for $K_1(r, \rho)$ and $K_2(r, \rho)$ for subsonic flows are as follows:

$$K_1(r, \rho) = U(\tau_R) \left(\frac{\beta^2}{R^2} + \frac{i\omega}{Rc} \right) G_R(r, \rho) \quad (17)$$

$$K_2(r, \rho) = U(\tau_R) \left(\frac{3\beta^4}{R^2} + \frac{3i\omega\beta^2}{Rc} - \frac{\omega^2}{c^2} \right) G_R(r, \rho) \quad (18)$$

where $U(\tau_R)$ and $G_R(r, \rho)$ are shown in Eq. (6). Using the expression in Eq. (7) and substituting the resulting expression for $K_{\phi}(r, \rho)$ into Eq. (16), $k_{\phi}(k, l, l^*)$ becomes

$$k_{\phi}(k, l, l^*) = \{\cos(\gamma - g)k_1(k, l^*) + k_2(k, l, l^*)\} \times \exp\left\{-\frac{i\omega L(k, l, l^*)}{V}\right\} \quad (19)$$

where

$$k_1(k, l^*) = -\frac{1}{4\pi} \iint_{l^*} \left\{ \frac{\beta^2}{R^3(k)} + \frac{i\omega}{c} \frac{1}{R^2(k)} \right\} \times \exp\left\{-\frac{i\omega}{\beta^2 c} [R(k) - R(k, l^*) + M\xi - M(l^*)]\right\} \times f(l^*, \xi, \sigma) d\xi d\sigma \quad (20)$$

$$k_2(k, l, l^*) = \frac{-v(k)}{4\pi} \iint_{l^*} \left\{ \frac{3\beta^4}{R^5(k)} + \frac{3i\omega\beta^2}{cR^4(k)} - \frac{\omega^2}{c^2} \frac{1}{R^3(k)} \right\} \times \exp\left\{-\frac{i\omega}{\beta^2 c} [R(k) - R(k, l^*) + M\xi - M\xi(l^*)]\right\} \times n(\xi, \sigma) f(l^*, \xi, \sigma) d\xi d\sigma \quad (21)$$

$$L(k, l, l^*) = \xi(l^*) - \xi(l) + \frac{M^2}{\beta^2} \{ \xi(l^*) - \xi(k) \} + \frac{M}{\beta^2} R(k, l^*) \quad (22)$$

In the above expressions, $R(k, l)$ is R derived for the points k and l , while $R(k)$ is R derived for the points k and ρ . Also, $n(\xi, \sigma)$ is the n -coordinate of the point ξ, σ on the sending element.

Mid point constant potential (MPCP) rectangular elements: The simplest derivation of the integrals in Eq. (19) can be obtained by insuring that the point l^* is essentially the mid-point of the element l^* and then evaluating the integrand at that point. Assuming a uniform potential distribution with $f(l^*, \xi, \sigma)$ equal to unity,

$$k_1(k, l^*) = - \frac{A(l^*)}{4\pi} \left\{ \frac{\beta^2}{R^3(k, l^*)} + \frac{i\omega}{c} \frac{1}{R^2(k, l^*)} \right\} \quad (23)$$

$$k_2(k, l^*) = \frac{-A(l^*) \mathbf{v}(k) n(l^*)}{4\pi}$$

$$\times \left\{ \frac{3\beta^4}{R^5(k, l^*)} + \frac{3i\omega\beta^2}{cR^4(k, l^*)} - \frac{\omega^2}{c^2R^3(k, l^*)} \right\} \quad (24)$$

where $A(l^*)$ is the area of the element l^* . For the remaining subsonic aerodynamic elements, the same out-of-plane term as shown in Eq. (24) will be used.

Zero order constant potential (ZOCP) rectangular elements: In reference 1, the same expressions were used as for the MPCP rectangular elements in the first evaluation of the in-plane steady state case. It was found that they did not provide correct results. Therefore, $k_1(k, l^*)$ was rederived for a rectangular element. Since only the steady-state term, independent of the radial frequency ω , was involved, it is referred to as the zero order element. The resulting expression for $k_1(k, l^*)$ can be written as:

$$k_1(k, l^*) = k_{SS}(k, l^*) - \frac{i\omega A(l^*)}{4\pi c R^2(k, l^*)} \quad (25)$$

where

$$\begin{aligned}
k_{SS}(k, \ell^*) &= \frac{-\beta^2}{4\pi} \iint_{\text{rectangle } \ell^*} \frac{1}{R^3(k)} d\xi d\sigma \\
&= \left\{ \left[F_{SS}(k, \xi, \sigma) \right] \begin{matrix} \xi_{AFT}(\ell^*) \\ \xi_{FOR}(\ell^*) \end{matrix} \right\} \begin{matrix} \sigma_{OUT}(\ell^*) \\ \sigma_{IN}(\ell^*) \end{matrix} \quad (26)
\end{aligned}$$

$F_{SS}(k, \xi, \sigma)$ can be obtained using the standard integral formula listed in Appendix B.

$$F_{SS}(k, \xi, \sigma) = \frac{1}{4\pi v(k)} \tan^{-1} \frac{v(k)R(k)}{X(k)S(k)} \quad (27)$$

$$R(k) = \sqrt{X^2(k) + \beta^2 S^2(k) + \beta^2 v^2(k)} \quad (28)$$

$$X(k) = \xi - \xi(k) \quad (29)$$

$$S(k) = \sigma - \sigma(k) \quad (30)$$

The terms $\xi_{AFT}(\ell^*)$ etc. define the coordinates of the edges of the rectangle making up the region ℓ^* and are shown in Fig. 3. When the receiving point k is coplanar with the sending region ℓ^* , $v(k)$ is zero, and one must be careful to program the limiting equations accordingly.

First order constant potential (FOCP) rectangular elements: In order to improve the accuracy of the results, the complete integrand of Eq. (20) was expanded to the first order term in ω , and then integrated. The result being:

$$k_1(k, \ell^*) = k_{SS}(k, \ell^*) \left\{ 1 + \left[\frac{i\omega}{\beta^2 c} R(k, \ell^*) + M\xi(\ell^*) - M\xi(k) \right] \right\} + \frac{i\omega M}{c} k_{US}(k, \ell^*)$$

where k_{SS} is shown in Eq. (26) and (31)

$$\begin{aligned}
k_{US}(k, \ell^*) &= \frac{1}{4\pi} \iint_{\text{rectangle } \ell^*} \{X(k)/R^3(k)\} d\xi d\sigma \\
&= \left\{ \left[F_{US}(k, \xi, \sigma) \right] \begin{matrix} \xi_{AFT}(\ell^*) \\ \xi_{FOR}(\ell^*) \end{matrix} \right\} \begin{matrix} \sigma_{OUT}(\ell^*) \\ \sigma_{IN}(\ell^*) \end{matrix} \quad (32)
\end{aligned}$$

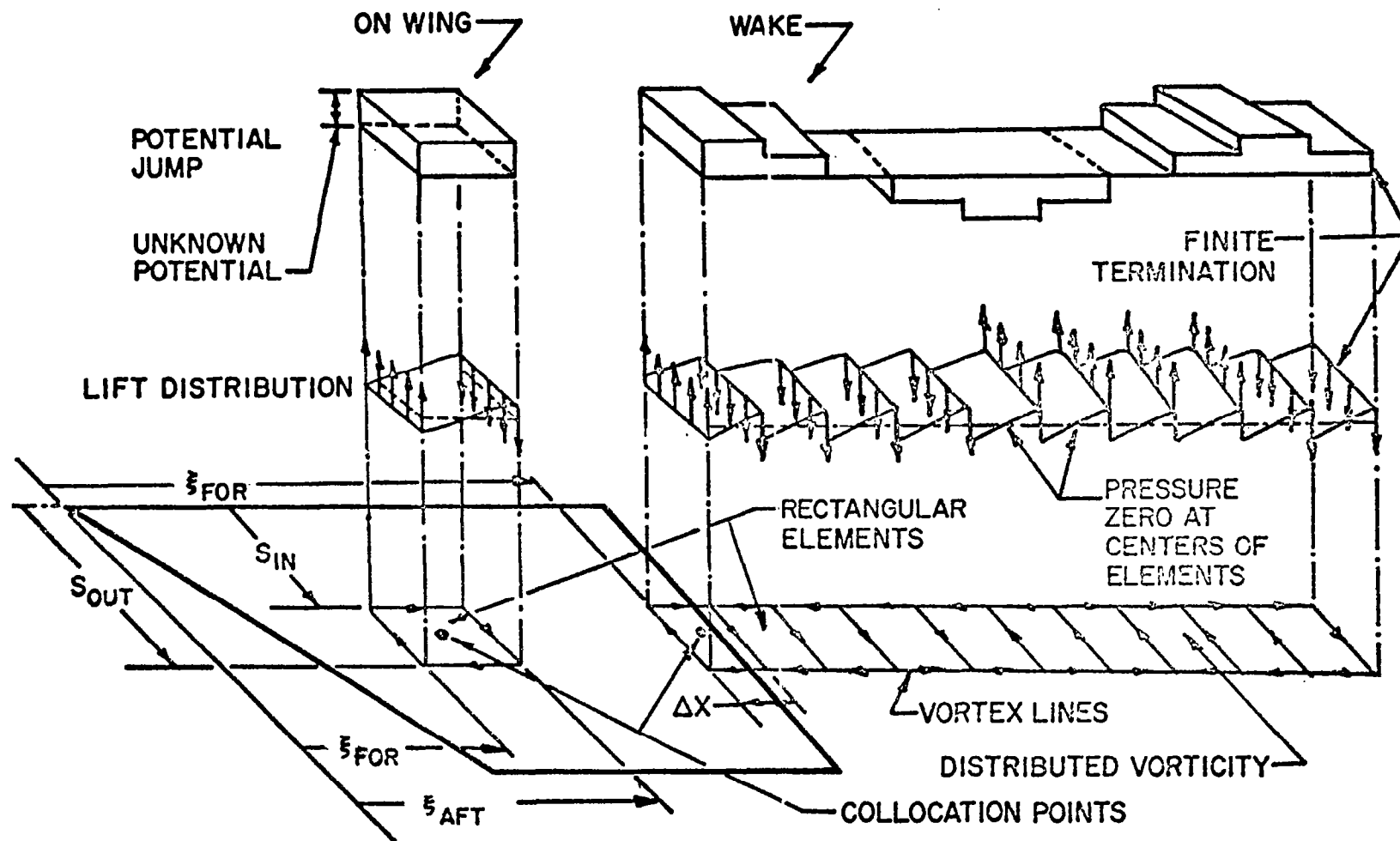


Fig. 3. Constant Potential Elements

$$F_{US}(k, \xi, \sigma) = \frac{1}{4\pi\beta} \log_e \{R(k) + \beta S(k)\} \quad (33)$$

Numerical difficulties will occur whenever a collocation point k is near a corner of the rectangular element ℓ^* . This situation should thus be avoided.

First order zero pressure (FOZP) rectangular elements: If the potential is varied in such a way that the distributed pressure remains zero, as shown in Fig. 4, the stepped potential of Fig. 3 is avoided, and the derivation of the forces acting on the elements is simplified. The modification consists of using the shape factor

$$f(\ell^*, \xi, \sigma) = \exp \{-i\omega[\xi - \xi(\ell^*)]/V\} \quad (34)$$

In Eq. (20) and the resulting expression for $k_1(k, \ell^*)$ is written as:

$$k_1(k, \ell^*) = k_{SS}(k, \ell^*) \left\{ 1 + \frac{i\omega}{\beta^2 V} [MR(k, \ell^*) + \xi(\ell^*) - \xi(k)] \right\} + i\omega k_{US}(k, \ell^*)/V \quad (35)$$

This is slightly different in form from that given in Eq. (31).

Supersonic aerodynamic elements.—As a first step in the development of supersonic rectangular elements, the in-plane case is considered. Much of the subsonic formulation is directly applicable to the supersonic formulations. Completing the differential indicated in Eq. (9), the expression for $K_1(r, \rho)$ in supersonic flow becomes

$$\begin{aligned} K_1(r, \rho) &= -\frac{\beta^2}{R} \frac{\partial G(r, \rho)}{\partial R} \\ &= \frac{1}{4\pi} \left[\frac{\beta^2}{R} \frac{\partial}{\partial R} \left\{ \frac{U(\tau_R)}{R} \right\} - \frac{i\omega}{c} \frac{U(\tau_R)}{R^2} \right] e^{-\frac{i\omega}{\beta^2 c} \{R-M(x'-\xi)\}} \\ &\quad + \frac{1}{4\pi} \left[\frac{\beta^2}{R} \frac{\partial}{\partial R} \left\{ \frac{U(\tau_A)}{R} \right\} + \frac{i\omega}{c} \frac{U(\tau_R)}{R^2} \right] e^{-\frac{i\omega}{\beta^2 c} \{-R-M(x'-\xi)\}} \end{aligned} \quad (36)$$

Now Eq. (16) can be written in the form

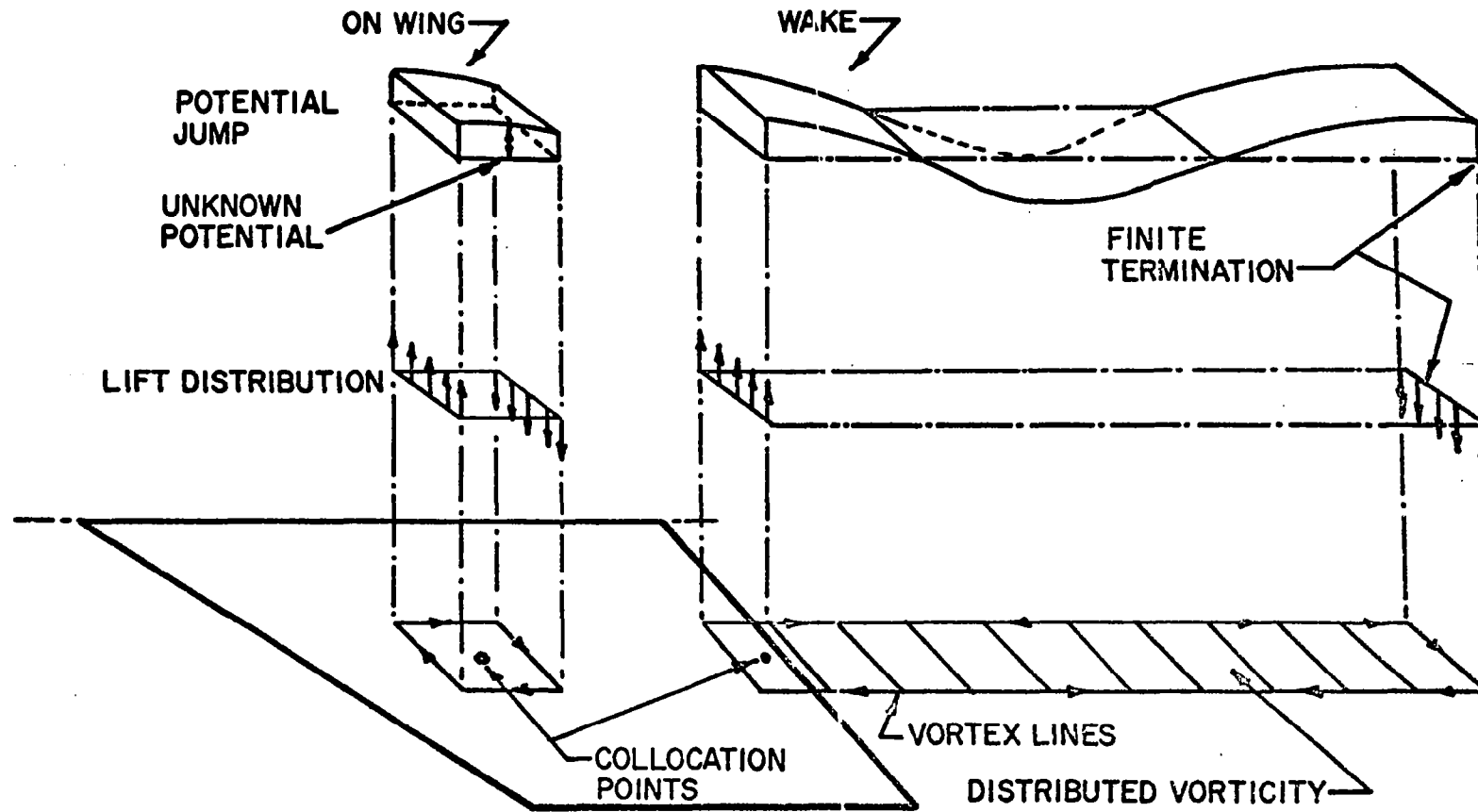


Fig. 4. Zero Pressure Elements

$$k_{\phi}(k, l, l^*) = \{k_{IR}(k, l^*) + k_{IA}(k, l^*)\} \exp\left\{-\frac{i\omega}{V} L(k, l, l^*)\right\} \quad (37)$$

where

$$k_{IR}(k, l^*) = \frac{1}{4\pi} \int \int_{\text{element } l^*} \left[\frac{\beta^2}{R} \frac{\partial}{\partial R} \left\{ \frac{U(\tau_R)}{R} \right\} - \frac{i\omega}{c} \frac{U(\tau_R)}{R^2} \right] \times \exp \left[-\frac{i\omega}{\beta^2 c} \{R(k) + M\xi - M\xi(l^*)\} \right] f(l^*, \xi, \sigma) d\xi d\sigma \quad (38)$$

$$k_{IA}(k, l^*) = \frac{1}{4\pi} \int \int_{\text{element } l^*} \left[\frac{\beta^2}{R} \frac{\partial}{\partial R} \left\{ \frac{U(\tau_A)}{R} \right\} + \frac{i\omega}{c} \frac{U(\tau_A)}{R^2} \right] \times \exp \left[-\frac{i\omega}{\beta^2 c} \{-R(k) + M\xi - M\xi(l^*)\} \right] f(l^*, \xi, \sigma) d\xi d\sigma \quad (39)$$

$$L(k, l, l^*) = \xi(l^*) - \xi(l) + \frac{M^2}{\beta^2} \{\xi(l^*) - \xi(k)\} \quad (40)$$

For a uniform potential distribution with $f(l^*, \xi, \sigma)$ equal to unity,

$$k_{IR}(k, l^*) = \left\{ k_{SS}(k, l^*) \left[1 + \frac{i\omega}{\beta^2 c} \{R(k, l^*) + M\xi(l^*) - M\xi(k)\} \right] + \frac{i\omega M}{c} k_{US}(k, l^*) \right\} \exp \left\{ -\frac{i\omega R(k, l^*)}{\beta^2 c} \right\} \quad (41)$$

$$k_{IA}(k, l^*) = \left\{ k_{SS}(k, l^*) \left[1 + \frac{i\omega}{\beta^2 c} \{-R(k, l^*) + M\xi(l^*) - M\xi(k)\} \right] + \frac{i\omega M}{c} k_{US}(k, l^*) \right\} \exp \left\{ -\frac{i\omega R(k, l^*)}{\beta^2 c} \right\} \quad (42)$$

Thus, the expression for $k_{\phi}(k, l^*)$ becomes

$$\begin{aligned}
k_{\phi}(k, l^*) = 2k_{SS}(k, l^*) & \left[\left\{ 1 + \frac{i\omega M}{\beta^2 c} [\xi(l^*) - \xi(k)] \right\} \right. \\
& \times \cos \left\{ \frac{\omega R(k, l^*)}{\beta^2 c} \right\} + \frac{\omega}{\beta^2 c} R(k, l^*) \sin \left\{ \frac{\omega R(k, l^*)}{\beta^2 c} \right\} \left. \right] \\
& + \frac{2i\omega M}{c} k_{US}(k, l^*) \cos \left\{ \frac{\omega R(k, l^*)}{\beta^2 c} \right\}
\end{aligned} \quad (43)$$

where

$$k_{SS}(k, l^*) = \frac{-1}{4\pi} \int \int_{\text{element } l^*} \frac{\beta^2}{R(k)} \frac{\partial}{\partial R(k)} \left\{ \frac{U(\tau_R, \tau_A)}{R(k)} \right\} d\xi d\sigma \quad (44)$$

$$k_{US}(k, l^*) = \frac{-1}{4\pi} \int \int_{\text{element } l^*} \frac{X(k) \beta^2}{R(k)} \frac{\partial}{\partial R(k)} \left\{ \frac{U(\tau_R, \tau_A)}{R(k)} \right\} d\xi d\sigma \quad (45)$$

In-plane steady supersonic (IPSS) rectangular elements: In the steady-state case, Eq. (43) reduces to

$$k_{\phi}(k, l^*) = 2 k_{SS}(k, l^*) \quad (46)$$

where $k_{SS}(k, l^*)$ is the expression given in Eq. (44). If one makes the following substitutions:

$$\begin{aligned}
U &= U(\tau_R, \tau_A) \\
X &= X(k) = \xi - \xi(k) \\
S &= S(k) = \sigma - \sigma(k) \\
N &= N(k) = v - v(k) \\
a^2 &= M^2 - 1 \\
R^2 &= R^2(k) = X^2 - a^2 S^2 - a^2 N^2
\end{aligned} \quad (47)$$

then, in the planar case, where $v(k) \rightarrow 0$,

$$-\frac{a^2}{R} \frac{\partial}{\partial R} \left(\frac{U}{R} \right) = \frac{\partial^2}{\partial N^2} \left(\frac{U}{R} \right) \quad (48)$$

but

$$\left(-a^2 \frac{\partial^2}{\partial X^2} + \frac{\partial^2}{\partial S^2} + \frac{\partial^2}{\partial N^2} \right) \left(\frac{U}{R} \right) = 0 \quad (49)$$

Therefore,

$$\begin{aligned} k_{SS}(k, \ell^*) &= \frac{-1}{4\pi} \iint_{\text{element } \ell^*} \left(\frac{\partial^2}{\partial S^2} - a^2 \frac{\partial^2}{\partial X^2} \right) \left(\frac{U}{R} \right) d\xi d\sigma \\ &= \frac{1}{4\pi} \iint_{\text{element } \ell^*} \left(\frac{\partial Q}{\partial X} - \frac{\partial P}{\partial S} \right) dX dS \end{aligned} \quad (50)$$

where

$$P = \frac{\partial}{\partial S} \left(\frac{U}{R} \right), \quad Q = a^2 \frac{\partial}{\partial X} \left(\frac{U}{R} \right)$$

Using Green's theorem (ref. 21)

$$\begin{aligned} k_{SS}(k, \ell^*) &= \frac{1}{2\pi} \oint_C [P dX + Q dS] \\ &= \frac{1}{4\pi} \oint_C \left[a^2 \frac{\partial}{\partial X} \left\{ \frac{U}{R} \right\} dS + \frac{\partial}{\partial S} \left\{ \frac{U}{R} \right\} dX \right] \end{aligned} \quad (51)$$

The cutoff function in the above equation may be written in the form:

$$U = U(-a|S| - X) \quad (52)$$

with

$$\frac{\partial U}{\partial X} = \frac{1}{a} \frac{\partial U}{\partial S} \quad (53)$$

Derivatives of the step function give rise to the impulse function, otherwise called the Dirac delta function. For example,

$$\begin{aligned}\frac{\partial}{\partial X} U(x) &= \delta(x) = 0 & (x \neq 0) \\ \frac{\partial}{\partial X} U(x) &= \delta(x) = \infty & (x = 0)\end{aligned}\tag{54}$$

A useful integral property of this delta function is

$$\int f(x)\delta(x) dx = f(0)\tag{55}$$

The next step is to make use of these properties and to perform the line integration indicated in Eq. (51) for complete and partial rectangular elements as sketched in Fig. 5.a. The figure shows an example of a rectangular wing broken up in 3×3 rectangular elements. Mach lines from one receiving point are shown to illustrate the complete and partial elements inside the aft Mach lines. Thus, the system of points and regions for steady supersonic calculations is slightly different from the subsonic case as shown in Fig. 2. The collocation points lie on the forward edge of each element. There is no need to consider the wake element in this case. The particular arrangement of collocation points used in these calculations is shown in Fig. 5.a. It is different from that used in the subsonic case but was selected for convenience, and does not, by any means, represent the final method recommended.

The integration along the periphery of a complete element (see Fig. 5.b) gives

$$k_{SS}(k, \ell^*) = \frac{1}{4\pi} \left\{ \left. \frac{R}{XS} \right|_B - \left. \frac{R}{XS} \right|_A - \left. \frac{R}{XS} \right|_C + \left. \frac{R}{XS} \right|_D \right\}\tag{56}$$

For partial elements such as No. 2 in Fig. 5.a which are cut by Mach lines, the path of integration is taken as indicated in Fig. 5.c. In this case,

$$\begin{aligned}k_{SS}(k, \ell^*) &= \frac{-a^2}{4\pi} \int_C^B \left(\frac{1}{aR} \frac{\partial U}{\partial S} - \frac{X}{R^3} \right) dS \\ &+ \frac{1}{4\pi} \int_C^A \left(\frac{a}{R} \frac{\partial U}{\partial X} - \frac{a^2 S}{R^3} \right) dX = \left. \frac{R}{XS} \right|_C\end{aligned}\tag{57}$$

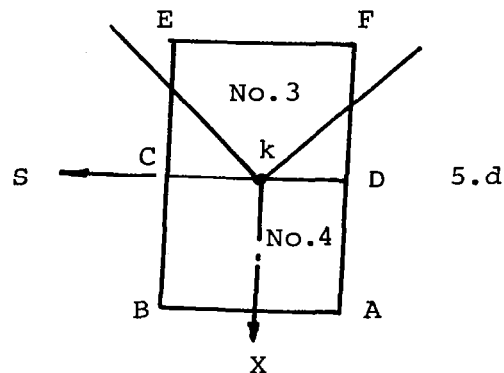
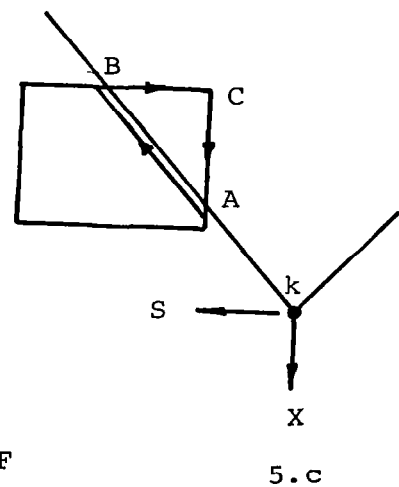
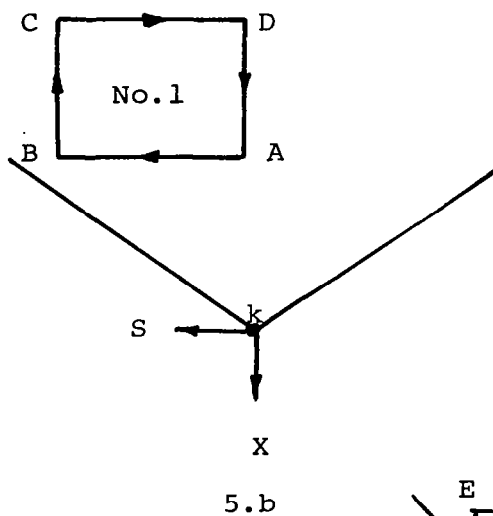
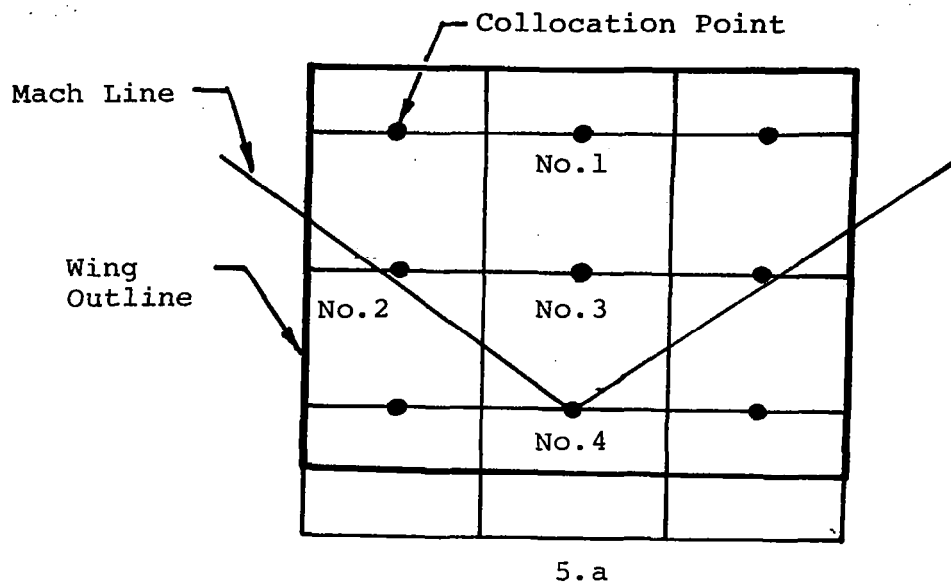


Fig.5 Paths of Integration for Complete and Partial Rectangular Elements Inside Aft Mach Lines

For the elements No. 3 and 4 in Fig. 5.a, the line integrations similar to those used for elements No. 1 and No. 2 are no longer applicable because of the singularity problem when $X(k) = 0$.

However, the nature of this singularity is well known because it results from the two-dimensional flow solution relating pressure at a point to local angle of attack at that point. According to this, the two-dimensional component of normal velocity under a lift line is characterized by a Dirac delta function.

Therefore, the solution for the cross-section of a two-dimensional supersonic wing consists of a stepped section. However, the section is known to be characterized by a straight line at a uniform angle of attack. Either one must abandon the uniform potential element, or one must use some suitable smoothing process in which a smooth curve is found which is a best fit to the stepped profile. The latter approach is used here.

The aerodynamic matrix is obtained in two parts. The first part gives the three-dimensional relationship along the lines described already. The second gives the two-dimensional component and in order to obtain this part correctly, the arrangement of collocation points shown in Figure 5 was selected. It will be noted that each collocation point is on the forward edge of a corresponding element (also a lift line because this is where the velocity potential jumps). Thus, the two-dimensional contribution to the aerodynamic matrix can be obtained by inverting the two-dimensional expression for lift due to angle of attack. This leads to the following procedure for the contributions of elements No. 3 and 4 to the downwash at collocation point No. 4.

The lift coefficient per unit span of a two-dimensional lifting flat plate is

$$C_L = \frac{L}{\frac{1}{2} \rho V^2 \Delta x} = \frac{4\alpha}{\sqrt{M^2 - 1}} \quad (58)$$

Lift is related to velocity potential as follows:

$$\frac{L}{\frac{1}{2} \rho V^2 \Delta x} = - \frac{\Delta \phi}{\frac{1}{2} V \Delta x} \quad (59)$$

Downwash is related to velocity potential by

$$\frac{w_k}{V} = \frac{\Delta\phi}{V} \left(\frac{-\sqrt{M^2 - 1}}{2\Delta x} \right) = \alpha \quad (60)$$

Comparing this with Eq. (12), it may be seen that

$$A_{k,k} = \frac{-\sqrt{M^2 - 1}}{2\Delta x} = -K \quad (61)$$

Thus, the contribution to downwash at collocation point No. 4 (= k) from element No. 4, as in Fig. 5.d, is -K, while the contribution from element No. 3 consists of the sum of the values K (because collocation No. 4 is on the near edge of element No. 3) and $\left. \frac{R}{XS} \right|_{E,F}$. This scheme represents a process of averaging out the downwash over the element resulting from the physical consideration that the downwash is continuously distributed over the surface rather than concentrated along a line.

It will be noted that the two-dimensional part of the aerodynamic matrix has -K on the diagonal, with +K at certain other elements.

The listing of the additional subroutines used in steady supersonic calculations and modifications made in subroutine DMATR are included in Appendix C.

Calculation of Aerodynamic Forces

Basic approach.— Let the downwash w_k be the sum of the contributions from all of the complex amplitudes \tilde{q}_i of generalized coordinate. Then the normal flow velocity at each collocation point, w_k , can be expressed in the complex form:

$$\frac{w_k}{V} = \sum_{i=1}^N \frac{w_{i,k}}{V} \tilde{q}_i = \sum_{i=1}^N \{ \alpha_{i,k} + \frac{i\omega}{V} h_{i,k} \} \tilde{q}_i \quad (62)$$

where $h_{i,k}$ and $\alpha_{i,k}$ are the amplitudes of displacement and local angle of attack, respectively, at each collocation point k for unit amplitude of the

generalized coordinate \tilde{q}_i , and N is the number of modes. Also, let

$$\Delta\phi_{\ell} = \sum_{i=1}^N \Delta\phi_{i,\ell} \tilde{q}_i \quad (63)$$

then

$$\frac{\Delta\phi_{i,\ell}}{V} = \sum_{k=1}^{N_{RP}} A_{k,\ell}^{-1} \frac{w_{i,k}}{V} \quad (64)$$

Thus, given the inverse of the aerodynamic influence matrix $A_{k,\ell}$ and the modal components of downwash $w_{i,k}$, the modal components of the velocity potential can be calculated.

Generalized forces.— The generalized forces \tilde{Q}_i can be expressed in the form:

$$\tilde{Q}_i = \sum_{j=1}^N \iint d(i,x,s) \Delta P(j,x,s) \tilde{q}_j \, dx \, ds \quad (65)$$

where $d(i,x,s)$ and $\Delta P(j,x,s)$ are the modal deflection and net pressure at point (x,s) , respectively. Eq. (65) can be put in the form:

$$\tilde{Q}_i = -\rho V^2 \sum_{j=1}^N C_{i,j} \tilde{q}_j \quad (66)$$

where ρ is the density of air.

The flutter airforce matrix, $C_{i,j}$, is given as

$$C_{i,j} = -\sum \iint d(i,x,s) \frac{\Delta P(j,x,s)}{\rho V^2} \, dx \, ds \quad (67)$$

Note that $\Delta\phi$ and ΔP are given in the same sense and are thus positive when the algebraic value is highest on the negative ($-n$) side of the airfoil. A positive ΔP then results in a force in the plus n direction. It can be shown that the pressure differential and velocity potential differential are related by the following equation:

$$\frac{\Delta P(j, x, s)}{\rho V^2} = - \left\{ \frac{\partial f(\ell, x, s)}{\partial x} + \frac{i\omega}{V} f(\ell, x, s) \right\} \frac{\Delta \phi_{j, \ell}}{V} \quad (68)$$

where $f(\ell, x, s)$ is the shape factor factor mentioned in Eq. (13). Eq. (67) now can be expressed in terms of velocity potentials by the above relationship.

On integration of Eq. (68),

$$\frac{\Delta \phi f(x, s)}{V} = -\exp \left(\frac{-i\omega x}{V} \right) \int_{-\infty}^x \frac{\Delta P(\lambda, s)}{\rho V^2} \exp \left(\frac{i\omega \lambda}{V} \right) d\lambda \quad (69)$$

The velocity potential in the wake is related to the velocity potential near the trailing edge by the requirement that the pressure differential sustained by the wake is zero. Thus, if $\Delta \phi_{TE}$ is the velocity potential differential at x_{TE} near the trailing edge, then

$$\Delta \phi f(x, s) = \Delta \phi_{TE} \exp \left\{ - \frac{i\omega}{V} (x - x_{TE}) \right\} \quad (70)$$

This can be derived readily from Eq. (69).

Flutter airforce matrix for constant potential case.— In this case, the velocity potential varies as shown in Fig. 3, leading to lift lines at the front and rear of the rectangular element. The forward lift is negative (i.e., in the negative n -direction). When the velocity potentials $\frac{\Delta \phi_{i, \ell}}{V}$ are solved from Eq. (64), the rectangular element moves as a rigid body so that

$$d(i, x, s) = h_{i, \ell} + \{x - x(\ell)\} \alpha_{i, \ell} \quad (71)$$

The contribution to the airforce matrix is obtained from Eqs. (67) and (68) as follows:

$$\Delta C_{i, j} = \left\{ \int_{\text{element}} \int_{\ell} \left[h_{i, \ell} + \{x - x(\ell)\} \alpha_{i, \ell} \right] \left[\frac{\partial f(\ell, x, s)}{\partial x} + \frac{i\omega}{V} f(\ell, x, s) \right] dx ds \right\} \frac{\Delta \phi_{j, \ell}}{V} \quad (72)$$

Under the assumption that the velocity potential is constant over the rectangle and that the point l is at its center, the contribution to $C_{i,j}$ for the surface elements becomes

$$\Delta C_{i,j} = -A(l) \left\{ \alpha_{i,l} - \frac{i\omega}{V} h_{i,l} \right\} \frac{\Delta \phi_{j,l}}{V} \quad (73)$$

The velocity potential on each element in the wake is given by Eq. (70). The strength of the lifting line at the leading edge of the wake is thus equal to the velocity potential in the first element as follows:

$$\Delta \phi\{x_{FOR}(l^*), s\} = \Delta \phi(l^*) \exp \left\{ -\frac{i\omega}{V} [x_{FOR}(l^*) - x(l^*) + \frac{1}{2} \Delta x(l^*)] \right\} \quad (74)$$

and the contribution to $C_{i,j}$ is

$$\begin{aligned} \Delta C_{i,j} = \Delta s(l^*) \{ h_{i,l^*} + [x_{FOR}(l^*) - x(l^*)] \alpha_{i,l} \} \\ \times \frac{\Delta \phi_{i,l^*}}{V} \exp \left\{ -\frac{i\omega}{V} [x_{FOR}(l^*) - x(l^*) + \frac{1}{2} \Delta x(l^*)] \right\} \end{aligned} \quad (75)$$

where $x_{FOR}(l^*)$ is the x-coordinate of the leading edge of the wake strip, and $\Delta x(l^*)$ is the chord of the first rectangular element in the wake, as shown in Fig. 3. If the wake is terminated at a finite distance (as in Fig. 3), there is a lift line in the wake which has negligible effect and is therefore ignored.

Flutter airforce matrix for zero pressure case.— The proper interpretation of the pressures in the wake is open to question when constant potential elements are used. No such questions arise, however, when the zero pressure element is used. Here the velocity potential is assumed to vary across a rectangular element in such a way that the pressure is zero except under lift lines at forward and rearward edges. Thus, in a region influenced by the velocity potential $\Delta \phi(l)$, the shape factor is expressed as

$$f(\ell, x, s) = \exp \left\{ -\frac{i\omega}{V} [x - x(\ell)] \right\} \quad (76)$$

The contribution to the flutter airforce matrix in this case is obtained by applying Eq. (72) and using the shape factor $f(\ell, x', s)$ varying as in Eq. (76).

$$\begin{aligned} \Delta C_{i,j} = \Delta s(\ell) & \left\{ [h_{i,\ell} + \{x_{FOR}(\ell) - x(\ell)\} \alpha_{i,\ell}] \right. \\ & \times \exp \left[-\frac{i\omega}{V} \{x_{FOR}(\ell) - x(\ell)\} \right] \\ & - [h_{i,\ell} + \{x_{AFT}(\ell) - x(\ell)\} \alpha_{i,\ell}] \\ & \times \exp \left[-\frac{i\omega}{V} \{x_{AFT}(\ell) - x(\ell)\} \right] \left. \right\} \frac{\Delta \phi_{i,\ell}}{V} \end{aligned} \quad (77)$$

The lift at the leading edge of the wake strip is similar to the lift at the leading edge of a rectangular region in Eq. (77), so that

$$\begin{aligned} \Delta C_{i,j} = \Delta s(\ell^*) & [h_{i,\ell^*} + \{x_{FOR}(\ell^*) - x(\ell^*)\} \alpha_{i,\ell^*}] \\ & \times \exp \left[-\frac{i\omega}{V} \{x_{FOR}(\ell^*) - x(\ell^*)\} \right] \frac{\Delta \phi_{i,\ell^*}}{V} \end{aligned} \quad (78)$$

COMPUTED RESULTS AND DISCUSSIONS

Computer Program

A computer program was written in FORTRAN IV language to perform the calculations outlined in the section on METHOD OF SOLUTION. The description of the program, input instructions, and sample problems along with the listing of the program are included in Appendix A.

To date, four versions of aerodynamic elements all using rectangular elements have been formulated. They are summarized as follows:

<u>Subroutines</u>	<u>Type of Elements</u>
ACON5, ACON6 and CCON5, CCON6	Zero Order Constant Potential (ZOCP) Rectangular Elements
ACON7, ACON8 and CCON5, CCON7	First Order Constant Potential (FOCP) Rectangular Elements
ACON11, ACON12 and CCON11, CCON12	First Order Zero Pressure (FOZP) Rectangular Elements
ACON3, ACON4 and CCON11, CCON12	In-Plane Steady Supersonic (IPSS) Rectangular Elements

Scope of Computations

A total of eight planforms were considered and are shown in Figures 6 to 13 with the details of their geometry. Table I gives the details of the cases for which calculations were made. Subsonic calculations including cases 1 through 3 are presented in reference 3.

Discretization of Surfaces

The breaking up or division of a surface into rectangular elements was accomplished by defining a chordwise strip of wing, locating its centerline, dividing the length into a specified number of chordwise elements, and laying these out by shifting one quarter of the chord of an element back from the leading edge. Collocation points were then located at their centers. These were extended into the wake with approximately equal chordwise dimensions and terminated about five to ten wing chord lengths back. This method of locating elements is illustrated in Fig. 14 for a rectangular wing and is compared with a similar wing divided up into winglets with a lift line at the quarter chord of each and a collocation point at the three-quarter chord as employed by Hedman (ref. 2).

Only the half wing is shown divided up in Fig. 14, because the symmetry logic of the computer program takes care of the effects of the other half. Other planforms used in the present calculations also have one or two planes of symmetry and these symmetries were used whenever applicable in an attempt to save computational effort.

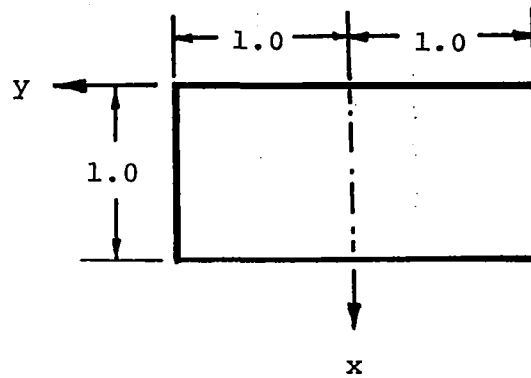


Fig. 6 Rectangular Wing A.R. = 2 (Planform No. 1)

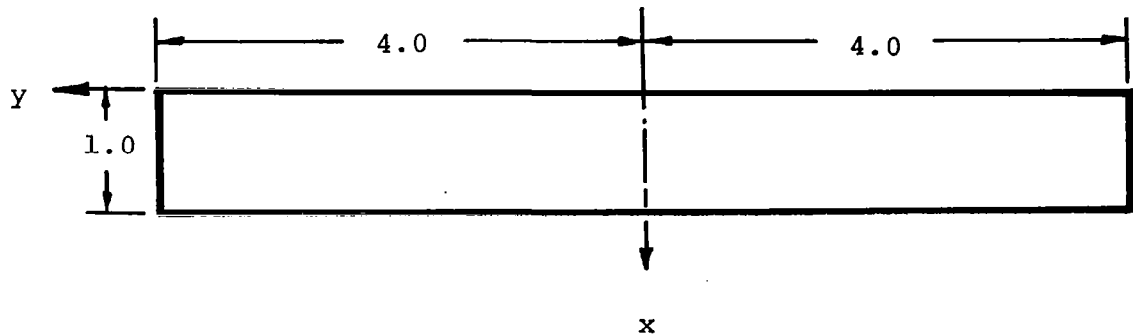


Fig. 7 Rectangular Wing A.R. = 8 (Planform No. 2)

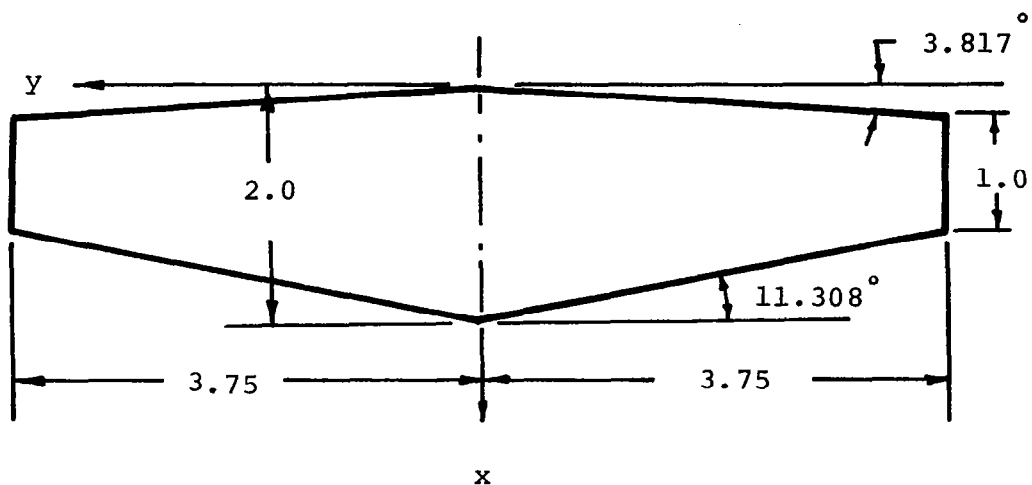


Fig. 8 Tapered Wing A.R. = 5.0 (Planform No. 3)

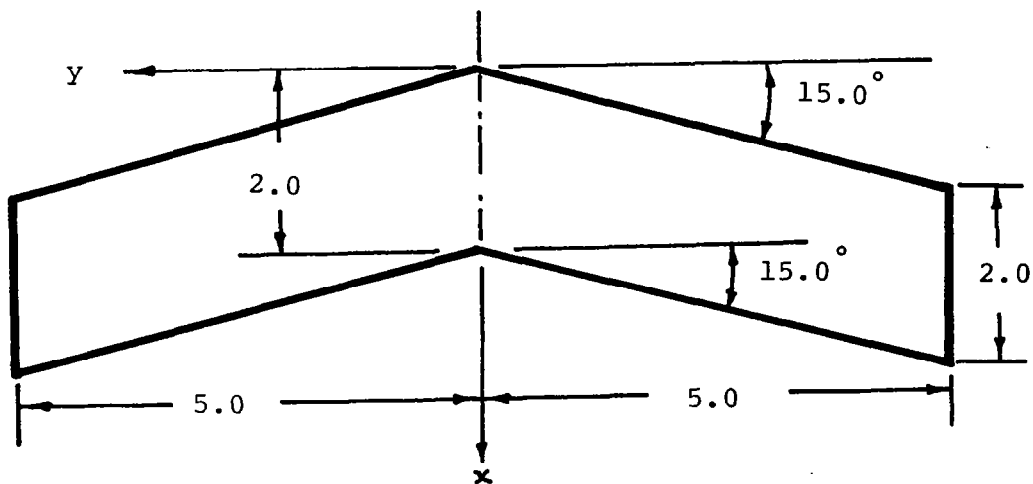


Fig. 9 Swept Wing A.R. = 5.0 (Planform No. 4)

Control Surface chord = $.712 \times \text{Local semichord}$
 Taper Ratio = $.2378$

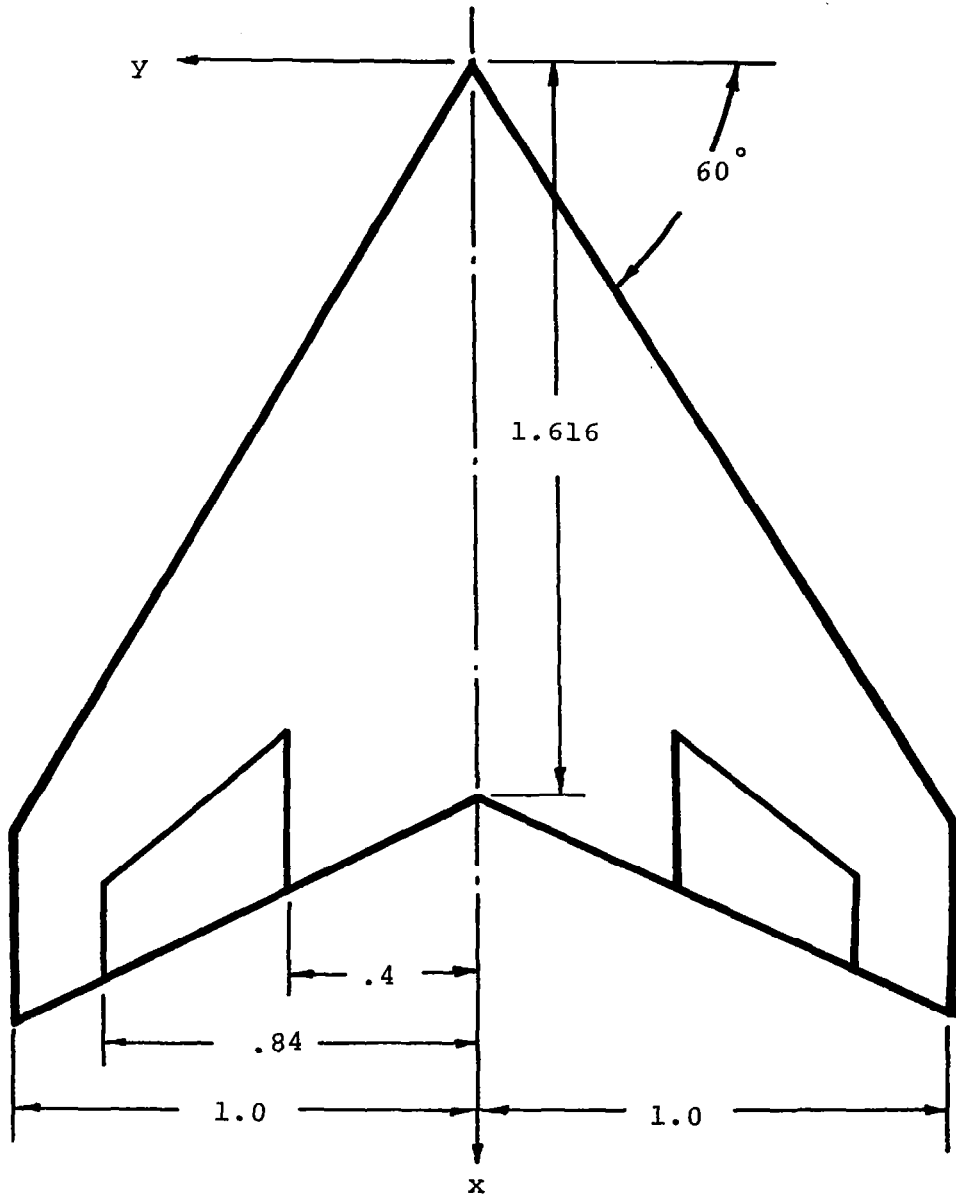


Fig. 10. Swept Wing with Partial-Span Flaps
 A.R. = 2 (Planform No. 5)

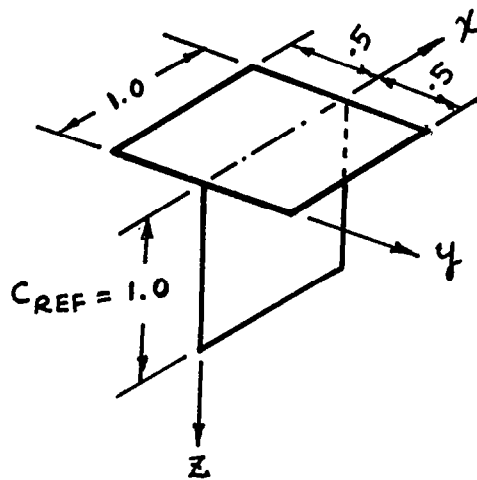


Fig. 11 Rectangular T-tail (Planform No. 6)

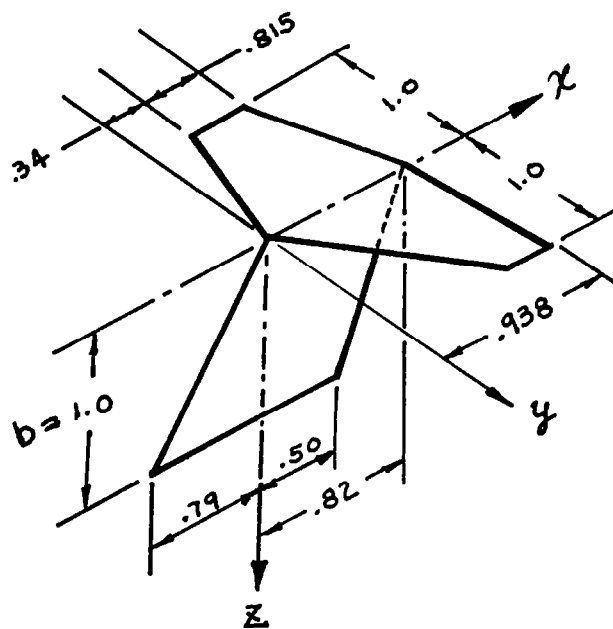
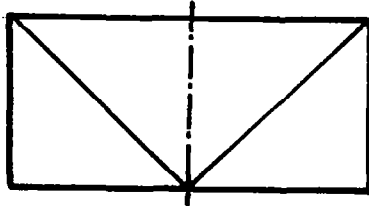
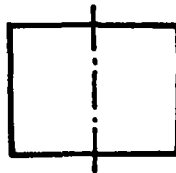


Fig. 12 Stark's T-tail (Planform No. 7)



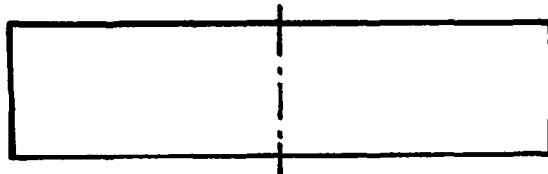
<u>Mach No.</u>	<u>Aspect Ratio</u>
1.2	3.015
1.4	2.041
1.6	1.613
1.8	1.336



Mach No. = 1.3
Aspect Ratio = 1.2039



Mach No. = 1.3
Aspect Ratio = 2.0



Mach No. = 1.3
Aspect Ratio = 4.0

Fig. 13 Rectangular Wings for Supersonic Calculations
(Planform No.8)

Table I
Calculations Performed

Case No.	Planform Number	Mach Number	Reduced Frequency	Derivatives	Remarks
1	1. Rectangular Wing A.R. = 2	0.9	0.5	$C_{L\alpha}, C_{M\alpha}$	Evaluation of the effective wake length
2	1. Rectangular Wing A.R. = 2	0 0.8, 0.9	0, .2, .4, .6, .8, .9 0, .15, .25, .35, .5	$C_{L\alpha}, C_{M\alpha}$	Comparison with Kernel function method and Doublet Lattice method
3	2. Rectangular Wing A.R. = 8	0	0	C_{ℓ}, C_m	Strip width variation, and Comparison with Kernel function method
4	3. Tapered Wing, A.R. = 5, Taper Ratio = .5 Sweep angle = 3.817 deg	.15	0	C_{ℓ}, C_m C_{PM}, C_L	Comparison with tabulation by Thomas and Wang (ref. 26)
	4. Untapered Wing A.R. = 5 Sweep angle = 15.0 deg	.12	0	C_{PM}, C_{BM} BMCP, PMCP See "Results and Discussion, Case 4"	
5	5. Swept Wing with Partial span flap A.R. = 2, L.E. Sweep angle = 60 deg	0, .7, 0.8, .9	0.5	$C_{i,j}$ (See Appendix A)	Comparison with the results reported by Stark (ref. 24)
6	6. Rectangular T-tail	0, .25	0.2	$C_{L\alpha}, C_{M\alpha}$	Comparison with Clevenson & Leadbetter (ref. 28) and Kalman (ref. 23) et. al.
	7. Stark's T-tail	0.8	0.3, .45	$Q_{m,n}$	Comparison with Stark's results (ref. 24)

Table I Continued

Calculation Performed

Case No.	Planform Number	Mach Number	Reduced Frequency	Derivatives	Remarks
7	8. Rectangular Wings with various Aspect Ratios	1.2, 1.4, 1.6, 1.8	0	$C_{L\alpha}, C_{M\alpha}$ (See "Results and Discussion, Case 7)	Comparison with Ref. 30
	8. Rectangular Wings with Various Aspect Ratios	1.3	0	$C_{L\alpha}, C_{M\alpha}$	Comparsion with Nelson, et al. (ref. 31)

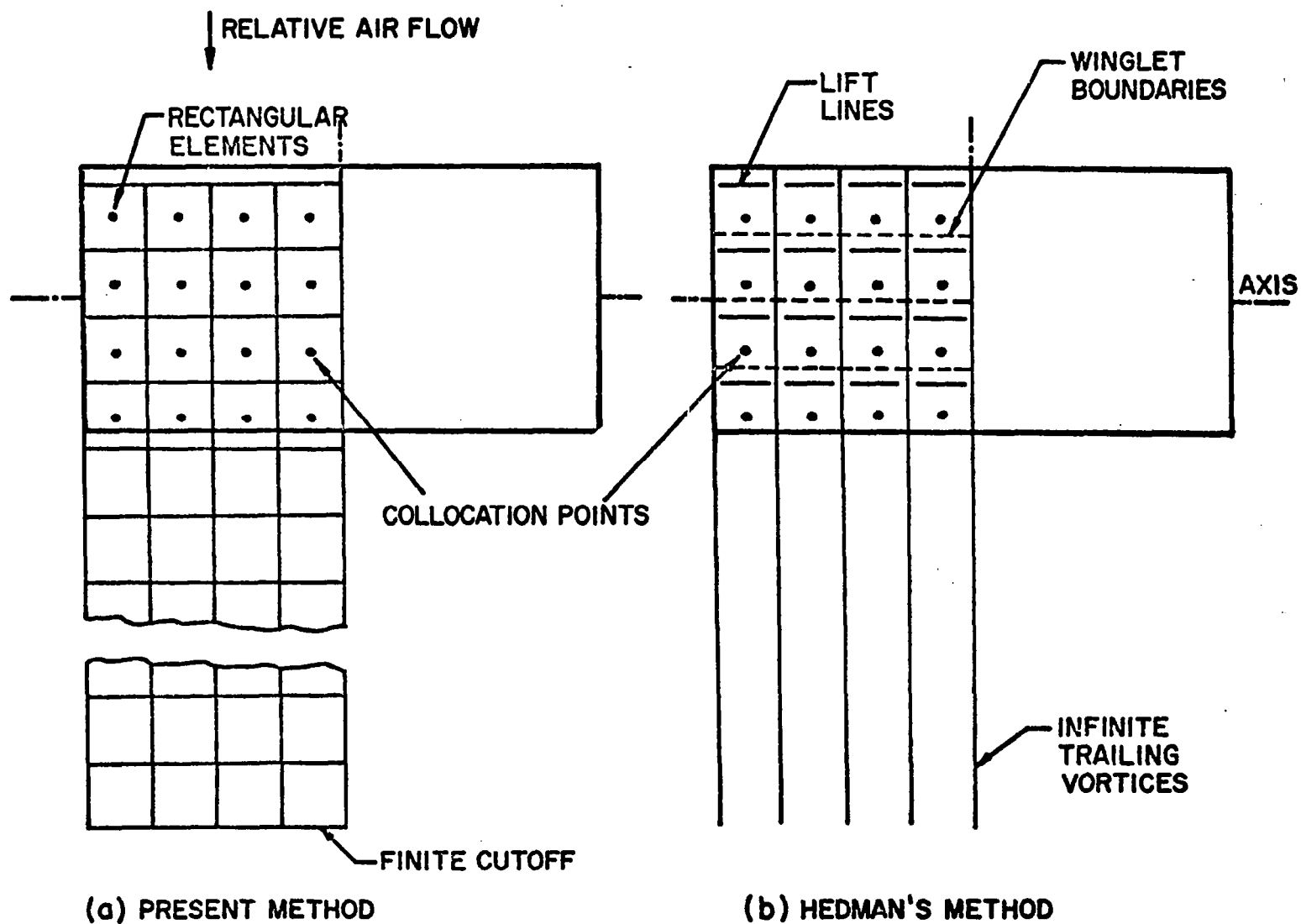


Fig. 14. Comparison of Four-by-Four Arrays,
Present Method and Hedman's (ref. 2)

Results and Discussions

Case 1: convergence of the results with the wake length.- Case 1 consisted of a check into the convergence of the results when the number of chord lengths included in the wake is varied. This is expressed as the ratio F which is equal to the length of the wake divided by the chord. Results shown in Table II were obtained for a four-by-four arrangement on a rectangular wing (planform No. 1) using first order zero pressure rectangular elements. The reduced frequency was 0.5, and the Mach number was 0.9. (Reduced frequency is defined as $\omega b/V$, where b is the half chord of the wing).

TABLE II

Convergence of Calculated Results for Aspect Ratio
Two Rectangular Wings, Oscillating about Mid-Chord at Reduced Frequency of
0.5 and Mach Number 0.9, as Ratio Wake Length/Chord ($=F$) is Changed

Ratio F	Lift Derivative		Moment Derivative	
	Real	Imaginary	Real	Imaginary
1	3.5454	0.5387	.6146	-1.8636
5	3.5622	0.5444	.5986	-1.8542
10	3.5622	0.5440	.5992	-1.8542
20	3.5623	0.5435	.5996	-1.8542

In the remaining calculations, F was taken equal to ten (10) which is well within one percent error according to Table II.

Case 2: rectangular wing pitching about midchord.- Case 2 was concerned with calculations on a rectangular wing (planform No. 1) to compare with two different references. First, calculations were made to compare with the results of the kernel function method reported by Runyan and Woolston (ref. 22) for the zero Mach number case and for reduced frequencies ranging up to 0.9. Second, calculations were made to compare with the results of the doublet lattice method reported by Kalman, Rodden, and Giesing (ref. 23) for Mach numbers of 0.8 and 0.9, and for reduced frequencies up to 0.5. These results have been reported in reference 3.

Using the key to the symbols given in Fig. 15, the results of these comparisons can be seen in Figs. 15 to 18 for comparison with the kernel function method and in Figs. 19 to 22 for comparison with the doublet lattice method. In the first comparison, generally fair agreement is noted except that the real part of the moment derivative does not agree well at zero frequency. Such a disagreement was noted earlier (ref. 1) when it was seen that the kernel function method and the downwash-velocity potential method gave different centers of pressure on a high aspect ratio wing. Otherwise, agreement with the first order zero pressure elements is generally high. The constant potential elements have the next highest agreement and the zero order calculations appear to have least agreement. At zero frequency, these three methods are of course identical. Improved agreement is also noted with the eight-by-eight arrangement as compared to the four-by-four arrangement. This indicates convergence as the number of collocation points (N_{RP}) is increased. One result by Stark (ref. 24) is shown for comparison and is seen to be in very close agreement with the results of Runyan and Woolston (ref. 22). In the second comparison, agreement at zero frequency is now good. This should be expected considering that the doublet lattice method gives the Hedman results at zero frequency. Agreement at a reduced frequency of 0.5 and a Mach number of 0.9 is good when first order zero pressure elements are used in an eight-by-eight array. Results given by Laschka (ref. 25) and one result by Stark (ref. 24) are also shown.

Definitions of the derivatives shown in the figures are as follows:

$$\text{Reduced Frequency} = K_r = \frac{wC}{2V}$$

$$\text{Lift Derivative} = \frac{\partial L}{\partial \alpha} \div qS$$

$$\text{Moment Derivative} = \frac{\partial M}{\partial \alpha} \div \frac{1}{2} qSc$$

where L is the lift in the sense of the negative n -axis, α is the angle of rotation about the mid chord, q is the dynamic pressure, S is the wing area, M is the moment about the mid chord line, and c is the chord. Both α and M are positive in the same sense.

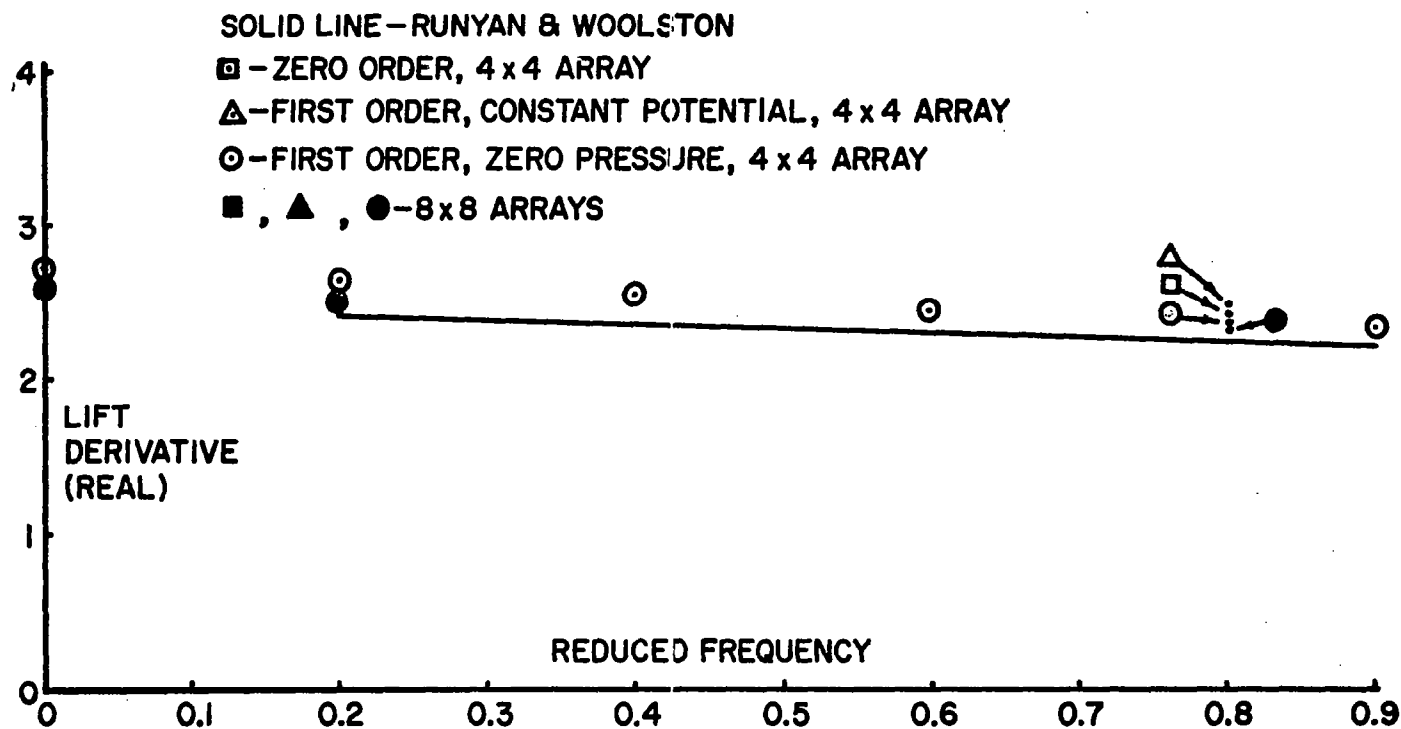


Fig. 15. Lift Derivative (Real Part) for Aspect Ratio Two Rectangular Wing Rotating about Mid-Chord at Zero Mach Number

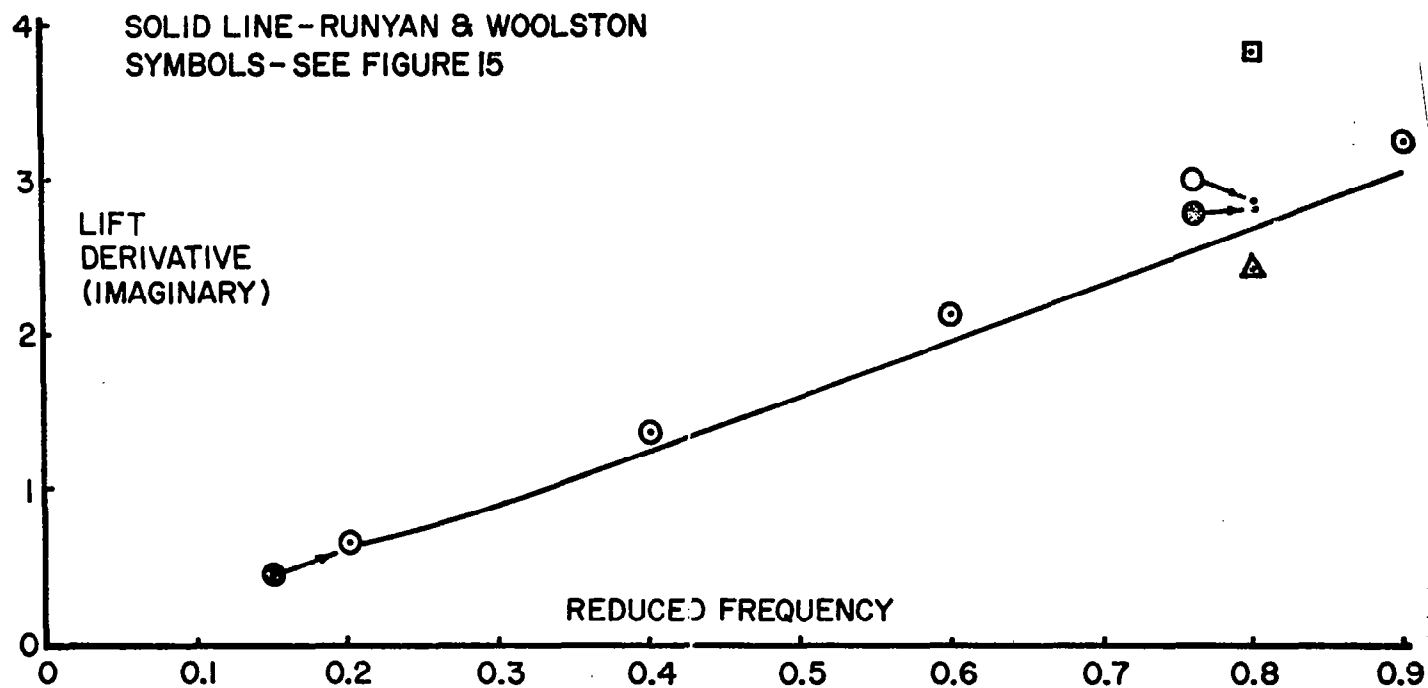


Fig. 16. Lift Derivative (Imaginary Part) for Aspect Ratio Two Rectangular Wing Rotating about Mid-Chord at Zero Mach Number

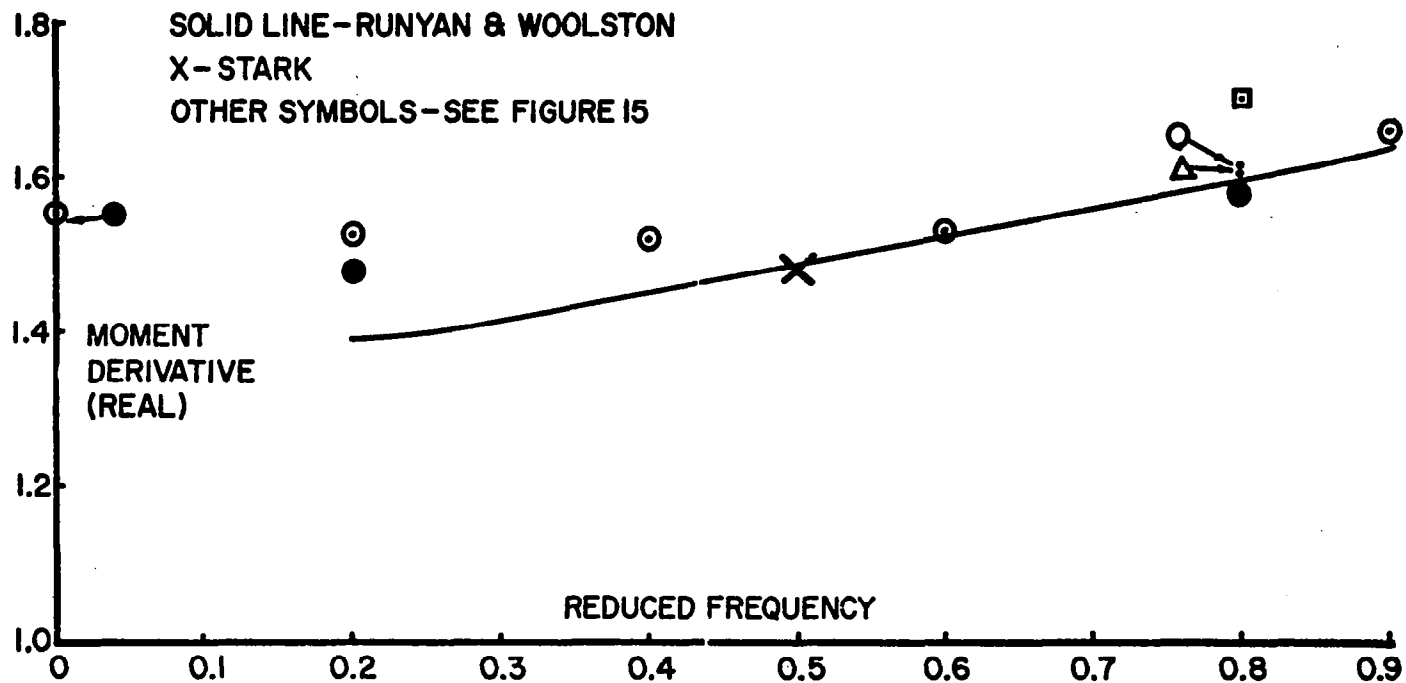


Fig. 17. Moment Derivative (Real Part) for Aspect Ratio Two Rectangular Wing Rotating about Mid-Chord at Zero Mach Number

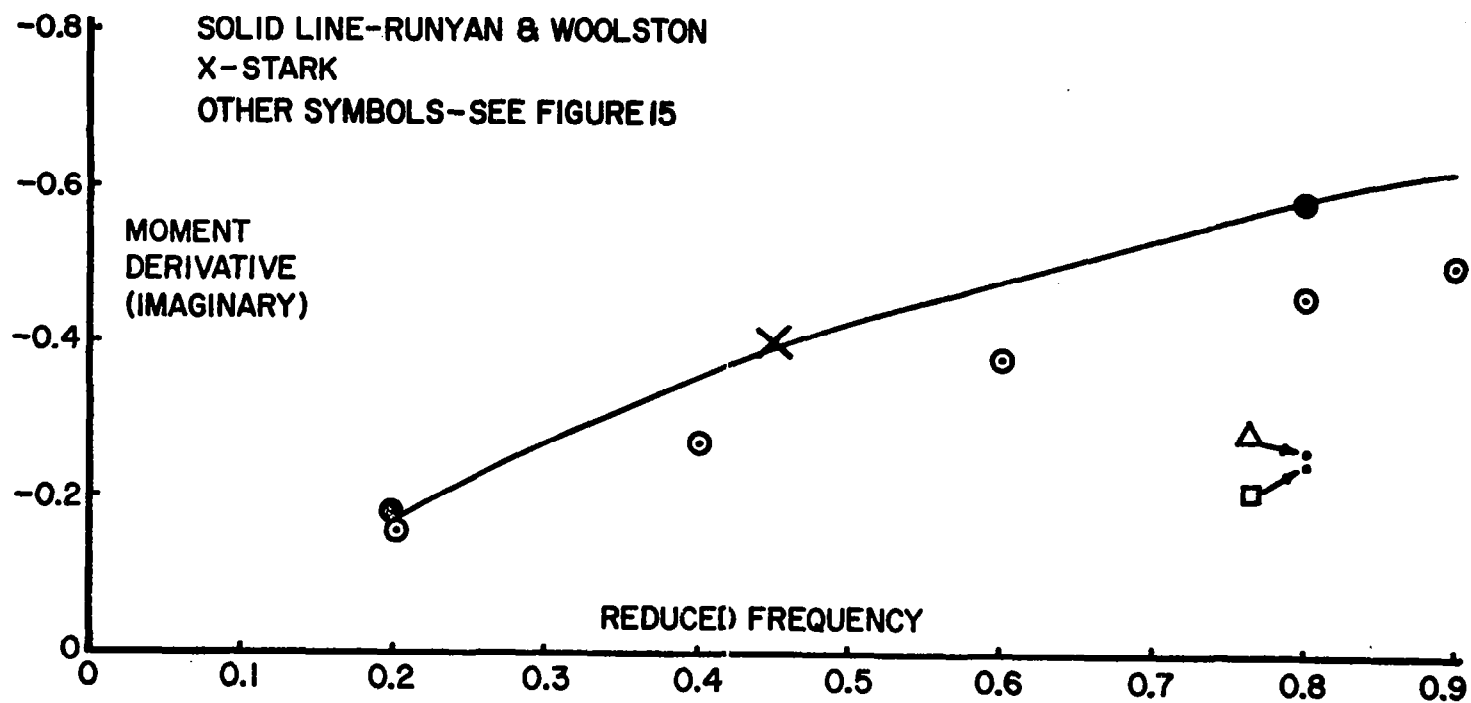


Fig. 18 Moment Derivative (Imaginary Part) for Aspect Ratio Two Rectangular Wing Rotating about Mid-Chord at Zero Mach Number.

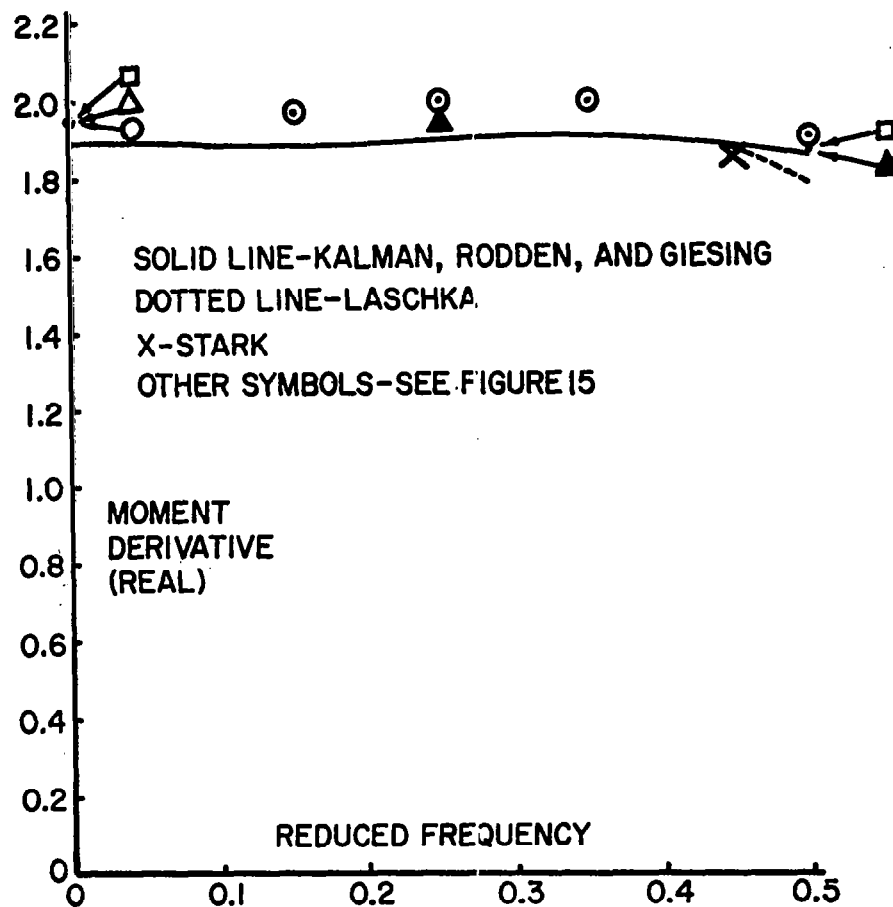


Fig. 19 Moment Derivative (Real Part) for Aspect Ratio Two Rectangular Wing Rotating about Mid-Chord at Mach Number 0.8.

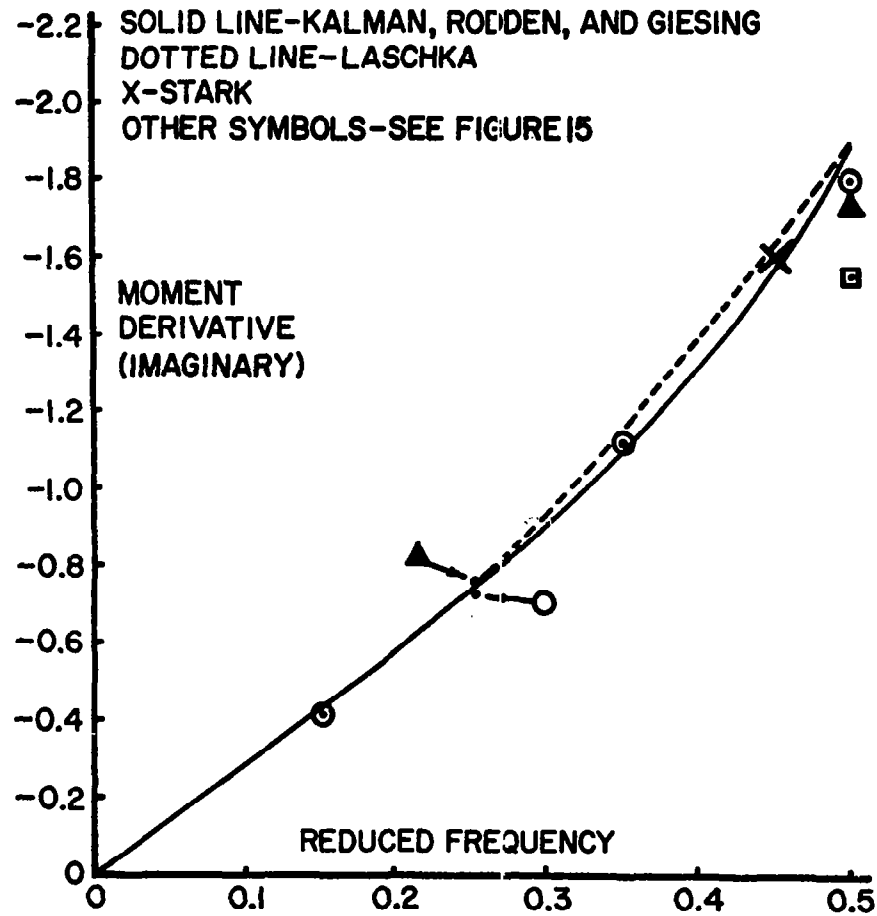


Fig. 20 Moment Derivative (Imaginary Part) for Aspect Ratio Two Rectangular Wing Rotating about Mid-Chord at Mach Number 0.8.

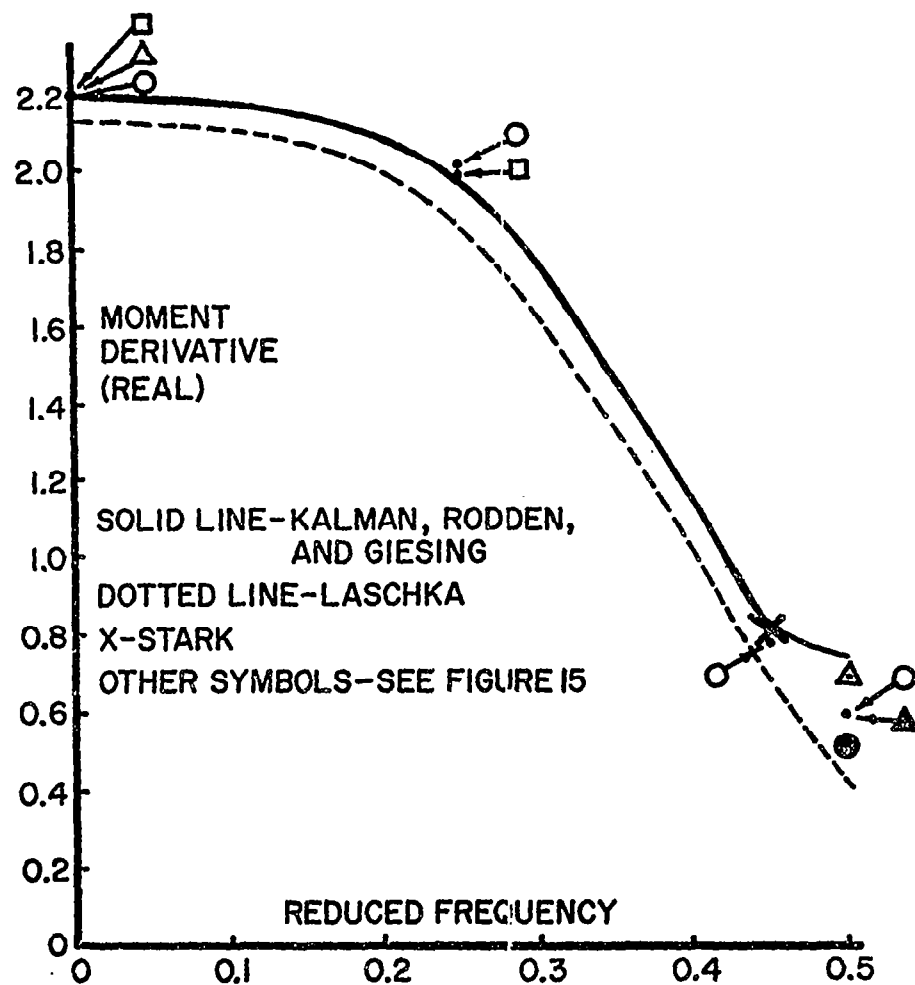


Fig. 21.. Moment Derivative (Real Part) for Aspect Ratio Two Rectangular Wing Rotating about Mid-Chord at Mach Number 0.9.

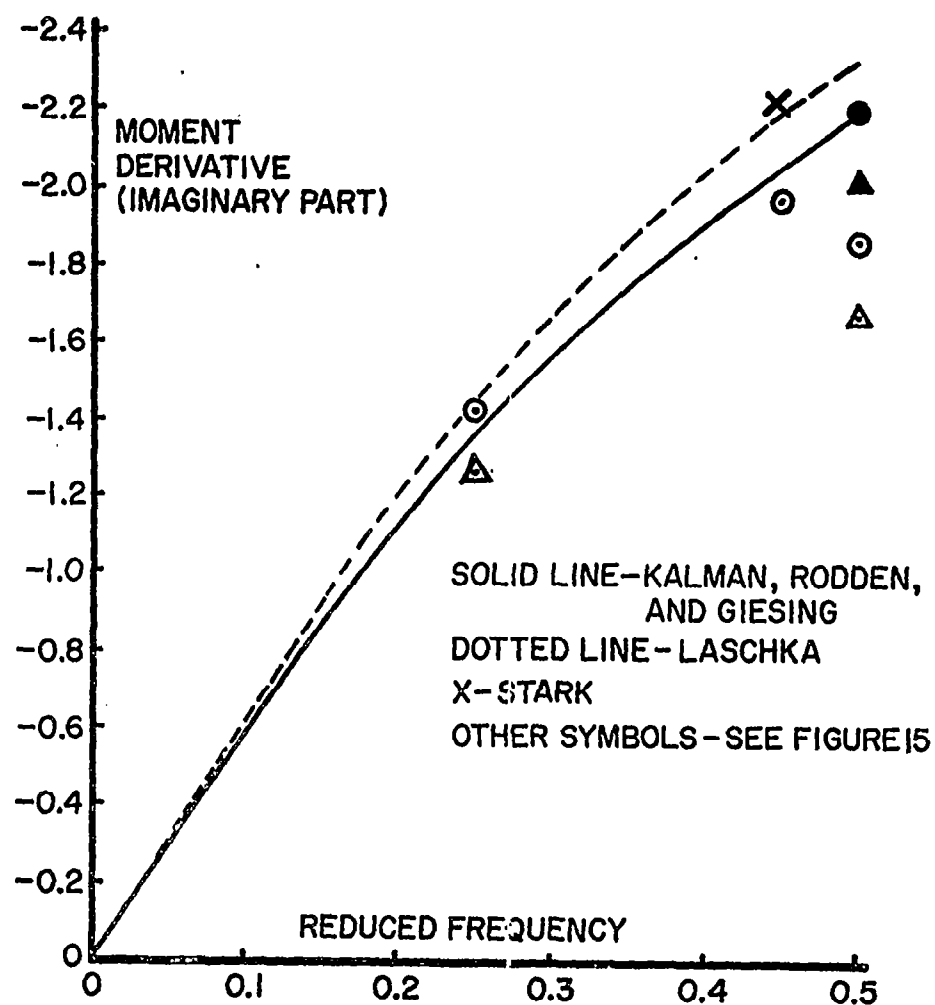


Fig. 22. Moment Derivative (Imaginary Part) for Aspect Ratio Two Rectangular Wing Rotating about Mid-Chord at Mach Number 0.9.

Case 3: lift distribution of a rectangular wing; subsonic steady.

Sectional lift slope, aerodynamic center total lift, and moment derivatives for an aspect ratio eight rectangular wing (planform No. 2) were evaluated in this case. In order to examine the effect of the strip width variations, one set of runs was made with an evenly spaced strip width as shown in Fig. 23. Another set of runs was made with the arrangement having reduced strip width towards the tip as shown in Fig. 24. The lift distributions and aerodynamic centers are plotted in Fig. 25 and Fig. 26, respectively, with results of the kernel function method for comparison (obtained by private communication from E. C. Yates, NASA Langley Research Center),

The sectional lift slope distribution in Fig. 25 shows that the present method gives lower values than the kernel function values, although the trend reverses towards the tip. Improved agreement was also noticed towards the tip when the arrangement of reduced strip width towards the tip, sketched in Fig. 24, was used. The aerodynamic centers calculated by the kernel function method using polynomial pressure modes are in closer agreement with the present results than those obtained by the kernel function method using the Glauert-Birnbaum series. This is shown in Fig. 25 with numerical data in Table III.

Case 4: tapered and swept wings; subsonic steady.- In this case, calculations were performed at the request of Langan and Wang of NSRDC (ref. 26) for the comparison of various numerical lifting surface theories with experimental results. Calculations were made for a tapered wing of aspect ratio five (planform No. 3) and for a swept wing of the same aspect ratio with no taper (planform No. 4). The arrangements of the aerodynamic elements used for these calculations are shown in Figs. 27 and 28.

Figures 29 and 30, and Tables IV and V were supplied by Langan and Wang (ref. 26). Tables IV and V present the wing loading characteristics for the tapered wing and the swept wing as computed by 15 programs and as obtained from the experimental results. The programs are listed in Tables IV and V and are identified by the names of those who contributed the data. Mach number for which the calculations were made, lift coefficient C_L , pitching moment center of pressure (PMCP) measured from the wing apex divided by the

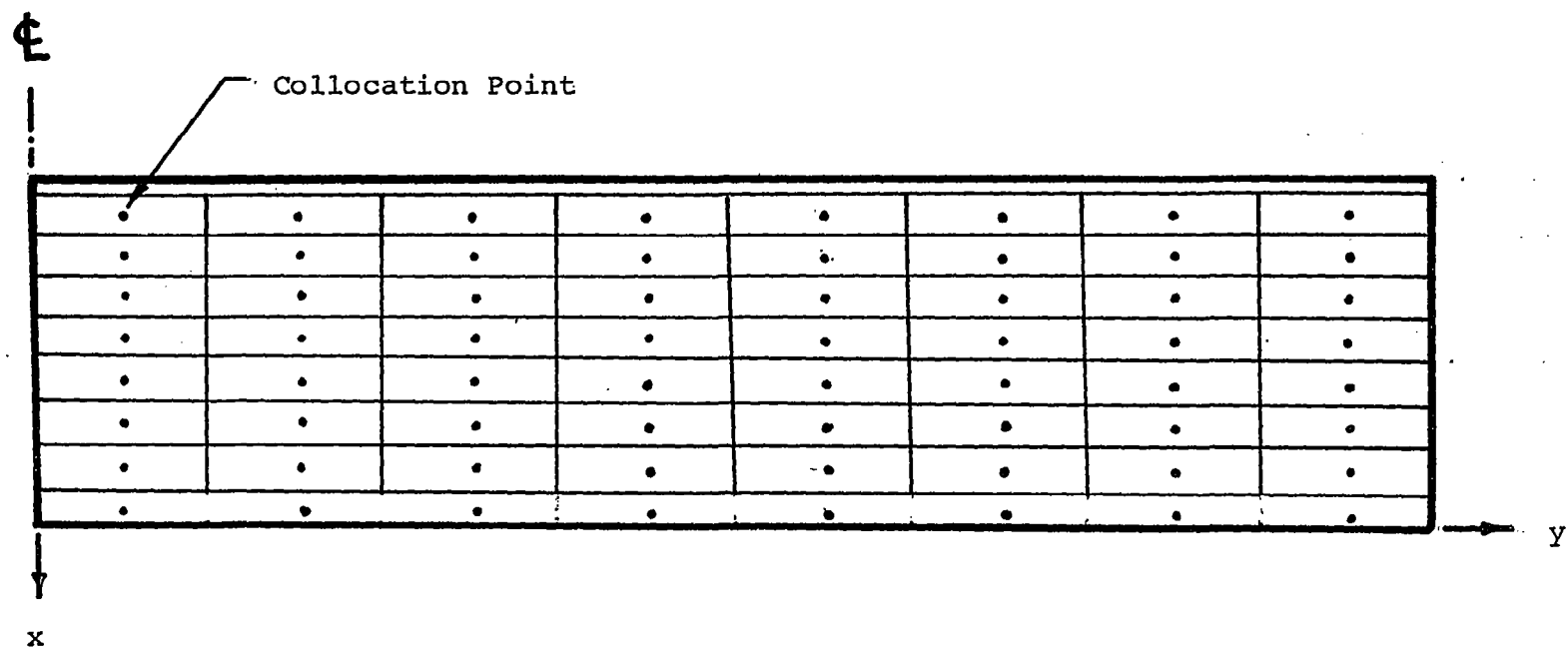


Fig. 23 Planform for Aspect Ratio 8 Rectangular Wing with 8×8 Arrays of Points, Evenly Spaced.

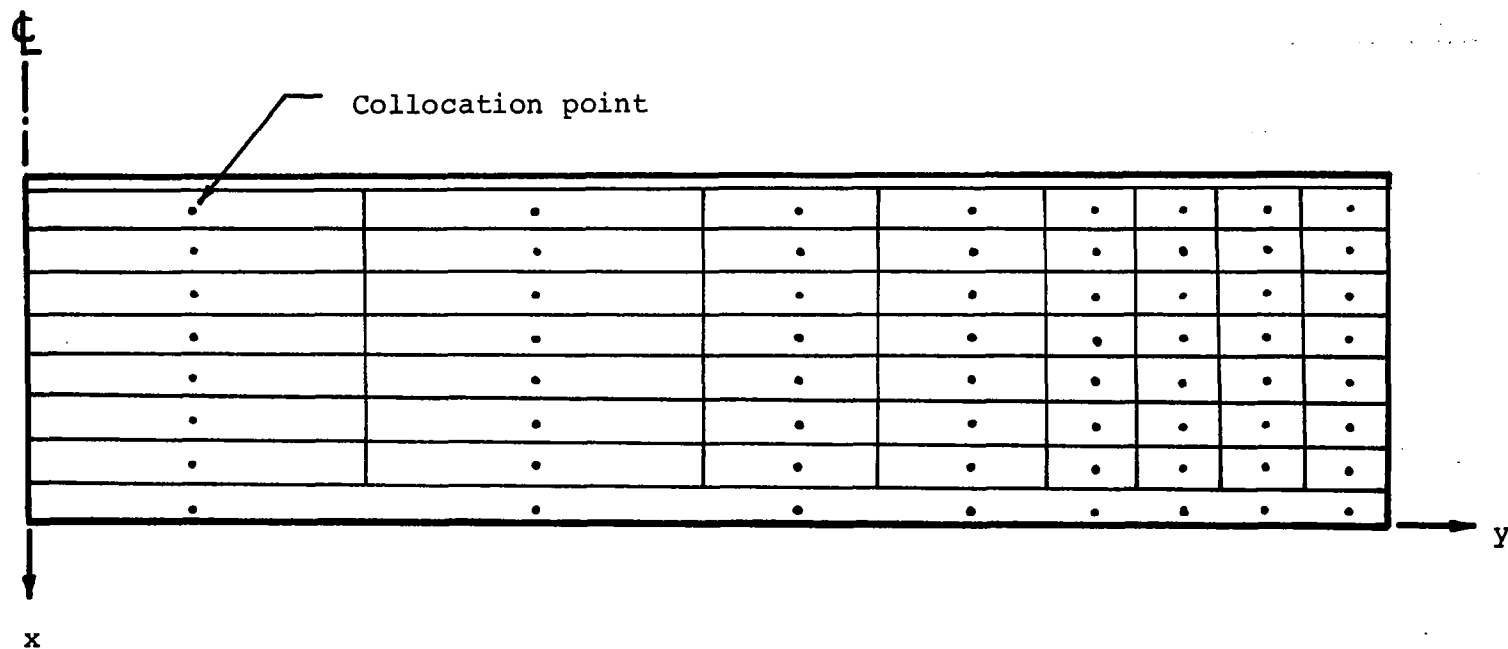


Fig. 24 Planform for Aspect Ratio 8 Rectangular Wing with 8×8 Arrays of Elements and Strip Width Reduced Towards Tip.

- Kernel Function Method - 40 Stations (4×4), Glauert Birnbaum Series
- First Order, Zero Pressure, 8×8 Array, Evenly Spaced Strips
- △— First Order, Zero Pressure, 8×8 Array, Reduced Strip Width Towards the Tip
- Kernel Function Method - (6×6), Langley Kernel Function Program Using Polynomial Pressure Modes

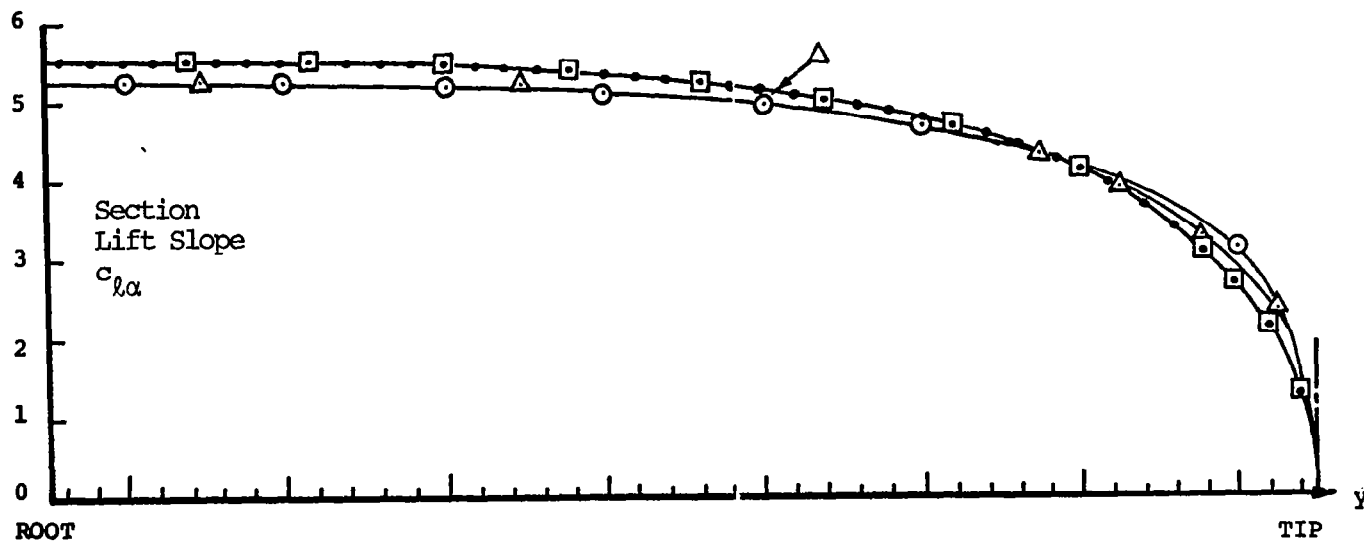


Fig. 25 Comparison of Section Lift Slope For An Aspect Ratio 8 Rectangular Wing
Mach No. = 0, $k = 0$

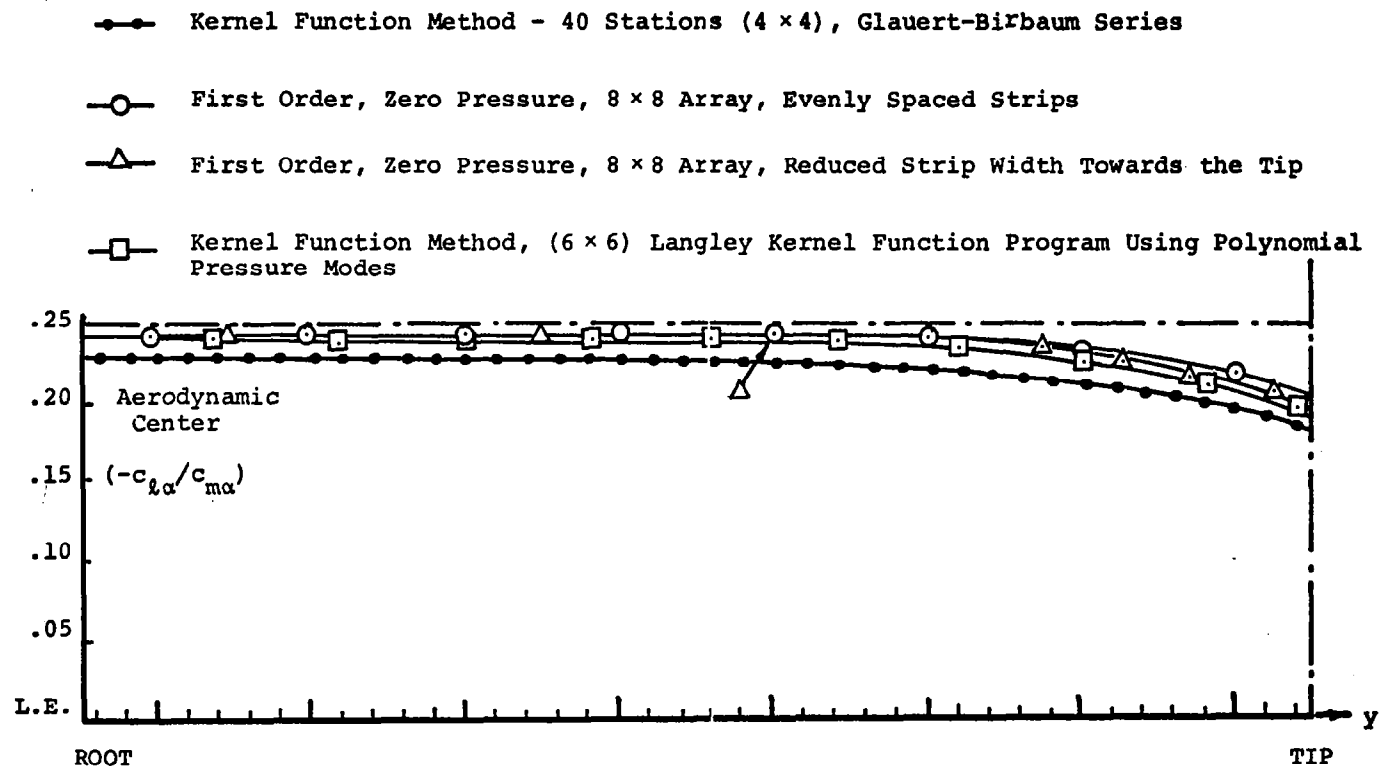


Fig. 26 Comparison of Aerodynamic Center For An Aspect Ratio 8 Rectangular Wing
 Mach No. = 0, $k = 0$

Table III

Sectional Lift Slope and Aerodynamic Centers, Total Lift and Moment for Aspect Ratio 8 Rectangular Wing with the variations in station spacing. Mach number = 0, $K_x = 0$, constant downwash $\alpha = 1.0$

Aerodynamic Element	Strip Spacing	$\eta = \frac{y}{b}$	C_l	C_m	c_m/c_l	C_L	C_M
First Order Zero Press.	Even Spacing (See Fig. 23)	.0625	5.3187	1.3194	0.2481	4.7226	1.1474
		.1875	5.2896	1.3113	0.2479		
		.3125	5.2253	1.2931	0.2475		
		.4375	5.1147	1.2616	0.2467		
		.5625	4.9359	1.2102	0.2452		
		.6875	4.6426	1.1248	0.2423		
		.8125	4.1314	0.9747	0.2359		
		.9375	3.1128	0.6843	0.2198		
		.1250	5.3132	1.3177	0.2480		
First Order Zero Press.	Adjusted spacing with reduced strips towards tip (see Fig. 24)	.3750	5.1936	1.2844	0.2473	4.6898	1.1393
		.5625	4.9559	1.2164	0.2454		
		.6875	4.6588	1.1300	0.2426		
		.78125	4.2873	1.0206	0.2381		
		.84375	3.8688	0.8976	0.2320		
		.90625	3.2858	0.7308	0.2224		
		.96875	2.3371	0.4809	0.2058		

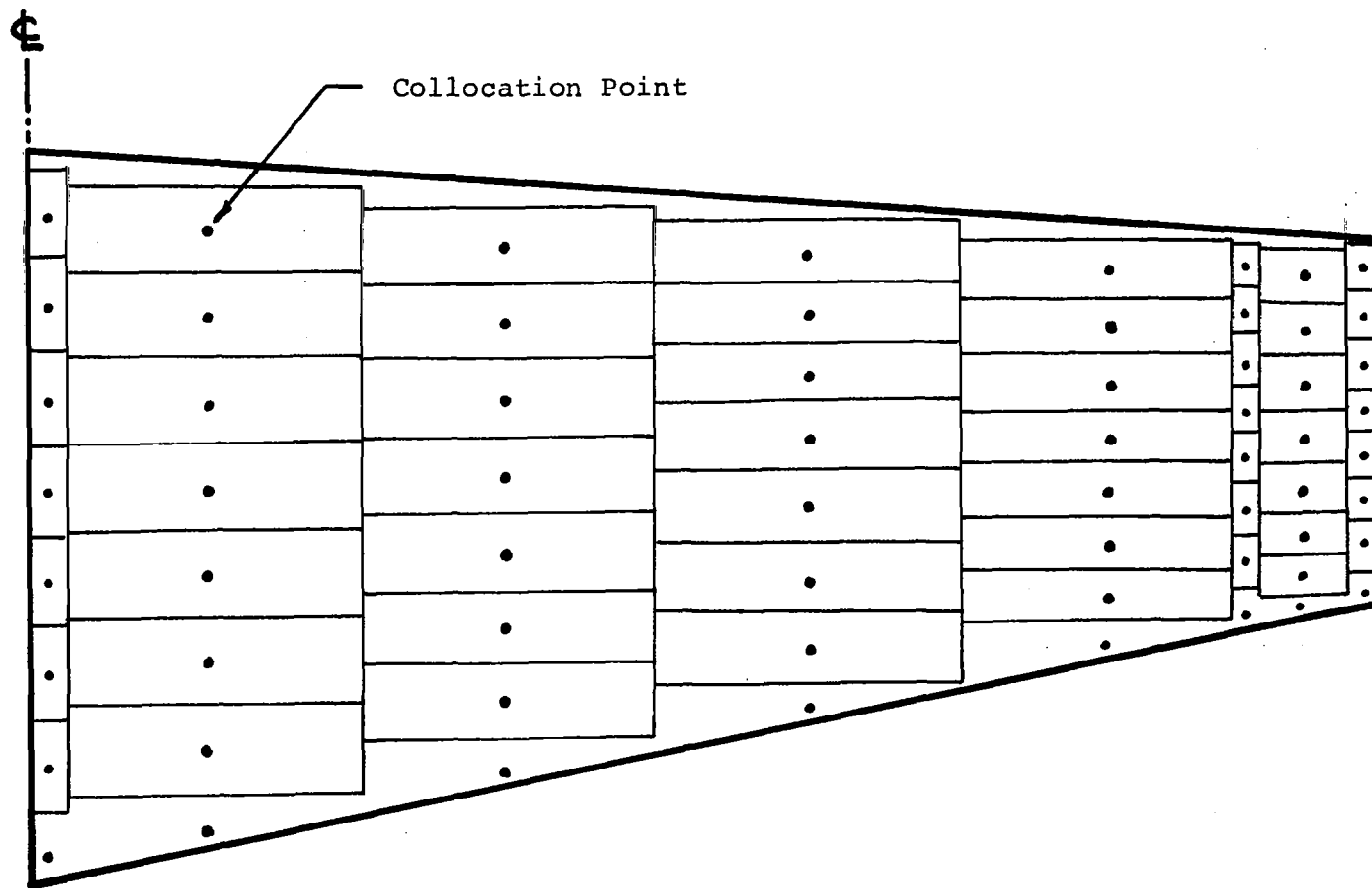


Fig. 27 Arrangement of Aerodynamic Elements for Aspect Ratio 5.
 Tapered Wing (Taper Ratio = 0.5, Leading Edge Sweep Angle = 3.817° ,
 Trailing Edge Sweep Angle = 11.308°)

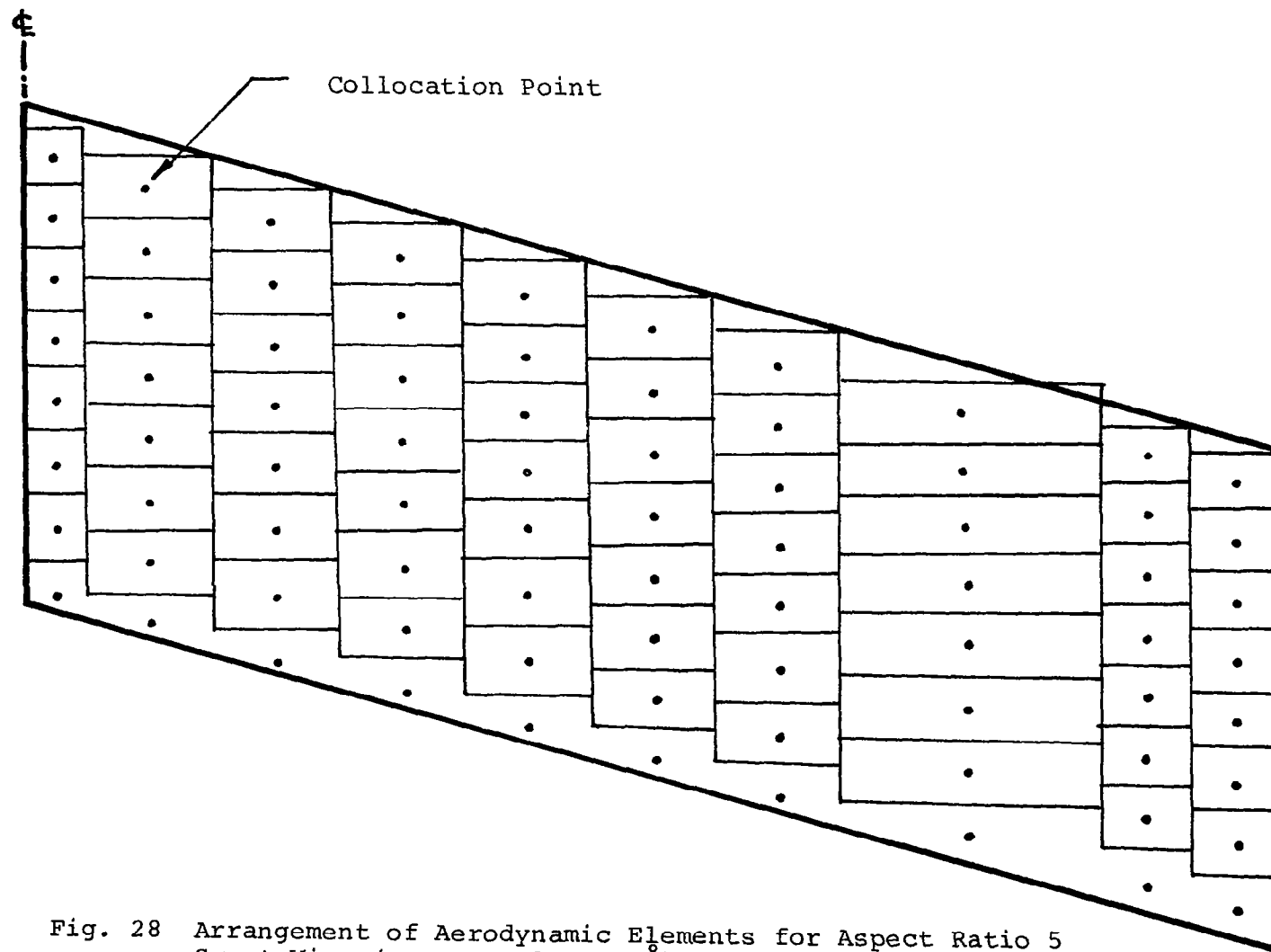


Fig. 28 Arrangement of Aerodynamic Elements for Aspect Ratio 5
Swept Wing (sweep angle = 15°)

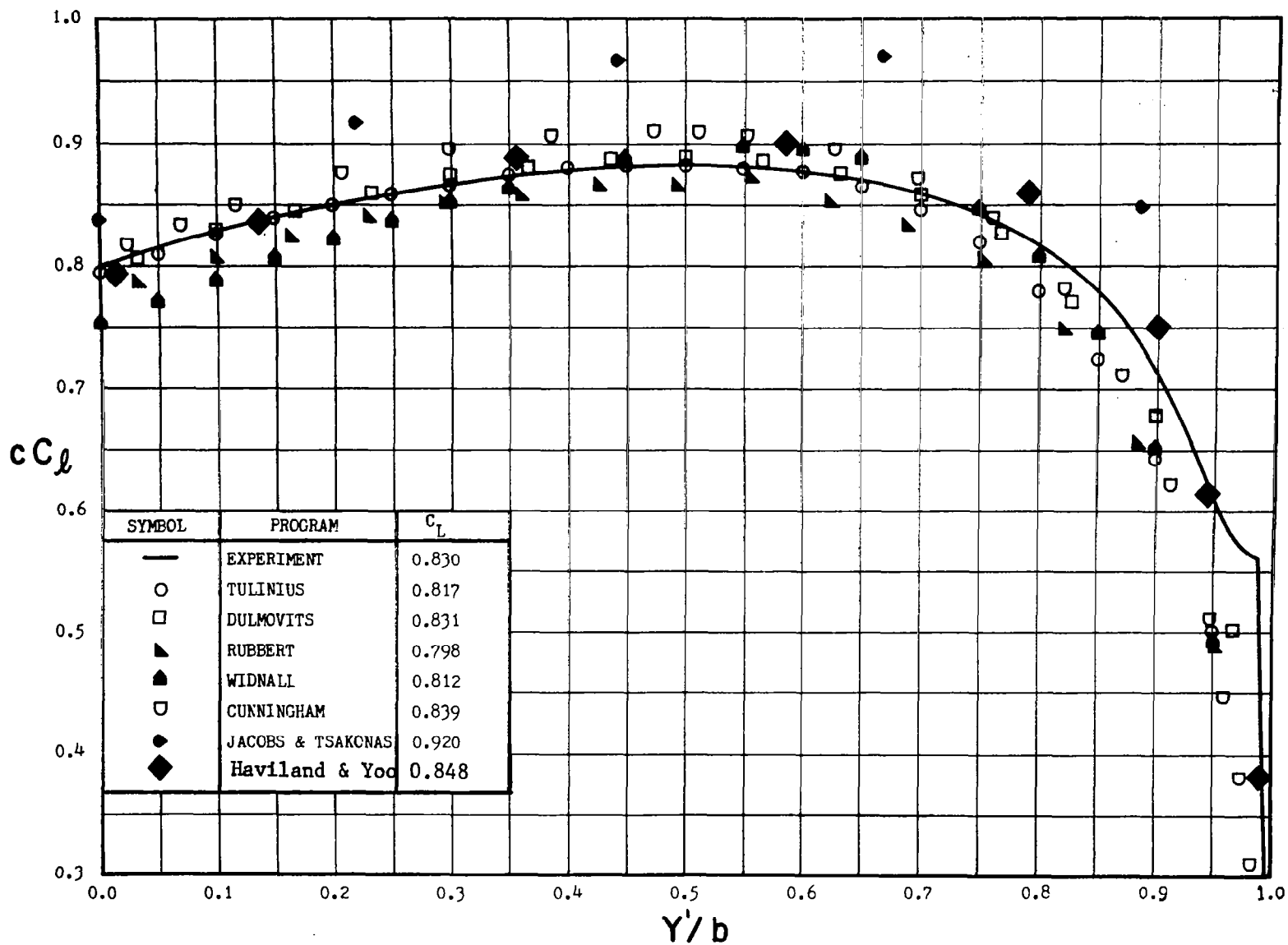


Fig. 29 Spanwise Lift Distribution for Tapered Wing at 11.4° Angle of Attack, From Langan and Wang²⁶

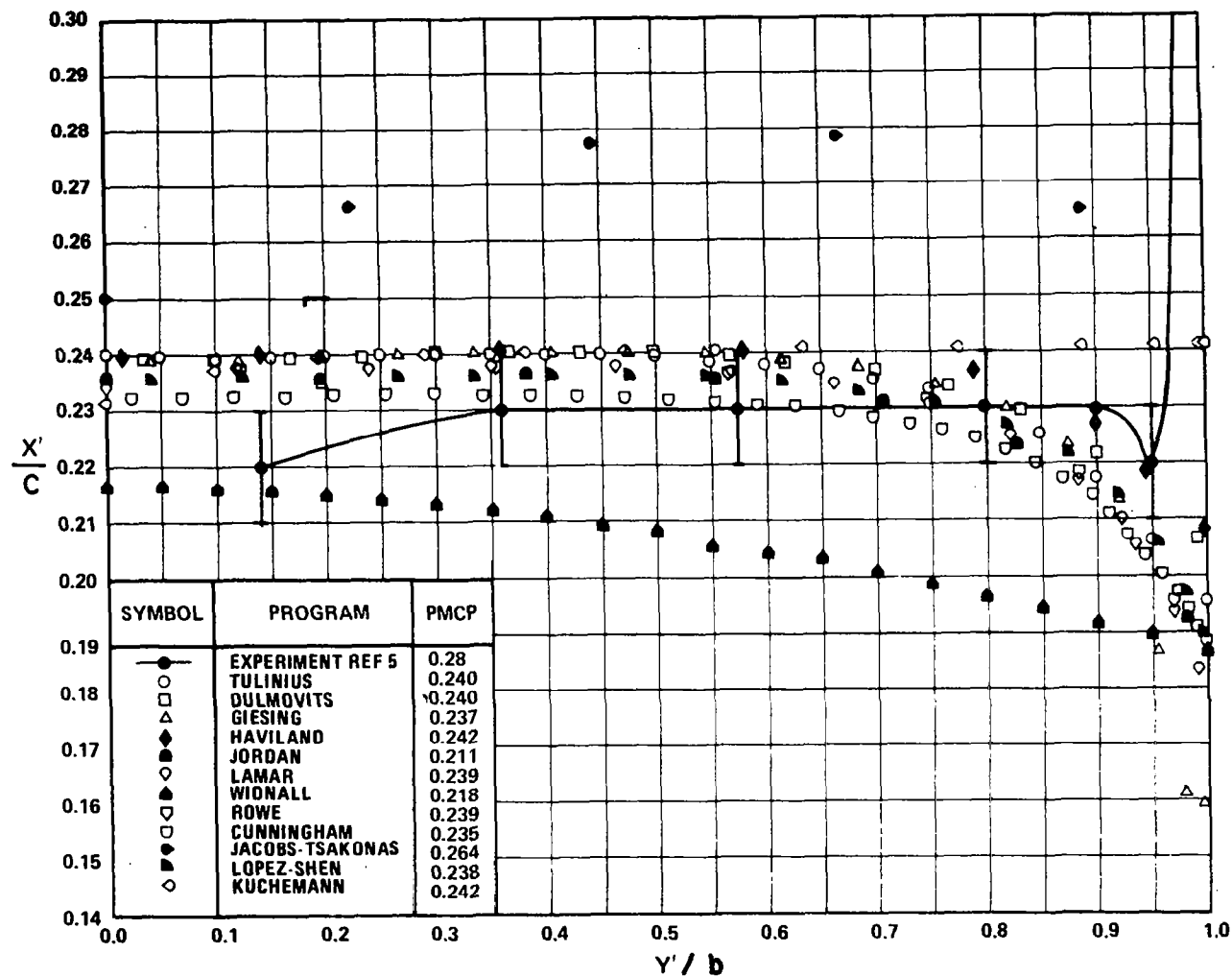


Fig. 30 - Spanwise Distribution of Chordwise Location of Center of Pressure for the Tapered Wing at 11.4-Degree Angle of Attack From Langan and Wang²⁶

TABLE IV - Tapered Wing at 11.4-Degree Angle of Attack

Program	Mach	C_L	PMCP	BMCP	C_{DI}	NCM x NSM	Time sec	Computer
Tulinus	0.15	0.817	0.240	0.425	0.043	420 ^(a)	25	CDC 6600
Dulmovits	↑	0.831	0.240	0.431		10 x 15	96	IBM 360/75
Margason-Lamar	↓	0.831	0.240	0.432		10 x 12	142	CDC 6700 ^(f)
Giesing	0.15	0.829	0.237		0.044	11 x 17	120C	IBM 360/65
Rubbert	0.00	0.798	0.238	0.420	0.041	10 x 15	117	CDC 6600
Lopez & Shen	0.00	0.814	0.238		0.042	8 x 17	105C	IBM 360/65
Haviland	0.15	0.848	0.242	0.438		8 x 8	291	CDC 6400
Jordan	0.00	0.820	0.211		0.043	2 x 15	9	UNIVAC 1108
Lamar	0.00	0.806	0.239	0.423	0.041	4 x 13	98	IBM 360/65
Widnall	0.15	0.812	0.218	0.431		10 x 2	63	CDC 6700 ^(f)
Bandler	0.00	0.807	0.238		0.042	4 x 4	8	CDC 6700 ^(f)
Rowe	0.15	0.815	0.239	0.428		4 x 6	13	CDC 6600
Cunningham	0.15	0.839	0.235	0.424		4 x 5	14	IBM 370/155
Jacobs-Tsakonas	0.00	0.920	0.264	0.439		5 ^(b)	40C	CDC 6600
Lopez (Küchemann)	0.15	0.852	0.242		0.047	16 ^(c)	12C	IBM 360/65
Experiment ^(e)	0.15	0.83	0.28	0.44				
Additional Computer Runs								
Giesing	0.00	0.823	0.240		0.044	11 x 17	121C	IBM 360/75
Jordan	↑	0.808	0.212		0.042	2 x 7	5	UNIVAC 1108
		0.819	0.211		0.043	2 x 15 ^(d)	10	
		0.817	0.213		0.043	2 x 31	28	
		0.811	0.211		0.042	3 x 15	31	
Jordan	0.00	0.798	0.213		0.041	4 x 15	68	UNIVAC 1108
Cunningham	0.15	0.849	0.233	0.425		3 x 3	10	IBM 370/155
Lopez	0.00	0.845	0.242		0.046	16 ^(c)	12C	IBM 360/65
Widnall	0.15	0.826	0.217	0.426		10 x 3	73	CDC 6700
Notes:								
(a) Tulinus uses 420 horseshoe vortices with 6 chordwise and 6 spanwise functions relating their strengths. The system is solved by a least squares method with 99 pivotal points.								
(b) Chordal modes.								
(c) Spanwise modes.								
(d) The kink at the wing centerline has been rounded off for these calculations.								
(e) Experimental results are examined in detail in the section entitled, "Comparisons with Experimental Results." There is a difference between the wing tips in the experiment and those in the calculations.								
(f) Times for CDC 6700 are in terms of CDC 6400 time.								

From Langan and Wang²⁶

TABLE V - Uncambered Swept Wing

Program	Mach	$C_{L\alpha}$	PMCP *	BMCP	C_{DI}	NCH x NSH	Time sec	Computer
Tulinus	0.12	3.891	0.538	0.450	0.999	420 ^(a)	87	CDC 6600
Dulmovits	0.12	3.987	0.541	0.455		10 x 15	104	IBM 360/75
Margason-Lamar	0.10	4.008	0.532			10 x 12	71	CDC 6700 ^(g)
Giesing	0.12	3.973	0.540		1.053	11 x 17	123C	IBM 360/65
Rubbert ^(b)	0.00	3.868	0.535	0.447	0.966	10 x 15	351 ^(c)	CDC 6600
Lopez & Shen	0.00	3.916	0.536		1.000	8 x 17	110C	IBM 360/65
Haviland	0.12	4.021	0.583	0.463		8 x 10	463	CDC 6400
Jordan	0.00	3.910	0.531		0.999	2 x 15	13	UNIVAC 1108
Lamar	0.00	3.874	0.536	0.447	0.980	8 x 11	651	IBM 360/65
Widnall	0.12	4.080	0.502	0.443		10 x 2	60	CDC 6700 ^(g)
Bandler	0.00	4.030	0.528		1.052	4 x 4	10	CDC 6700 ^(g)
Rowe	0.12	3.921	0.534	0.447		8 x 9	95	CDC 6600
Cunningham	0.12	4.091	0.523	0.444		5 x 5	19	IBM 370/155
Jacobs-Tsakonas	0.00	4.253	0.553	0.464		5 ^(d)	80C	CDC 6600
Lopez	0.12	4.065	0.550		1.109	16 ^(e)		
Experiment								
Pressure	0.12	3.89		0.462				
Force	0.12	3.85		0.466				
Additional Computer Runs								
Margason-Lamar	0.00	3.996	0.532	0.457		10 x 12	144	CDC 6700 ^(g)
Giesing	0.00	3.956	0.540		1.044	11 x 17	123C	IBM 360/65
Jordan	0.00	3.894	0.532		0.993	2 x 15 ^(f)	20	UNIVAC 1108
Widnall	0.12	4.073	0.499	0.444		10 x 3	73	CDC 6700
Cunningham	0.12	4.043	0.524	0.445		8 x 5	115	IBM 370/155
Cunningham	0.12	4.145	0.523	0.443		3 x 3	7	IBM 370/155
Lopez	0.00	4.047	0.550		1.099	16 ^(e)	20	CDC 6600
Notes:								
(a) (Not applicable)								
(b) Rubbert's program is nonlinear. The above results were obtained by running the uncambered wing at $\alpha = 0.1$ radians.								
(c) Each of the Rubbert runs for the swept wing took 117 seconds.								
(d) Chordal modes.								
(e) Spanwise modes.								
(f) Rounds off the kink at the centerline for this run.								
(g) CDC 6700 time is in terms of time on a CDC 6400.								

From Langan and Wang²⁶

*Ref. 27 gives a value of 0.555 for PMCP.

root chord, and bending moment center of pressure (BMCP) measured from the wing centerline divided by semispan are presented for each program. In Table V, the lift derivatives are given in place of the lift coefficients.

Fig. 29 presents the spanwise lift distribution for the tapered wing at 11.4 degrees angle of attack. Fig. 30 shows the spanwise distribution of chordwise location of the center of pressure for the tapered wing at 11.4 degrees angle of attack.

Most of the results of the present method are in fair agreement with the computer results obtained by others and with the experimental results. The most noticeable disagreement is the spanwise lift distribution shown in Fig. 29 where the values of the present method are higher than the others towards the wing tip. A similar trend was noticed in the case of a rectangular wing reported in Case 3.

Case 5: swept wing with control surface - subsonic unsteady. - Case 5 consisted of calculations on a swept wing with partial-span flaps (planform No. 5) shown in Fig. 10 which compare with the results reported by Stark (ref. 24). The oscillating modes for wing and control surface and the corresponding aerodynamic coefficients are defined in Example 2 found in Appendix A.

The breakdown of the wing and the control surface is shown in Fig. 31 for the case of 40 collocation points. Fig. 32 shows the arrangement of the swept wing with even strip width and Fig. 33 shows the arrangement with reduced strip width towards the tip. The aerodynamic coefficients calculated by using these arrangements and for different numbers of collocation points are compared with those of Stark (ref. 24) and with the results obtained by the doublet lattice methods (obtained by private communication from J. Griffin, Vought Aeronautics Co.) in Fig. 34, and in Table VI. It is difficult to compare the relative computational efforts of the different methods used for the results reported here due to the lack of information available.

In general, the results for the swept wing are not in as good agreement with the referenced values as in the case of rectangular wing calculations. The lift coefficients are in good agreement except at high subsonic speed. At Mach number 0.9, the imaginary value of lift coefficient is considerably smaller than the referenced value. The real parts of moment coefficients

CONTROL SURFACE CHORD = $.712 \times$ LOCAL SEMI CHORD
 WING ASPECT RATIO = 2
 WING TAPER RATIO = $.2378$
 LEADING EDGE SWEEP ANGLE = 60°

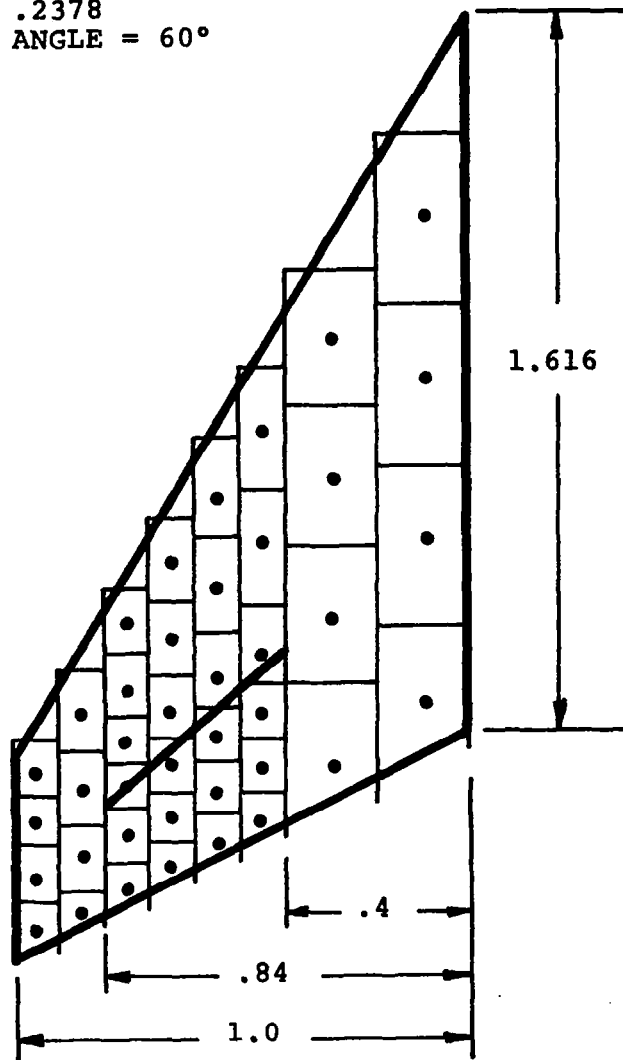


Fig. 31 Arrangement of Aerodynamic Elements for a Swept Wing with Partial-Span Control Surface

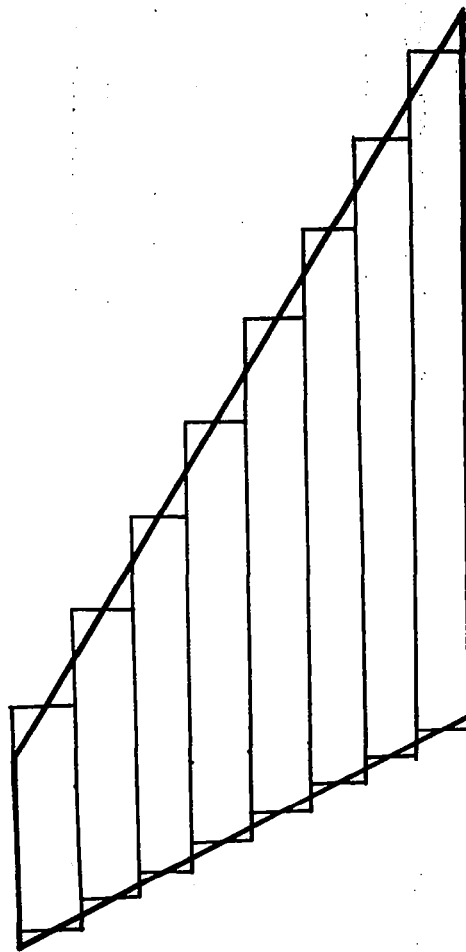


Fig.32 Arrangement with Evenly Spaced Strip Width for An Aspect Ratio Two Swept Wing (Leading edge sweep Angle 60° , Taper Ratio = .2376)

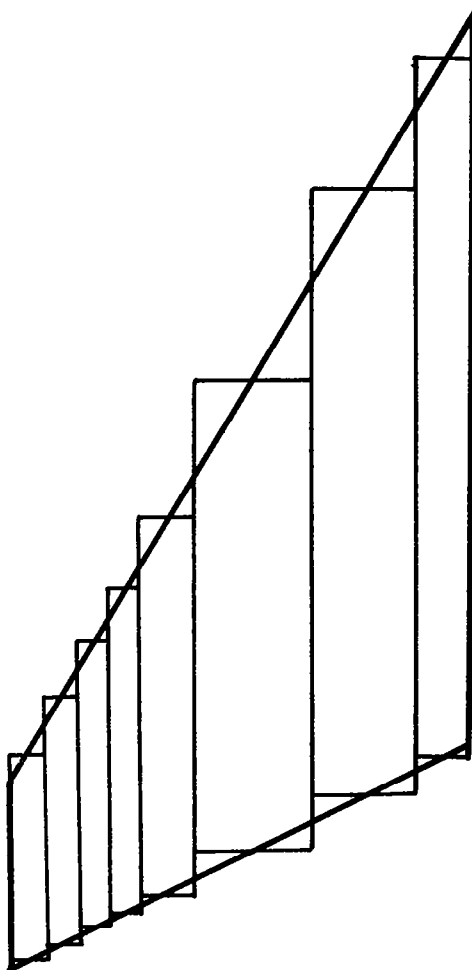


Fig. 33 Arrangement with Reduced Strip Width Towards Tip
For An Aspect Ratio Two Swept Wing (Leading Edge
Sweep Angle = 60° , Taper Ratio = .2376)

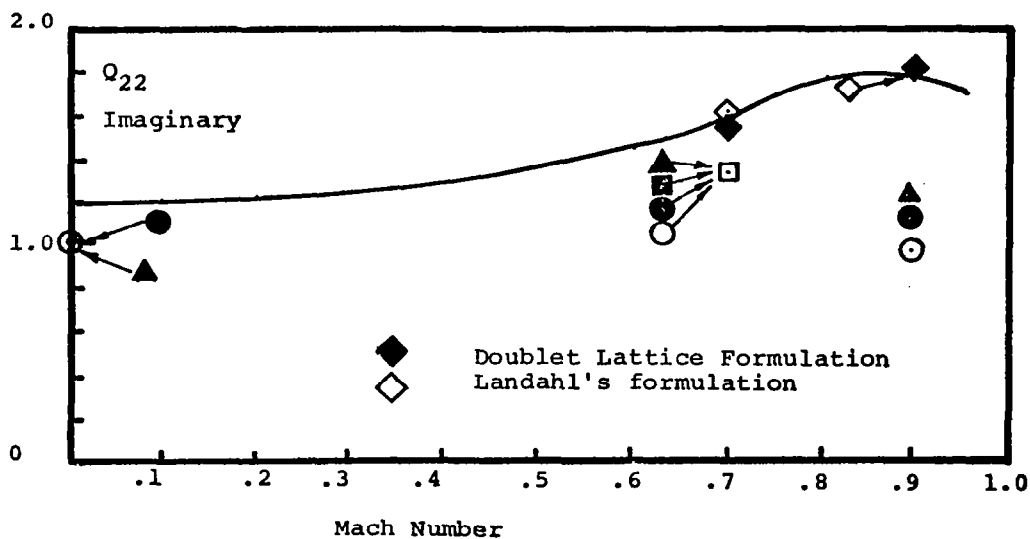
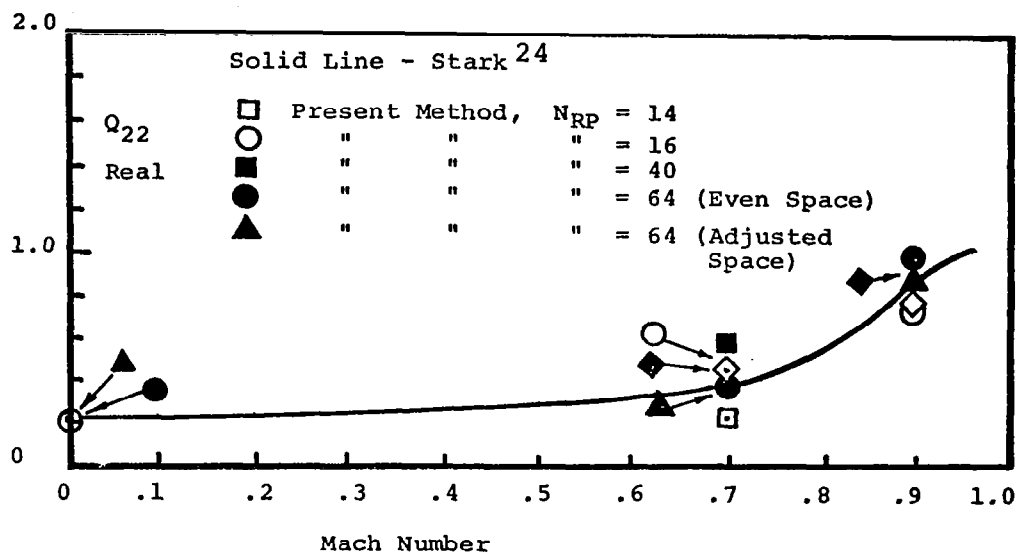


Fig. 34 Pitching Moment Coefficient For a Tapered Swept Wing Oscillating in Pitch

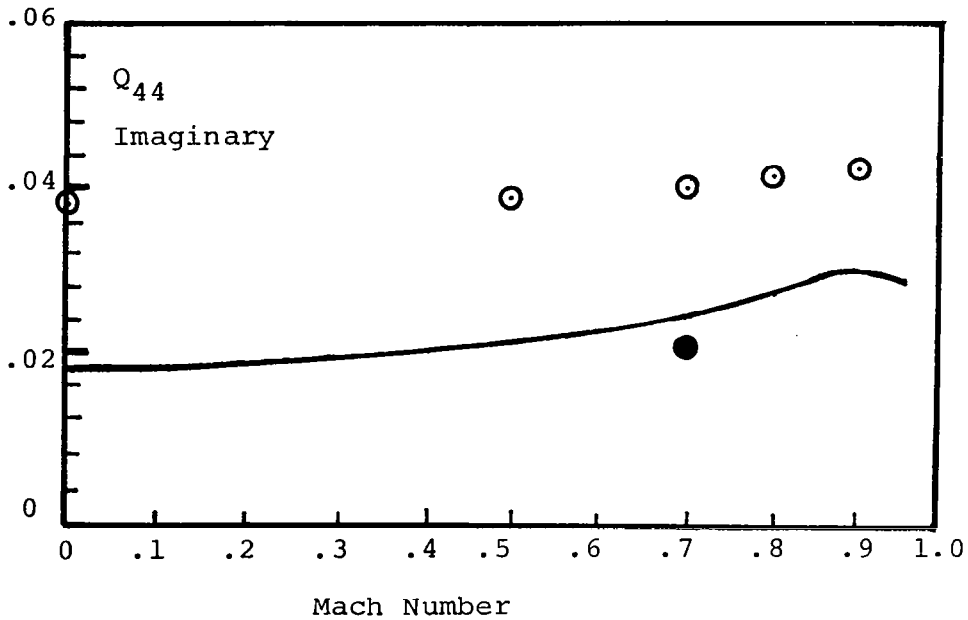
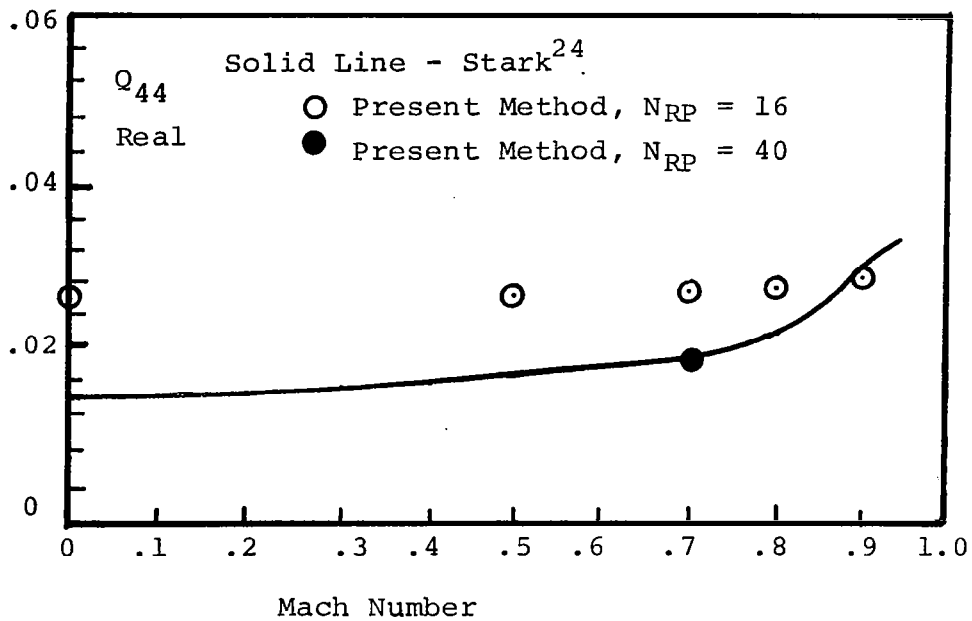


Fig. 35 Flap Moment Coefficient Due to
Control Surface Rotation, $K_r = .5$

Table VI. Lift and Moment Derivatives for Aspect Ratio
Two Swept Wing with Partial-Span Flaps
(Leading Edge Sweep Angle=60°, Taper Ratio=.2376)
Rotating about Root Midchord ($K_r = .5$)

Mach No.	Q_{mn}	Present Method				Reference		
		N_{RP}	Strip Width	Real	Imag.	Ref. No.	Real	Imag.
0	Q_{12}	16	Even	1.9277	2.7281	Stark 24	1.7399	2.6312
	"	64	"	1.8742	2.6369	D.L. (A)*	1.8039	2.5424
	"	64	Reduced	1.9179	2.6833	D.L. (B)**	1.8180	2.5493
	Q_{22}	16	Even	.2700	1.019	Stark 24	.2335	1.1844
	"	64	"	.2400	1.008	D.L. (A)*	.2987	1.221
	"	64	Reduced	.234	1.010	D.L. (B)**	.3034	1.2202
.7	Q_{12}	14	Even	1.9394	2.4229	Stark 24	2.3309	2.9015
	"	16	"	2.6948	2.8539	D.L. (A)*	2.3620	2.7519
	"	40	"	2.5694	2.2033	D.L. (B)**	2.3869	2.7426
	"	64	"	2.5962	2.8341			
	"	64	Reduced	2.6566	2.8936			
	Q_{13}	14	Even	.3846	.7713	Stark 24	.0984	.7658
	"	40	"	.1412	.7971			
	Q_{14}	14	Even	.7677	.3133	Stark 24	.8003	.0693
	"	40	"	.8346	.0211			
	Q_{22}	14	Even	.2234	1.3227	Stark 24	.3495	1.5228
	"	16	"	.4401	1.254	D.L. (A)*	.4326	1.5172
	"	40	"	.5655	1.2922	D.L. (B)**	.4484	1.5313
	"	64	"	.3857	1.277			
	"	64	Reduced	.3738	1.298			
	Q_{23}	14	Even	.1276	.5684	Stark 24	.0518	.5608
	"	40	"	.0153	.5641			
	Q_{24}	14	Even	.5332	.3479	Stark 24	.5663	.1917
	"	40	"	.5693	.1397			

Table VI. (Cont'd)

Mach No.	Q_{mn}	Present Method				Reference		
		N_{RP}	Strip Width	Real	Imag.	Ref. No.	Real	Imag.
.9	Q_{42}	14	Even	.02005	.05953	Stark 24	.0052	.0471
	"	40	"	.0165	.0410			
	Q_{43}	14	Even	.0190	.0338	Stark 24	.0130	.0211
	"	40	"	.0120	.0203			
	Q_{12}	16	Even	2.7525	1.6424	Stark 24	3.0654	2.6195
	"	64	"	3.404	1.596	D.L.(A)*	2.9741	2.6347
	"	64	Reduced	3.2915	1.9057	D.L.(B)**	2.9637	2.4395
	Q_{22}	16	Even	.686	.945	Stark 24	.8287	1.7606
	"	64	"	.945	1.068	D.L.(A)*	.7439	1.6998
	"	64	Reduced	.8546	1.185	D.L.(B)**	.8758	1.6792

* D.L.(A): Doublet Lattice Calculations by Rodemich's Formulation

** D.L.(B): " " " " Landahl's "

(Results obtained by private communication)

are in close agreement with the referenced values up to Mach number 0.9; imaginary parts are, however, consistently lower than the referenced values, giving the worst comparison at Mach number 0.9 as shown in Fig. 34. Improvements were noticed as a higher number of collocation points was used at Mach number 0.9.

The flap moment coefficients were calculated with only 14 collocation points for Mach numbers ranging 0 to .9. Considering the small number of collocation points used, the results are in fair agreement as is shown in Fig. 35. One calculation was made with 40 collocation points for Mach number 0.7 which resulted in marked improvement over the results obtained from 14 collocation points. This indicates convergence of the present results to the referenced values with a higher number of collocation points.

Case 6: T-tails - subsonic unsteady.- Two T-tails found in the literature were re-analyzed, using the first order zero pressure rectangular elements. The first was the rectangular T-tail (planform No. 6) shown in Fig. 11. Results are compared in Table VII with experimental results reported by Clevenston and Leadbetter (ref. 28) and with calculations by Kalman et al. (ref. 23). In the latter calculations, the effect of the tunnel wall as a reflecting plane was disregarded. In comparison, Kalman's calculations used 100 collocation point which is equivalent to using 200 points if the effects of symmetries had not been included in the computer program.

The second was Stark's (ref. 29) well-documented T-tail (planform No. 7) shown in Fig. 12. Results are shown in Table VIII compared with results reported by Stark and results by Kalman (ref. 23), using the doublet lattice method. The numbers of collocation points used for the present method were 18, 50, 60, 66, 70, and 72. Sixty-three collocation points were used in Stark's configuration and 230 in Kalman's. These numbers would have been higher if effects of symmetries had not been considered.

The computed results generally showed convergence towards the referenced values as the number of collocation points was increased up to 60 collocation points. Further increase of the number of collocation points to 66 and 72 initially gave erratic results. However, when the elements adjacent to the

Table VII. Comparison of Side Force and Moment Derivatives for A Rectangular T-tail Oscillating In Yaw about the Fin Midchord

Method	M	K_r^*	Side Force Deriv. $C_{Y,\psi}$		Moment Deriv. $C_{N,\psi}$	
			Real	Imag.	Real	Imag.
Present	.25	.2	1.5226	0.1931	.7221	-.09371
Clevenson and Leadbetter ²⁸	.25	.202	1.215	0.0	.635	-.194
	.25	.195	1.4	0.0	.636	-.195
Kalman et al ²³	0	.2	1.1738	.2494	.6437	-.0905

*Based on $\frac{1}{2} C_{REF}$ (See Fig. 11)

Table VIII. Comparison of Aerodynamic Coefficients for Stark's T-tail³¹
(Mach No. = .8)

Mode Derivatives		K_r^*	Yaw (j=1)		Slidesway (j=2)		Roll (j=3)	
			Real	Imag.	Real	Imag.	Real	Imag.
Yawing Moment (C _{1j})	Present, N _{RP} =18	.2	.0211	-.3919	.0367	-.0053	.0098	.0211
	Present, N _{RP} =50	.2	-.2849	-.4734	.02713	-.06099	.01244	.02705
	Present, N _{RP} =60	.2	-1.221	-.4316	.03197	-.03147	.01253	.02613
	Present, N _{RP} =66	.2	-.918	-.5868	.9731	-.4333	.1083	.00026
	Present, N _{RP} =70	.2	-.2719	-.4950	.02956	-.05899	-.01339	.02893
	Present, N _{RP} =72	.2	-.7165	2.1534	-.4507	.404	-.0029	.0350
	Kalman ²³	.2	-.0837	-.5270	.0470	-.0278	.0137	.0257
	Stark ³¹	.2	-.0961	-.4811	.412	.0300	.0125	.0239
Side Force (C _{2j})	Present, N _{RP} =18	.2	-.5861	-.3520	.0265	-.1177	.0133	-.0298
	Present, N _{RP} =50	.2	-.7818	-.3496	.01269	-.150	.01662	-.0362
	Present, N _{RP} =60	.2	-.6231	-.3446	.02160	-.1228	.01653	-.0347
	Present, N _{RP} =66	.2	-.3766	1.0956	.3863	-.6203	-.4012	.1477
	Present, N _{RP} =70	.2	-.7793	-.3602	.01468	-.1495	.01766	-.03592
	Present, N _{RP} =72	.2	-.7991	1.2299	-.2777	-.0483	.00833	-.0297
	Kalman ²³	.2	-.6270	-.3965	.0297	-.1260	.0171	-.0318
	Stark ³¹	.2	-.6108	-.3625	.0241	-.1211	.0158	-.0295
Rolling Moment (C _{3j})	Present, N _{RP} =18	.2	-.1262	-.1101	.0129	-.0264	.0120	-.0382
	Present, N _{RP} =50	.2	-.1231	-.1346	.0177	-.0266	.0201	-.0596
	Present, N _{RP} =60	.2	-.1295	-.1334	.01693	-.02769	.01967	-.0582
	Present, N _{RP} =66	.2	-.4012	.1477	-.0465	-.0632	.0142	-.0625
	Present, N _{RP} =70	.2	-.1236	-.1373	.01815	-.02657	.02065	-.0594
	Present, N _{RP} =72	.2	-.07963	-.3133	.0512	-.0310	.0211	-.0586
	Kalman ²³	.2	-.1270	.1267	.0154	-.0269	.0186	-.0529
	Stark ²⁹	.2	-.1247	-.1151	.0134	-.0255	.0179	-.0497
Yawing Moment	Present, N _{RP} =18	.3	.0458	-.6220	.0844	-.0160	.0244	.0331
	Stark ²⁹	.3	-.0690	-.7736	.0973	-.0549	.0315	.0403
Side Force	Present, N _{RP} =18	.3	-.6106	-.5145	.0552	-.1818	.0300	-.0458
	Stark ²⁹	.3	-.6471	-.5592	.0562	-.1895	.0379	-.0449
Rolling Moment	Present, N _{RP} =18	.3	-.1342	-.1613	.0269	-.0428	.266	-.0588
	Stark ²⁹	.3	-.1344	-.1729	.0299	-.0415	.0411	-.0770

* Based on $\frac{1}{3} b$ (See Fig. 12)

intersection of the two surfaces were kept to the same size as for the case of 60 collocation points, the results obtained with 70 collocation points showed a tendency to converge.

The evaluation of the three versions of rectangular subsonic elements for planar cases showed that the best agreement resulted from the "first order, zero pressure, rectangular element" followed by the "first order, constant potential, rectangular elements," with the "zero order, constant potential, rectangular elements" appearing to have the least agreement. These three methods were applied to the T-tail with 18 elements, but the results given in Table IX do not indicate that any one method is preferable over the others.

Definitions of aerodynamic coefficients used for the two T-tail calculations are as follows:

$$C_{Y,\psi} = \frac{F_Y}{\pi q S_{FIN}}$$

$$C_{N,\psi} = \frac{M_\psi}{\frac{1}{2} \pi q S_{FIN} C_{REF}}$$

where

$$F_Y = \text{Side Force}$$

$$M_\psi = \text{Pitching Moment}$$

$$S_{FIN} = \text{Fin Area}$$

Stark's T-tail:

$$C_{l,j} = \frac{1}{\pi q b} \iint_{Tail} J_m(x,y) \Delta P_n(x,y) dx dy$$

$$+ \iint_{Tail} J_m(x,z) \Delta P_n(x,z) dx dz$$

Table IX. Comparison of Various Aerodynamic Elements for Stark's²⁹
T-tail ($N_{RP} = 18$, $K_r = .2^*$)

Mode Derivative		Yaw (j=1)		Sidesway (j=2)		Roll (j=3)	
		Real	Imag.	Real	Imag.	Real	Imag.
Yawing Moment (C_{1j})	By ZOCP	0.321	-.4222	.0416	-.0045	.0114	.0214
	By FOCP	.0289	-.4080	.0389	-.0044	.0104	.0215
	By FOZP	.02094	-.3978	.0367	-.0053	.0098	.0211
	By Stark	-.0961	0.4811	.0412	-.0300	.0125	.0239
Side Force (C_{2j})	By ZOCP	-.5671	-.3575	.0289	-.1141	.0144	-.0289
	By FOCP	-.5787	-.3548	.0275	-.1163	.0138	-.0294
	By FOZP	-.5859	-.3519	.0265	-.1176	.0133	-.0297
	By Stark	-.6108	-.3625	.0241	-.1211	.0158	-.0295
Rolling Moment (C_{3j})	By ZOCP	-.1240	-.1083	.0127	-.0257	.0122	-.0377
	By FOCP	-.1252	-.1094	.0128	-.0261	.0122	-.0380
	By FOZP	-.1260	-.1100	.0219	0.0263	.0120	-.0382
	By Stark ³¹	-.1248	-.1151	.0134	-.0255	.0179	-.0497

* Based on $\frac{1}{3} b$ (See Fig. 12)

Effective wake length (F=6)

ZOCP = Zero-order, Constant Potential, Rectangular, Element

FOCP = First order, Constant Potential, Rectangular, Element

FOZP = First order, Zero Pressure, Rectangular, Element

where the oscillating modes considered are

$$J_n(x,y) = \begin{cases} 0 & , & n=1 \\ 0 & , & n=2 \\ y/b & , & n=3 \end{cases} \quad \text{for tail}$$

$$J_n(x,z) = \begin{cases} (x_0 - x)/c & , & n=1 \\ 1 & , & n=2 \\ -z/b & , & n=3 \end{cases} \quad \text{for fin}$$

$$i = 1 \dots m$$

$$j = 1 \dots n$$

$$c = b/3$$

x_0 = x-coordinate of fin tip mid chord

ΔP_n = Pressure jump corresponding to J_n

Case 7: rectangular wings - supersonic steady.- Using in-plane steady supersonic rectangular elements, two sets of calculations were made on rectangular wings of various aspect ratios. The first was for comparison with results previously obtained by Haviland (ref. 30) for Mach numbers ranging from 1.2 to 1.8 and aspect ratios as shown in Fig. 13. The second set was made to compare with the results reported by Nelson et al. (ref. 31) for Mach number 1.3 and aspect ratios as indicated in Fig. 13.

The breakdown of the wing surface for supersonic calculations is different from that for subsonic calculations. This has been illustrated in Fig. 36 for the case of 16 collocation points on an aspect ratio two rectangular wing. The lift and moment derivatives calculated for the rectangular wing pitching about the leading edge which compare with results by Haviland (ref. 30) are shown in Table X. The derivatives calculated to compare with the results reported by Nelson et al. (ref. 31) for rectangular wings pitching about the midchord are shown in Table XI.

Using 8 x 8 arrays of elements, the present results are within 5% of the referenced values for the whole Mach number range used in the calculations.

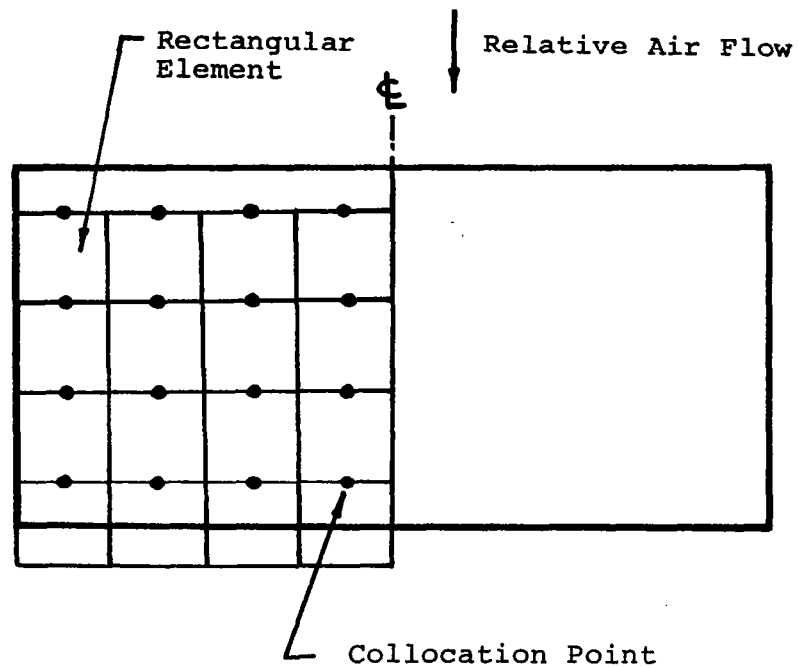


Fig. 36 Arrangement of Aerodynamic Elements
for Aspect Ratio Two Rectangular Wing
for Steady Supersonic Calculations

Table X. Comparison of Lift and Moment Derivatives
(about Leading Edge) for Rectangular Wings
in Steady Supersonic Flows

Method	No. of Points	Mach No.	Aspect Ratio	Lift Derivative	Moment Derivative
Haviland ³⁰	6 × 6	1.2	3.0151	4.49	-4.08
Present	4 × 4	"	"	4.878	-4.4056
"	5 × 5	"	"	4.8158	-4.3398
"	6 × 6	"	"	4.7507	-4.2595
"	8 × 8	"	"	4.694	-4.1979
Haviland ³⁰	6 × 6	1.4	2.0412	3.08	-2.77
Present	4 × 4	"	"	3.2922	-2.9683
"	5 × 5	"	"	3.2503	-2.9246
"	6 × 6	"	"	3.2161	-2.8836
"	8 × 8	"	"	3.1589	-2.8159
Haviland ³⁰	6 × 6	1.6	1.6013	2.42	-2.17
Present	4 × 4	"	"	2.5827	-2.3286
"	5 × 5	"	"	2.5499	-2.2943
"	6 × 6	"	"	2.5230	-2.2622
"	8 × 8	"	"	2.4984	-2.2369

Table X - Cont'd

Method	No. Points	Mach No.	Aspect Ratio	Lift Derivative	Moment Derivative
Haviland ³⁰	6 × 6	1.8	1.3363	2.01	-1.79
Present	4 × 4	"	"	2.1555	-1.538
"	5 × 5	"	"	2.1279	-1.9147
"	6 × 6	"	"	2.1054	-1.8876

Table XI. Comparison of Lift and Moment Derivatives (about Midchord) for Rectangular Wings in Steady Supersonic Flows Mach No. = 1.3

Method	No. of Points	Aspect Ratio	Lift Coefficient	Moment Coefficient
Nelson ³¹ et al.		1.2039	2.42	.40
Present	4 x 4	"	2.596	.465
Nelson ³¹ et al.		2.0	3.38	.245
Present	4 x 4	"	3.678	.234
"	8 x 8	"	3.494	.254
Nelson ³¹ et al.		4.0	4.16	.120
Present	4 x 4	"	4.347	.105
"	8 x 8	"	4.229	.115

Definitions of the derivatives shown in the tables are the same as those used in Case 2.

Computation Time

The four-by-four results took between thirteen (13) and twenty seven (27) seconds to run on the CDC 6400, using batch processing. The eight-by-eight results required 220 to 294 seconds. The time should be roughly proportional to the number of elements in the aerodynamic influence matrix, i.e., to the number of reference points (N_{RP}) squared, or 1:16 in the above case.

PROPOSED EXTENDED METHOD OF ANALYSIS

In this section, the method described previously is extended to polygonal elements for subsonic and supersonic flows in the out-of-plane case. Expressions are shown to be the same as those previously developed when applied to rectangular elements.

Statement of Problem

The problem of the extended method is identical to the original problem.

Coordinate System

This is identical to the original system outlined. However, for analytical convenience, use is made of the X,S,N coordinate system defined in Eq. (47). This gives the coordinate of the sending point in a system whose origin is the receiving point r . X is parallel to the x' axis, S is parallel to the plane of sending surface, and N is normal to it.

Governing Differential Equation

This is identical to Eq. (2).

Integral Equation

This is defined by Eqs. (4) and (5).

Expression for Green's function.— This is equivalent to Eq. (6). However, the cutoff function is redefined in terms of a real argument, and the results are expressed in terms of the X,S,N coordinate system.

Taking r at the collocation point k , the subsonic Green's Function is

$$G = G_R \{r(k), \rho\} = \frac{-1}{4\pi R} \exp \left\{ \frac{-i\omega}{\beta^2 c} [R + MX] \right\} \quad (79A)$$

Define also

$$G_A \{r(k), \rho\} = \frac{-1}{4\pi R} \exp \left\{ \frac{-i\omega}{\beta^2 c} [-R + MX] \right\} \quad (79B)$$

where

$$R = \sqrt{x^2 + \beta^2 S^2 + \beta^2 N^2}$$

The supersonic Green's function may then be expressed as:

$$G = U(F) [G_R \{r(k), \rho\} + G_A \{r(k), \rho\}] \quad (80)$$

U is the step function, defined by

$$U(x) = \begin{cases} 1; & x \geq 0 \\ 0; & x < 0 \end{cases}$$

and the cutoff function F (which is positive only in the forward Mach cone) is

$$F = -X - \sqrt{-\beta^2 S^2 - \beta^2 N^2}$$

as used by Watkins and Berman (ref. 14).

Expression for $K\phi$.— This is still defined by Eq. (5), but it is expressed in a different form than in Eq. (7). Note first that

$$\begin{aligned}\partial/\partial n &= -\hat{n} \cdot \hat{v} \partial/\partial v - \hat{n} \cdot \hat{\sigma} \partial/\partial \sigma \\ &= -\cos(\gamma - g) \partial/\partial v - \sin(\gamma - g) \partial/\partial \sigma\end{aligned}\quad (81)$$

where γ and g are the angles between the local normal and the z-axis on the sending and receiving surfaces respectively, as shown in Figure 1. Then

$$K_{\phi} = -\cos(\gamma - g) \partial^2 G / \partial v^2 - \sin(\gamma - g) \partial^2 G / \partial v \partial \sigma \quad (82)$$

Method of Solution

The method of solution is generally the same as suggested previously. However, expressions for irregular elements are developed for both subsonic and supersonic flow. No doubt the same can be done for sonic flows by deriving the limiting expressions correctly.

Integration by Discrete Elements

The expression for the "aerodynamic influence matrix" $A_{k,l}$ remains as in Eq. (12).

Aerodynamic Elements

The catalog of aerodynamic elements is extended. Due to the new form for K_{ϕ} expressed in Eq. (82), however, the new and old elements can only be compared for the in-plane case.

Basic form.— The zero-pressure form of element has given the best results up to now, and has therefore been chosen as the fundamental form for the extended method. Also, Eqs. (13) and (34) have been combined, f has been redefined, and the X, S, N , coordinate system has been introduced, resulting in

$$-\Delta\phi(l^*, X, S) = \Delta\phi_l f(l^*, X, S) \exp \left\{ \frac{-i\omega}{v} [X - X(l)] \right\} \quad (83)$$

The net pressure differential ΔP acting in the positive N direction is now given by

$$\frac{\Delta P}{\frac{1}{2} \rho V^2} = -2 \left\{ \frac{\partial}{\partial X} + \frac{i\omega}{V} \right\} \frac{\Delta\phi(\ell^*, X, S)}{V} \quad (84)$$

Therefore, for any element on which f equals 1, ΔP is zero, (the zero pressure element), while for any element on which f equals $\{x - x(\ell)\}$

$$\frac{\Delta P}{\frac{1}{2} \rho V^2} = -2 \frac{\Delta\phi\ell}{V} \exp \left\{ \frac{-i\omega}{V} [X - X(\ell)] \right\} \quad (85)$$

which is constant in the zero frequency case. The relative advantages of using polynomial forms for f are not understood at this time. However, the above two examples warrant further discussion.

In the first case with f equals 1 there is no pressure except at the edge of region ℓ^* where there is a lift line corresponding to the stepwise jump in $\Delta\phi$. This would be treated as a vortex loop in the steady state case, as is done for example, in the method of Rubbert and Saaris (ref. 5).

In the second case, the pressure varies harmonically. Further possibilities are polynomials with unknown coefficients. For example, if f is $1 + a \{x - x(\ell)\}$, we have two unknowns for each element, $\Delta\phi/V$ and a .

The expressions for the general terms $A_{k,\ell}$ of the aerodynamic influence matrix given in Eqs. (14) and (15) are retained. It might be noted that the form of Eq. (14) could be used for the on-surface elements as well as for the wake region elements if it were desired to subdivide them. Also, the form of Eq. (15) might be used for trailing edge elements, if the 'panelled' wake used in earlier parts of this report were to be replaced by integrals extending to infinity.

It is thus convenient to introduce a modified Green's function

$$\bar{G} = G \exp \left\{ -\frac{i\omega}{V} [X - X(\ell)] \right\} \quad (86)$$

Then using Eqs. (82) and (83), Eq. (16) can be rewritten as

$$k_{\phi}(k, \ell, \ell^*) = - \iint_{\ell^*} \{ \cos(\gamma - g) \partial^2 \bar{G} / \partial N^2 + \sin(\gamma - g) \partial^2 \bar{G} / \partial N \partial S \} f(\ell^*, X, S) dX dS \quad (87)$$

Subsonic aerodynamic elements.— After some manipulation, it can be shown that

$$\frac{\partial^2 \bar{G}}{\partial N^2} = \left[\left\{ 1 + \frac{i\omega R}{\beta^2 c} \right\} \frac{\partial^2}{\partial N^2} \left\{ \frac{1}{R} \right\} - \frac{\omega^2 N^2}{c^2 R^3} \right] R \bar{G}_R \quad (88)$$

and

$$\frac{\partial^2 \bar{G}}{\partial N \partial S} = \left[\left\{ 1 + \frac{i\omega R}{\beta^2 c} \right\} \frac{\partial^2}{\partial N \partial S} \left\{ \frac{1}{R} \right\} - \frac{\omega^2 NS}{c^2 R^3} \right] R \bar{G}_R \quad (89)$$

where

$$\begin{aligned} \bar{G}_R &= G_R \exp \left\{ - \frac{i\omega}{V} [X - X(\ell)] \right\} \\ &= - \frac{1}{4\pi R} \exp \left\{ - \frac{i\omega}{\beta^2 V} [MR + X - \beta^2 X(\ell)] \right\} \end{aligned} \quad (90)$$

Minimum first order expansion-subsonic: The argument of the exponential in the expression for \bar{G}_R , Eq. (90), can be expanded about the point ℓ^* as before for the development of the so called "first order" elements. Since the argument of the expanded exponential is of the form $i\omega\Delta/c$ (where Δ is a typical dimension of the element ℓ^*), expansion up to the first order term should be adequate when small elements are used. Then, from Eq. (90),

$$\begin{aligned} \bar{G}_R &\approx \frac{-1}{4\pi R} \left\{ 1 - \frac{i\omega}{\beta^2 c} [R - R(k, \ell^*)] - \frac{i\omega}{\beta^2 V} [X - X(\ell^*)] \right\} \\ &\times \exp \left\{ - \frac{i\omega}{\beta^2 V} [MR(k, \ell^*) + X(\ell^*) - \beta^2 X(\ell)] \right\} \end{aligned} \quad (91)$$

By substituting this into Eqs. (87), (88), and (89), the "Minimum First Order Expansion" results in which all terms in ω^2 and higher order are dropped. This leads to the following expression for k_ϕ

$$\begin{aligned}
 k_\phi(k, \ell, \ell^*) = & \left[\left\{ \frac{\cos(\gamma-g)}{4\pi} I_0'(k, \ell^*) + \frac{\sin(\gamma-g)}{4\pi} I_0''(k, \ell^*) \right\} \right. \\
 & \times \left\{ 1 + \frac{i\omega R(k, \ell^*)}{\beta^2 c} + \frac{i\omega X(\ell^*)}{\beta^2 V} \right\} - \left\{ \frac{\cos(\gamma-g)}{4\pi} I_1'(k, \ell^*) \right. \\
 & + \left. \left. \frac{\sin(\gamma-g)}{4\pi} I_1''(k, \ell^*) \right\} \left\{ \frac{i\omega}{\beta^2 V} \right\} \right] \exp \left\{ - \frac{i\omega}{\beta^2 V} [MR(k, \ell^*) \right. \\
 & \left. \left. + X(\ell^*) - \beta^2 X(\ell) \right] \right\} \quad (92)
 \end{aligned}$$

In the above expansion, terms such as $(\omega N/c)^2$ are dropped. The validity of this step is in question and is discussed later. The remaining terms dropped are of the form $(\omega \Delta/V)^2$ which are small if the elements are themselves small.

The "I" integrals have the form

$$I_0'(k, \ell^*) = \iint_{\ell^*} f(\ell^*, X, S) \frac{\partial^2}{\partial N^2} \left\{ \frac{1}{R} \right\} dXdS \quad (93)$$

$$I_1'(k, \ell^*) = \iint_{\ell^*} f(\ell^*, X, S) X \frac{\partial^2}{\partial N^2} \left\{ \frac{1}{R} \right\} dXdS \quad (94)$$

$$I_0''(k, \ell^*) = \iint_{\ell^*} f(\ell^*, X, S) \frac{\partial^2}{\partial N \partial S} \left\{ \frac{1}{R} \right\} dXdS \quad (95)$$

$$I_1''(k, \ell^*) = \iint_{\ell^*} f(\ell^*, X, S) X \frac{\partial^2}{\partial N \partial S} \left\{ \frac{1}{R} \right\} dXdS \quad (96)$$

Supersonic aerodynamic elements.— As with Eqs. (88) and (89), it can be shown that

$$\frac{\partial^2}{\partial N^2} U\bar{G}|_A^R = \left[\left\{ 1 \pm \frac{i\omega R}{\beta^2 c} \right\} \frac{\partial^2}{\partial N^2} \left\{ \frac{U}{R} \right\} \mp \frac{i\omega}{\beta^2 c} \frac{\partial^2 U}{\partial N^2} - \frac{\omega^2 U N^2}{c^2 R^3} \right] R\bar{G}|_A^R \quad (97)$$

$$\frac{\partial^2}{\partial N \partial S} U\bar{G}|_A^R = \left[\left\{ 1 \pm \frac{i\omega R}{\beta^2 c} \right\} \frac{\partial^2}{\partial N \partial S} \left\{ \frac{U}{R} \right\} \mp \frac{i\omega}{\beta^2 c} \frac{\partial^2 U}{\partial N \partial S} - \frac{\omega^2 U N S}{c^2 R^3} \right] R\bar{G}|_A^R \quad (98)$$

The notation $|_A^R$ refers to alternate choices of the subscripts, R (retarded) and A (advanced). The corresponding signs on the RH side are indicated by \pm or \mp as appropriate.

Minimum first order expansion-supersonic: Using the same procedure as in the subsonic case, an expression is obtained for k_ϕ which corresponds to that given by Eq. (92).

$$\begin{aligned} k_\phi(k, \ell, \ell^*) = & \left[\left\{ \frac{\cos(\gamma-g)}{4\pi} I_0'(k, \ell^*) + \frac{\sin(\gamma-g)}{4\pi} I_0''(k, \ell^*) \right\} \right. \\ & \times \left\{ 2\cos \frac{\omega R(k, \ell^*)}{\beta^2 c} + \frac{2\omega R(k, \ell^*)}{\beta^2 c} \sin \frac{\omega R(k, \ell^*)}{\beta^2 c} + \frac{2i\omega X(\ell)}{\beta^2 V} \cos \frac{\omega R(k, \ell^*)}{\beta^2 c} \right\} \\ & - \left\{ \frac{\cos(\gamma-g)}{4\pi} I_1'(k, \ell^*) + \frac{\sin(\gamma-g)}{4\pi} I_1''(k, \ell^*) \right\} \left\{ \frac{2i\omega}{\beta^2 V} \cos \frac{\omega R(k, \ell^*)}{\beta^2 c} \right\} \\ & - \left\{ \frac{\cos(\gamma-g)}{4\pi} J'(k, \ell^*) + \frac{\sin(\gamma-g)}{4\pi} J''(k, \ell^*) \right\} \left\{ \frac{2\omega}{\beta^2 c} \sin \frac{\omega R(k, \ell^*)}{\beta^2 c} \right\} \Big] \\ & \times \exp \left\{ - \frac{i\omega}{\beta^2 V} [X(\ell^*) - \beta^2 X(\ell)] \right\} + k_\phi''(k, \ell^*) \end{aligned} \quad (99)$$

The first term includes all contributions except from coincidence of the point k with the element ℓ^* which is covered by k_ϕ'' . The derivation of the corresponding integrals has been discussed. The second term which covers the coincidence effect appears only in the supersonic case.

Although this equation appears formidable at first sight, it has a symmetry which should make programming relatively simple.

The integrals are

$$I_0'(k, \ell^*) = \iint_{\ell^*} f(\ell^*, X, S) \frac{\partial^2}{\partial N^2} \left\{ \frac{U(F)}{R} \right\} dXdS \quad (100)$$

$$I_1'(k, \ell^*) = \iint_{\ell^*} f(\ell^*, X, S) \times \frac{\partial^2}{\partial N^2} \left\{ \frac{U(F)}{R} \right\} dXdS \quad (101)$$

$$I_0''(k, \ell^*) = \iint_{\ell^*} f(\ell^*, X, S) \frac{\partial^2}{\partial N \partial S} \left\{ \frac{U(F)}{R} \right\} dXdS \quad (102)$$

$$I_1''(k, \ell^*) = \iint_{\ell^*} f(\ell^*, X, S) \times \frac{\partial^2}{\partial N \partial S} \left\{ \frac{U(F)}{R} \right\} dXdS \quad (103)$$

$$J'(k, \ell^*) = \iint_{\ell^*} f(\ell^*, X, S) \frac{\partial^2 U(F)}{\partial N^2} dX, dS \quad (104)$$

$$J''(k, \ell^*) = \iint_{\ell^*} f(\ell^*, X, S) \frac{\partial^2 U(F)}{\partial N \partial S} dXdS \quad (105)$$

The first four "I" integrals differ from the corresponding subsonic ones only in that they contain the step function $U(F)$. The "J" integrals only appear in the supersonic case and their integrands are zero except on the forward Mach cone.

Evaluation of Integrals by Contour Integration

Evaluation of the "I" and "J" integrals begins with their reduction to contour form. These contours will be assumed to be polygons, so that it will

be necessary only to evaluate the contributions of straight line segments. Define the indefinite F integrals as follows:

$$F'_{m,n} = \iint X^m S^n \frac{\partial^2}{\partial N^2} \left\{ \frac{U(F)}{R} \right\} dX dS \quad (106)$$

$$F''_{m,n} = \iint X^m S^n \frac{\partial^2}{\partial N \partial S} \left\{ \frac{U(F)}{R} \right\} dX dS \quad (107)$$

It will be shown that these can be reduced to line integrals, thus, for example, if $f(\ell^*, X, S)$ equals unity, then I_1 can be expressed as the sum of line integrals along the sides of the polygons, so that

$$I_1''(k, \ell^*) = \sum_{i=1}^N \left\{ F''_{1,0} \right\}_i^{i+1} \quad (108)$$

where $i, i + 1$ are two consecutive points (in the right handed sense) around the contour, as shown in Figure 37. A transformation to an X, S, N coordinate system will be used to facilitate integration. The bracket $\{F\}_i^{i+1}$ has a particular significance. If the line i to $i + 1$ does not cross the Mach cone, it is identical to $[F]_i^{i+1}$, and has the conventional meaning "evaluate F at $i + 1$ and subtract value at i ." However, there is no contribution to the line integral from outside the Mach cone, but there is one from the intersection point, so that a different interpretation must be made when a line intersects a Mach cone.

In Eq. (108) above, the shape factor f corresponds to the zero pressure case which has already been discussed. In the harmonic pressure case, with f equal to $x - x(\ell)$, one would have

$$I_1''(k, \ell^*) = \sum_{i=1}^N \left\{ F''_{2,0} - X(\ell^*) F''_{1,0} \right\}_i^{i+1} \quad (109)$$

Given a method to evaluate the "F" integrals, a large range of elements is available. Five cases of interest can be identified concerning two consecutive points, 1 and 2 which are as follows:

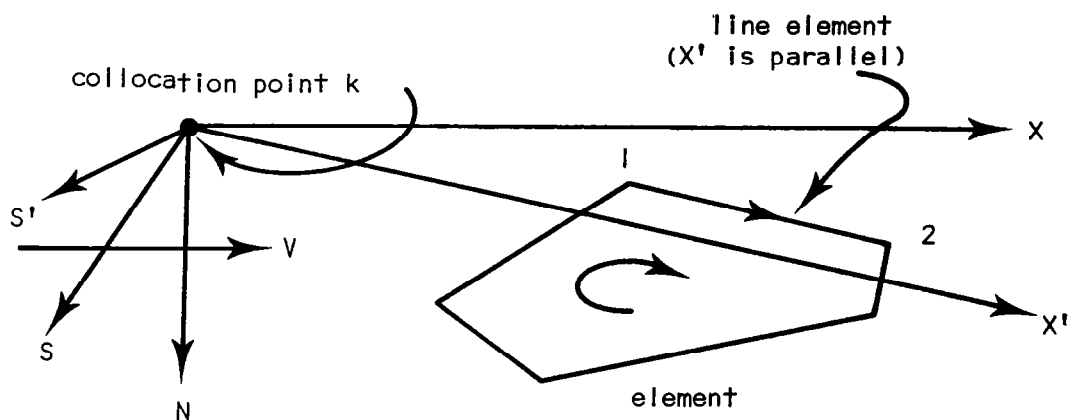


Figure 37: Contour Integral

- (I) Subsonic case, and supersonic case with points 1, 2 lying inside the Mach forward cone.
- (II) Supersonic case with point 1 inside the forward Mach cone and point 2 outside.
- (III) Supersonic case with points 1 and 2 reversed relative to II.
- (IV) Supersonic case with points 1 and 2 outside the forward Mach cone.
- (V) Supersonic case with collocation point k lying on element ℓ^* .

Cases I and II are discussed in the following subsections. Case III is easily deduced from II. Case IV yields zeros (for this line section, though not necessarily for the whole element). Finally, Case V introduces additional diagonal terms. (Note that a point lies inside the forward Mach cone if the cutoff function F defined under Eq. (80) is positive).

The following transformation of coordinates is used in the plane element ℓ^*

$$X = E_{1,2} \{X'(X_2 - X_1) - \beta^2 S'(S_2 - S_1)\} / R_{1,2} \quad (110)$$

$$S = E_{1,2} \{X'(S_2 - S_1) + S'(X_2 - X_1)\} / R_{1,2} \quad (111)$$

$$dXdS = dX'dS' \quad (112)$$

where X_1, S_1 , and X_2, S_2 are the coordinates of the points 1, 2 and 3

$$R_{1,2} = \sqrt{|(X_2 - X_1)^2 + \beta^2(S_2 - S_1)^2|} \quad (113A)$$

and

$$\begin{aligned} E_{1,2} &= 1 \text{ if } (X_2 - X_1)^2 + \beta^2(S_2 - S_1)^2 > 0 \\ &= -1 \text{ if } (X_2 - X_1)^2 + \beta^2(S_2 - S_1)^2 < 0 \end{aligned} \quad (113B)$$

In the supersonic case, $E_{1,2}$ in Eq. (113) is negative unity if the line from point no. 1 to point no. 2 makes a smaller angle with the S-axis than does the Mach line. Also, $R_{1,2}$ is zero when the line between the two points is parallel to a Mach line. This case is discussed later.

The inverse transformation to Eqs. (110) to (111) is

$$X' = \{X(X_2 - X_1) + \beta^2 S(S_2 - S_1)\} / R_{1,2} \quad (114)$$

$$S' = \{-X(S_2 - S_1) + S(X_2 - X_1)\} / R_{1,2} \quad (115)$$

In terms of the new coordinates,

$$R = \sqrt{E_{1,2}X'^2 + \beta^2 E_{1,2}S'^2 + N^2} \quad (116)$$

In the subsonic case the transformation can be represented by the following three transformations applied in order:

- (1) A Prandtl-Glauert Transformation
- (2) A rotation of axes so that the line from points 1 to 2 is parallel to the X' axis.
- (3) An inverse Prandtl-Glauert transformation.

In the supersonic case, the corresponding transformation which transforms the equations to rectangular hyperbolic is used (See, for example, the report by Heaslet and Lomax (ref. 32)), but the factor $E_{1,2}$ is introduced to avoid the use of imaginary numbers.

It is readily shown that

$$dX = \frac{E_{1,2}(X_2 - X_1)}{R_{1,2}} dX' - \frac{\beta^2 E_{1,2}(S_2 - S_1)}{R_{1,2}} dS' \quad (117)$$

$$dS = \frac{E_{1,2}(S_2 - S_1)}{R_{1,2}} dX' + \frac{E_{1,2}(X_2 - X_1)}{R_{1,2}} dS' \quad (118)$$

also that

$$\int dX' = E_{1,2} R_{1,2} \quad (119)$$

$$\int dS' = 0 \quad (120)$$

Note that it is possible for X' to be positive in the forward Mach cone, whereas X is always negative, as illustrated in Figure 38. A useful method of evaluating integrals can be derived from the following:

$$\left\{ \beta^2 \frac{\partial}{\partial X^2} + \beta^2 \frac{\partial}{\partial S^2} + \beta^2 \frac{\partial}{\partial N^2} \right\} \frac{1}{R} = \begin{cases} 4\pi \delta(0,0,0); & M < 1 \\ 2\pi \delta(0,0,0); & M > 1 \end{cases} \quad (121)$$

Case I. no Mach cone intersection.-

"F" integrals of the first kind: These integrals have the general form given in Eq. (106), but with $U(F) = 1$.

To cover the zero pressure case, with $f = 1$, we require $m = 0, 1$; $n = 0$

$$(a) \quad F'_{0,0} = \iint \frac{\partial^2}{\partial N^2} \left\{ \frac{1}{R} \right\} dXdS$$

Substituting from Eq. (121), using Green's Theorem (ref.21), and then Eqs. (114) and (115)

$$\begin{aligned} F'_{0,0} &= -\iint \left\{ \beta^2 \frac{\partial^2}{\partial X^2} + \frac{\partial^2}{\partial S^2} \right\} \left\{ \frac{1}{R} \right\} dXdS \\ &= -\beta^2 \oint \frac{\partial}{\partial X} \left\{ \frac{1}{R} \right\} dS + \oint \frac{\partial}{\partial S} \left\{ \frac{1}{R} \right\} dX \\ &= -\beta^2 \oint \frac{\partial}{\partial X'} \left\{ \frac{1}{R} \right\} dS' + \oint \frac{\partial}{\partial S'} \left\{ \frac{1}{R} \right\} dX' \end{aligned} \quad (122)$$

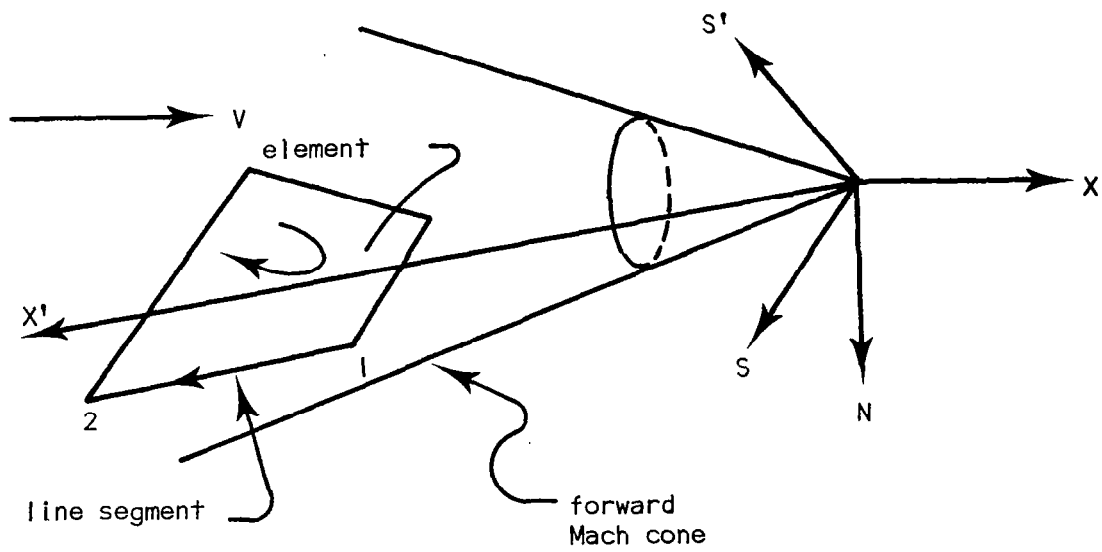


Figure 38. Case of Positive X' in Forward Mach Cone

Taking the straight line from point no. 1 to point no. 2 which is parallel to the X' axis, dS' is zero. Thus,

$$\left\{ F_{0,0}' \right\}_1^2 = \int_1^2 \frac{\partial}{\partial S'} \left\{ \frac{1}{R} \right\} dX' = \left[\frac{-E_{1,2} X' S'}{R(E_{1,2} S'^2 + N^2)} \right]_1^2 \quad (123)$$

It is convenient to leave the integral in this form since, for computer evaluation, X', S' can be found readily.

$$(b) \quad F_{1,0}' = \iint X' \frac{\partial^2}{\partial N^2} \left\{ \frac{1}{R} \right\} dXdS$$

Applying the same substitutions as before, together with Eq. (110), and using the rule for differentiation of products, one has

$$\begin{aligned} \left\{ F_{1,0}' \right\}_1^2 &= \frac{E_{1,2}(X_2 - X_1)}{R_{1,2}} \int_1^2 X' \frac{\partial}{\partial S'} \left\{ \frac{1}{R} \right\} dX' \\ &\quad - \frac{\beta^2 E_{1,2} S' (S_2 - S_1)}{R_{1,2}} \int_1^2 \frac{\partial}{\partial S'} \left\{ \frac{1}{R} \right\} dX' + \frac{\beta^2 E_{1,2} (S_2 - S_1)}{R_{1,2}} \int_1^2 \frac{dX'}{R} \\ &= \left[\frac{\beta^2 S'}{R R_{1,2}} \left\{ E_{1,2}(X_2 - X_1) + \frac{X' S' (S_2 - S_1)}{(E_{1,2} S'^2 + N^2)} \right\} \right. \\ &\quad \left. + \frac{\beta^2 \sqrt{E_{1,2}} (S_2 - S_1)}{R_{1,2}} \log \left\{ \sqrt{E_{1,2}} X' + R \right\} \right]_1^2 \quad (124) \end{aligned}$$

Note that the last term in Eq. (124) is complex if $E_{1,2}$ is negative. Evaluation of the integrals in Eqs. (123) and (124) is facilitated by the standard integrals of Appendix B.

"F" Integrals of the second kind: These "F" integrals have the general form given in Eq. (107):

$$(a) \quad F_{0,0}'' = \iint \frac{\partial^2}{\partial N \partial S} \left\{ \frac{1}{R} \right\} dXdS$$

Integrating first with respect to dS

$$F_{0,0}'' = - \oint \frac{\partial}{\partial N} \left\{ \frac{1}{R} \right\} dX \quad (125)$$

then transforming and taking the straight line element from point 1 to 2

$$\begin{aligned} \left\{ F_{0,0}'' \right\}_1^2 &= - \frac{E_{1,2}(X_2 - X_1)}{R_{1,2}} \int_1^2 \frac{\partial}{\partial N} \left\{ \frac{1}{R} \right\} dX' \\ &= \left[\frac{E_{1,2}NX'(X_2 - X_1)}{RR_{1,2}(E_{1,2}S'^2 + N^2)} \right]_1^2 \end{aligned} \quad (126)$$

$$(b) \quad F_{1,0}'' = \iint X \frac{\partial^2}{\partial N \partial S} \left\{ \frac{1}{R} \right\} dXdS$$

As before, for the straight line element from point 1 to 2:

$$\begin{aligned} \left\{ F_{1,0}'' \right\}_1^2 &= - \frac{E_{1,2}(X_2 - X_1)^2}{(R_{1,2})^2} \int_1^2 X' \frac{\partial}{\partial N} \left\{ \frac{1}{R} \right\} dX' \\ &\quad + \frac{\beta^2 S'(X_2 - X_1)(S_2 - S_1)}{(R_{1,2})^2} \int_1^2 \frac{\partial}{\partial N} \left\{ \frac{1}{R} \right\} dX' \\ &= \left[- \frac{\beta^2 N(X_2 - X_1)}{R(R_{1,2})^2} \left\{ E_{1,2}(X_2 - X_1) + \frac{X'S'(S_2 - S_1)}{(E_{1,2}S'^2 + N^2)} \right\} \right]_1^2 \end{aligned} \quad (127)$$

Case II with Mach cone intersection.— Let point C lie on the intersection of the forward Mach cone with a straight line path from points 1 to 2 so that point no. 2 lies outside of the cone. The integrands of the "I" and "J" integrals are now zero beyond point C, but most of their terms are singular at C. This arrangement is illustrated in Figure 39.

First note, that when point no. 2 is outside the Mach cone, function $U(F)$ goes from unity to zero at a point C which lies between points 1 and 2 as shown in Figure 39. Then, since the derivative of the step function is the Dirac delta function $\delta(X)$, it follows that for any function $Y(X)$

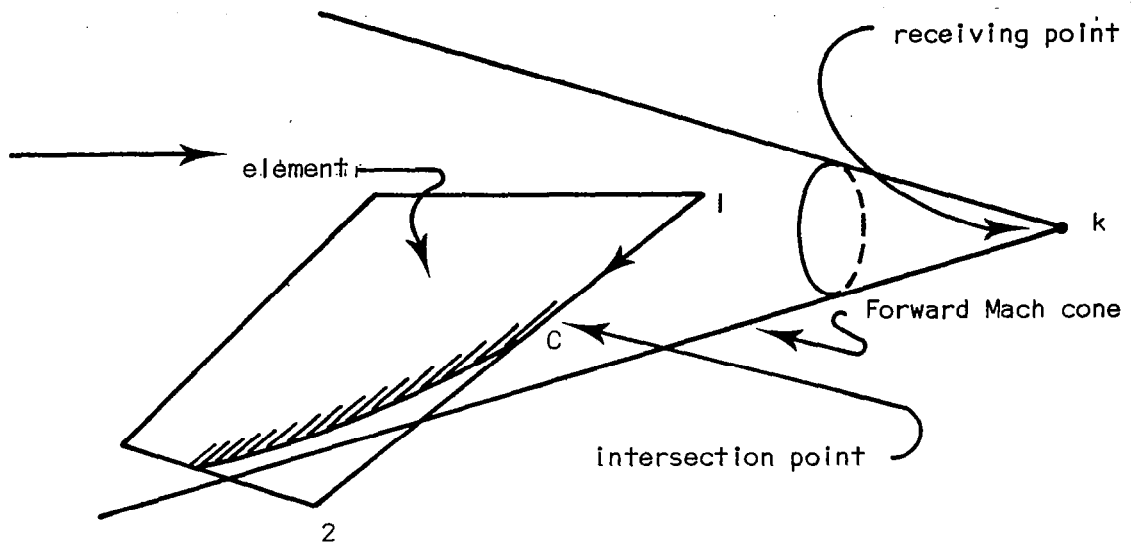


Figure 39: Intersection with Forward Mach Cone

$$\int Y(X) \partial U(X)/\partial X dX = \int Y(X) \delta(X) dX = Y(0)$$

In the more general form, applicable to the case in point

$$\begin{aligned} & \int Y(X,S,N) \frac{\partial}{\partial \alpha} U \{F(X,S,N)\} dX \\ &= Y(X,S,N) \frac{\partial F/\partial \alpha}{1 \partial F/\partial X} \Big|_C \end{aligned} \quad (128)$$

where α is X , S or N . Equation (116) for R can be factored in the form

$$R = \sqrt{-E_{1,2} F' F'_A} \quad (129)$$

where

$$F' = -X' - \sqrt{-\beta^2 S'^2 - \beta^2 E_{1,2} N^2} \quad (130A)$$

$$F'_A = X' - \sqrt{-\beta^2 S'^2 - \beta^2 E_{1,2} N^2} \quad (130B)$$

It is not easy to identify the cut-off function for the forward Mach cone. For the following derivation, it will be assumed that it is F' as given by Eq. (130A), which would be the case if points 1 and 2 were aligned in a positive direction along the X axis.

Note that, at a point C on the forward Mach cone

$$X'_C = -\sqrt{-\beta^2 S'^2_C - \beta^2 N^2_C} \quad (131)$$

First, the following indefinite integral is evaluated at C

$$\begin{aligned} \int \frac{\partial}{\partial S'} \left\{ \frac{U(F')}{R} \right\} dX' \Big|_C &= \int \left\{ \frac{1}{R} \frac{\partial U(F')}{\partial S'} - \frac{\beta^2 U(F') S'}{R^3} \right\} dX' \Big|_C \\ &= \left\{ \frac{\beta^2 S'}{R \sqrt{-\beta^2 S'^2 - \beta^2 N^2}} - \frac{\beta^2 X' S'}{R(\beta^2 S'^2 + \beta^2 N^2)} \right\} \Big|_C \end{aligned}$$

$$= - \frac{\beta^2 R S'}{X'(\beta^2 S'^2 + \beta^2 N^2)} \Big|_C = 0 \quad (132)$$

By interchanging variables

$$\int \frac{\partial}{\partial N} \left\{ \frac{U(F')}{R} \right\} dX' \Big|_C = 0 \quad (133)$$

Also, the following indefinite integral

$$\begin{aligned} \int X' \frac{\partial}{\partial S'} \left\{ \frac{U(F')}{R} \right\} dX' \Big|_C \\ = \left\{ \frac{\beta^2 S' X'}{R \sqrt{\beta^2 S'^2 + \beta^2 N^2}} - \int \frac{\beta^2 U(F') X' S'}{R^3} dX' \right\} \Big|_C \\ = \left\{ - \frac{\beta^2 S'}{R} + \frac{\beta^2 S'}{R} \right\} \Big|_C = 0 \end{aligned} \quad (134)$$

Again, by interchanging variables

$$\int X' \frac{\partial}{\partial N} \left\{ \frac{U(F')}{R} \right\} dX' \Big|_C = 0 \quad (135)$$

It follows from Eqs. (132) to (135) that all of the singular terms in the "F" integrals vanish on the Mach cone. Presumably, the same results would follow from the application of the method of determining the principal values of Improper integrals given by Mangler (ref. 33).

"F" integrals of the first kind with Mach cone intersection:

$$(a) \quad F'_{0,0} = \iint \frac{\partial^2}{\partial N^2} \left\{ \frac{U(F')}{R} \right\} dX dS$$

Proceeding as for Eq. (123) but substituting from Eq. (132)

$$\left\{ F'_{0,0} \right\} = \int_1^2 \frac{\partial}{\partial S'} \left\{ \frac{U(F')}{R} \right\} dX' = \frac{E_{1,2} X' S'}{R(E_{1,2} S'^2 + N^2)} \Big|_1 \quad (136)$$

Thus an element in the form of a polygon would have contributions from the vertices inside the forward Mach cone only.

$$(b) \quad F'_{1,0} = \iint X \frac{\partial^2}{\partial N^2} \left\{ \frac{U(F)}{R} \right\} dXdS$$

As for Eq. (124) but substituting from Eqs. (133) and (134)

$$\left\{ F'_{1,0} \right\}_1^2 = - \frac{\beta^2 S'}{RR_{1,2}} \left\{ E_{1,2}(X_2 - X_1) + \frac{X'S'(S_2 - S_1)}{(E_{1,2}S'^2 + N^2)} \right\} \Big|_1^C + \left[\frac{\beta^2 \sqrt{E_{1,2}}(S_2 - S_1)}{R_{1,2}} \log \{ \sqrt{E_{1,2}} X' + R \} \right]_1^C \quad (137)$$

Thus there is a contribution at point C from the finite term.

"F" integrals of the second kind with Mach cone intersection:

$$(a) \quad F''_{0,0} = \iint \frac{\partial^2}{\partial N \partial S} \left\{ \frac{U(F)}{R} \right\} dXdS$$

As for Eq. (126), but substituting from Eq. (133)

$$\left\{ F''_{0,0} \right\}_1^2 = - \frac{E_{1,2}NX'(X_2 - X_1)}{RR_{1,2}(E_{1,2}S'^2 + N^2)} \Big|_1 \quad (138)$$

$$(b) \quad F''_{1,0} = \iint X \frac{\partial^2}{\partial N \partial S} \frac{U(F)}{R} dXdS$$

Again, as for Eq. (127), but substituting from Eqs. (133) and (134)

$$\left\{ F''_{1,0} \right\}_1^2 = \frac{\beta^2 N(X_2 - X_1)}{R(R_{1,2})^2} \left\{ E_{1,2}(X_2 - X_1) + \frac{X'S'(S_2 - S_1)}{(E_{1,2}S'^2 + N^2)} \right\} \Big|_1 \quad (139)$$

"K" integrals of first and second kind: In order to evaluate the "J" integrals, we first define the "K" integrals which are similar to the "F" integrals of Eqs. (106) and (107)

$$K'_{m,n} = \iint X^m S^n \frac{\partial^2 U(F)}{\partial N^2} dX dS \quad (140)$$

$$K''_{m,n} = \iint X^m S^n \frac{\partial^2 U(F)}{\partial N \partial S} dX dS \quad (141)$$

Then, for example, if $f(l^*, X, S) = 1$, we have

$$J''(k, l^*) = \sum_{i=1}^N \left\{ K''_{0,0} \right\}_i^{i+1} \quad (142)$$

There is evidently no contribution except at a Mach cone intersection.

$$(a) \quad K'_{0,0} = \iint \frac{\partial^2 U(F)}{\partial N^2} dX dS$$

As for $F'_{0,0}$ in Eq. (123)

$$\begin{aligned} \left\{ K'_{0,0} \right\}_1^2 &= \int_1^2 \frac{\partial U(F')}{\partial S'} dX' \\ &= \left. \frac{-\beta^2 S'}{\sqrt{-\beta^2 S'^2 - \beta^2 N^2}} \right|_C = - \left. \frac{\beta^2 S'}{X'} \right|_C \end{aligned} \quad (143)$$

Note that the sign would be reversed if the point 1 were outside the Mach cone, and point 2 were inside.

$$(b) \quad K''_{0,0} = \iint \frac{\partial^2 U(F)}{\partial N \partial S} dX dS$$

As for $F''_{0,0}$ in Eq. (126)

$$\begin{aligned} \left\{ K''_{0,0} \right\} &= \frac{E_{1,2}(X_2 - X_1)}{R_{1,2}} \int_1^2 \frac{\partial U(F')}{\partial N} dX' \\ &= \left. \frac{\beta^2 (X_2 - X_1) N}{R_{1,2} X} \right|_C \end{aligned} \quad (144)$$

Additional Supersonic Terms

In evaluating the "I" and "J" integrals of Eqs. (100) to (105), the RH term of Eq. (121) was omitted. The term k''_ϕ in Eq. (99) replaces this, and must be evaluated for supersonic flows.

In the original calculations for rectangular elements, the collocation points were placed directly over the lifting lines, as shown in Fig. 5. However, the procedure for calculating k''_ϕ could be described as follows: The wing is divided up into rectangular winglets, as in Hedman's method for the subsonic case, (see Fig. 14) but, in place of the lift lines at the quarter chords and the collocation points at the three-quarter chords of the winglets, the lift line and collocation point are both placed at mid-chord. Then, for the purpose of calculating the effect of a lift-line directly on the collocation point with which it coincides, the lift line is replaced by the same total lift uniformly distributed over the element. Because we are actually concerned with an aerodynamic matrix which relates velocity potential to downwash, the resulting matrix has some off-diagonal terms. The lift and downwash on a two-dimensional supersonic wing are directly related through the so-called "Ackeret result" (reference 4), so that the wing section consistent with a lift-line is stepped, nevertheless, the procedure outlined above gives correct lift and moment when applied to two-dimensional wings. As with the subsonic case, the simplified method used for rectangular elements will no longer be as effective when applied to arbitrary elements.

Numerical Problems in Computation

In evaluating the expressions for the "F" and "K" integrals, numerical problems may arise in the computer due to division by zero in such cases as the following:

- (a) $R = 0$
- (b) $S' = N = 0$
- (c) $R_{1,2} = 0$

It will be necessary to take care of these cases either by taking special precautions during preparation of input by programming additional computer logic.

(a) $R = 0$. This occurs when there is a collocation point k on a vertex of an

element. This situation should be avoided. In the supersonic case, it may be that R is very nearly zero because a vertex is nearly on the Mach cone. If $R < \epsilon$, where ϵ is an arbitrary small number, calculations should proceed as though the Mach cone is intercepted.

(b) $S' = N = 0$. This occurs when the collocation point is on the extension of a side of an element. It can easily be shown from Eq. (115) that, if S' is zero anywhere on a straight line element, it is zero all along it. If $N = 0$ also, this could lead to division by zero in all four integrals. In all such cases, however, the limiting contributions are zero. Therefore, on the computer, terms with $S'^2 + N^2$ in the denominator can be disregarded when $S'^2 + N^2$ is small.

(c) $R_{1,2} = 0$. This occurs when the line segment is parallel to a Mach line. Since $R_{1,2}$ appears in the denominators of X' and S' , the limiting expressions must be evaluated carefully. Resulting limits on Eqs. (123), (124), (126) and (127) are,

$$\{F'_{0,0}\}_1^2 \rightarrow \left[\frac{-\bar{X}'}{\bar{S}'R} \right]_1^2 \quad (145)$$

$$\{F'_{1,0}\}_1^2 \rightarrow \left[\frac{\beta^2 S}{R} \right]_1^2 \quad (146)$$

$$\{F''_{1,0}\}_1^2 \rightarrow \left[\frac{N\bar{X}'(X_2 - X_1)}{R(\bar{S}')^2} \right]_1^2 \quad (147)$$

$$\{F''_{1,0}\}_1^2 \rightarrow \left[-\frac{\beta^2 NS(X_2 - X_1)}{R\bar{S}'} \right]_1^2 \quad (148)$$

where \bar{X}' and \bar{S}' are evaluated as for X' and S' but with $R_{1,2}$ taken as equal to unity.

Comparison of Extended Method with Previous Results

As was pointed out earlier, it is only possible to make a comparison of the final expressions for the in-plane case. However, for parallel airfoils (where angles γ , g are equal), Eqs. (82) and (88) can be written as follows:

$$K_{\phi} = \left\{ \beta^2/R^2 + i\omega/cR \right\} \bar{G}_R + \left\{ -N^2/R^2 \right\} \left\{ 3\beta^4/R^2 + 3i\omega\beta^2/cR - \omega^2/c^2 \right\} \bar{G}_R \quad (149)$$

This agrees with Eq. (7), after substitution from Eqs. (17) and (18) and taking T_1 equal to unity and T_2 equal to $-N^2/R$.

In the case of an in-plane airfoil, Eq. (92) can be written in a form directly comparable with Eq. (35)

$$k_{\phi}(k, \ell, \ell^*) = \left[\left\{ \frac{I_0'(k, \ell^*)}{4\pi} \right\} \left\{ 1 + \frac{i\omega R(k, \ell^*)}{\beta^2} + \frac{i\omega X(\ell^*)}{\beta^2 V} \right\} - \left\{ \frac{i\omega}{V} \right\} \left\{ \frac{I_1'(k, \ell^*)}{4\pi\beta^2} \right\} \exp \left\{ -\frac{i\omega}{\beta^2 V} [MR(k, \ell^*) + X(\ell^*) - \beta^2 X(\ell)] \right\} \right] \quad (150)$$

Now from Eqs. (26) and (93) with f equal to unity

$$\begin{aligned} \frac{I_0'(k, \ell^*)}{4\pi} &= \frac{1}{4\pi} \iint_{\ell^*} \frac{\partial^2}{\partial N^2} \left\{ \frac{1}{R} \right\} dXdS \\ &= \frac{-\beta^2}{4\pi} \iint_{\ell^*} \left\{ \frac{1}{R^3} \right\} dXdS \\ &= k_{SS}(k, \ell^*) \end{aligned} \quad (151)$$

also, from Eq. (32) and (94) with f equal to unity

$$\frac{-I_1'(k, \ell^*)}{4\pi} = -\frac{1}{4\pi\beta^2} \iint_{\ell^*} X \frac{\partial^2}{\partial N^2} \left\{ \frac{1}{R} \right\} dXdS$$

$$= \frac{1}{4\pi} \iint_{\ell^*} \frac{X}{R^3} dXdS = k_{US}(k, \ell^*) \quad (152)$$

Substituting back from Eqs. (151) and (152) into (150), it is found that the expression k_ϕ is identical to that given by Eqs. (19) and (35). Thus the extended method leads to expressions which are identical to those developed earlier when parallel, zero pressure elements are used. As a further verification, Eqs. (151) and (152) can be compared directly for the rectangular element shown in Figure 40. First, we evaluate I_0' according to Eqs. (108) and (123). The contribution of each point comes from two terms. Transforming, using Eqs. (114) and (115), and noting that $(X_B - X_A)$ and $(S_C - S_B)$ are both zero, we have the following:

$$\begin{aligned} \frac{I_0(k, \ell^*)}{4\pi} &= \frac{1}{4\pi R_A} \left\{ -\frac{X_A}{S_A} - \frac{\beta^2 S_A}{X_A} \right\} + \dots = -\left(\frac{X_A^2 + \beta^2 S_A^2}{4\pi R_A X_A S_A} \right) + \dots \\ &= -\frac{R_A}{4\pi X_A S_A} + \frac{R_B}{4\pi X_B S_B} - \frac{R_C}{4\pi X_C S_C} + \frac{R_D}{4\pi X_D S_D} \end{aligned} \quad (153)$$

where R_A is R evaluated at the point A . The above expression is identical to that for k_{SS} given in Eq. (26). Using the same approach in dealing with I_1' and substituting from Eq. (124), the contributions of the first two terms cancel at each point. This leaves only the contributions of the logarithmic expression along the lines A to B and C to D . Thus,

$$\frac{I_1'(k, \ell^*)}{4\pi\beta^2} = \left[\frac{1}{4\pi\beta} \log(\beta S + R) \right]_A^B - \left[\frac{1}{4\pi\beta} \log(-\beta S + R) \right]_C^D \quad (154)$$

It can, however, be shown that

$$-\log(-\beta S + R) = \log(\beta S + R)$$

therefore the above expression is identical to that given for k_{US} in Eq. (32).

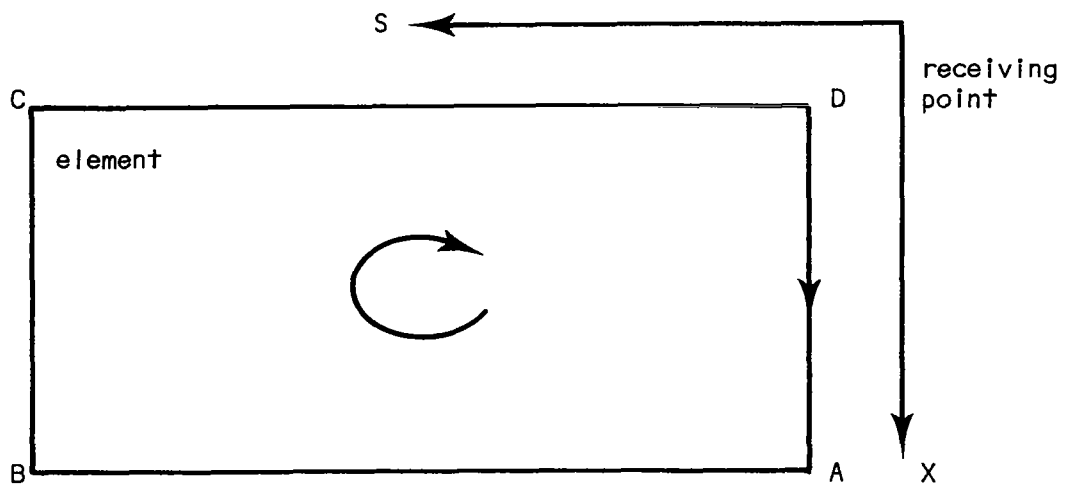


Figure 40: Derivation of I'_O for Rectangle

Only the steady state in-plane case has been previously developed for supersonic flow. From Eqs. (46) and (99), we now have

$$k_{\phi}(k, l^*) = 2k_{SS}(k, l^*) = 2I_0'(k, l^*)/4\pi \quad (155)$$

Comparing Eqs. (153) and (56) it is seen that the extended method is compatible in the supersonic case also.

In summary, it has been shown that the methods given in this section are identical to those given previously when applied to in-plane, first order, zero pressure, rectangular elements in the subsonic case and to in-plane, steady state, rectangular elements in the supersonic case. Computations based on both of these cases have already been evaluated. The extended method would give identical results in the cases discussed.

Computer Program

The expressions developed here could be included as new elements in the computer program described in Appendix A. However, it would be considerably less time consuming to precompute as much as possible and then to calculate the aerodynamic matrix from the precomputed data for each value of ω . An examination of Eqs. (92) and (99) shows that the aerodynamic matrix $A_{k,l}$ could be written as follows:

$$A_{k,l} = \{A'_{k,l} + \omega A''_{k,l} + i\omega A'''_{k,l}\} \exp i\omega L(k,l) + k''_{\phi}(k, l, l) + \sum (l^*) k_{\phi}(k, l, l^*) \quad (156)$$

In the above expressions, five real matrices of the same size as $A_{k,l}$ are required. The indicated summation is over wake elements which can be rectangular, and can therefore be evaluated more rapidly than polygonal elements.

In the present program, the normal flow (downwash) at each collocation point is assumed to be known, and generalized forces are calculated after the velocity potentials have been solved. The same could be done with the extended

method; however, since the aerodynamic elements can now be made to conform with structural elements, it might be better to determine location and downwash of the collocation point from deflections at structural nodes and, finally to compute equivalent forces at the nodal points. If zero pressure elements are used, the forces act along the perimeter. The force per unit length on a line element when taken right-handed is proportional to its projection along the σ axis. It is thus in the negative direction (i.e. opposite to the positive normal coordinate v) when the projection of the line is positive.

Thus if dF is an element of force on the perimeter, as shown in Figure 41,

$$dF = \rho v^2 \Delta \phi_\ell \exp \left\{ -\frac{i\omega}{V} [\xi - \xi(\ell)] \right\} d\sigma \quad (157)$$

Missing Term

A first order expression is used to replace the exponential terms before integration. However, a term in $(\omega N/c)^2$, where N is the normal distance from collocation point to sending surface, is ignored (this cannot be expressed by a contour integral). If it should later prove to be important, it may be necessary to evaluate the surface integral by its midpoint value using the approach described previously.

Summary of Extended Method

The principal aim of this section has been to develop the expressions for arbitrary out-of-plane polygon aerodynamic elements. Each expression is in the form of a contour integral so that it is only necessary to compute the contribution of each straight-line element. The expressions developed are generally applicable for subsonic and supersonic flow, but special steps are necessary when a line element intercepts the forward Mach cone from a receiving point.

This method has been proven to be identical to the one developed and checked out earlier in this report when applied to in-plane surfaces. Thus, much of the experience acquired to date remains valid.

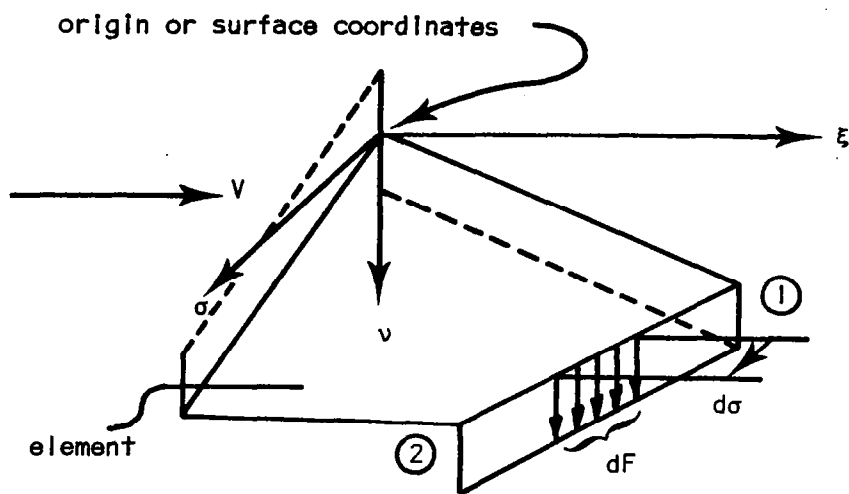


Figure 41: Aerodynamic Forces

The problem of defining the Ackeret lift term is not discussed in detail because it is believed to require considerable numerical experimentation and careful programming. Certainly, the idea that the pressure at a given point contributes directly to the flow at that point is straightforward. Also, the problem of finding optimum ways of locating collocation points has not been discussed. In the applications to rectangular elements discussed earlier, special schemes were used for locating collocation points and the rectangles themselves. However, if the aerodynamic elements are to be compatible with structural elements, such favorable arrangements will no longer be possible. Computed results may thus turn out to be unreliable because the normal flow distribution corresponding to constant potential or zero pressure elements is singular on the edges of the elements on which there are finite vortices. If selection of collocation points were arbitrary, then it would be necessary to use more uniform potential distributions so that finite vortices could be eliminated. The polynomial forms envisioned in Eqs. (106) and (107) might possibly prove adequate for this purpose.

CONCLUDING REMARKS

In the present investigation, a numerical method has been developed on the basis of the linearized theory by which the generalized airforce matrix can be calculated for steady or oscillating wings in subsonic and supersonic flows. The use of the downwash-velocity potential relationship in preference to more commonly employed downwash-pressure relationship gives a somewhat simplified form of the kernel function. The approximations made in the evaluation of the integrals involved avoid some of the difficulty incurred in evaluating the improper integrals. Thus, one of the advantages of the method proposed here is numerical simplicity in comparison to other existing methods. The present method has been tested quite extensively for rectangular elements in steady and unsteady cases in subsonic flows. Its application in supersonic flow has been limited to steady planar rectangular wings. The results of these calculations are summarized in the following paragraphs.

It has been demonstrated that accurate results can be obtained for cases of steady and oscillating planar rectangular wings in subsonic flows using the downwash-velocity potential method. Among the three types of aerodynamic

elements evaluated, the best results were obtained with the so called "first order, zero pressure" rectangular elements, followed by "first order, constant potential" rectangular elements. The "zero order, constant potential rectangular elements, although considerably simpler than the other two types of elements provided the least favorable results. Results appear to be convergent with respect to the total number of boxes used. The wake can safely be terminated in five chord lengths or less.

The lift distributions on rectangular and tapered wings in subsonic flows indicate that the use of rectangular elements gives excess lift towards the tips. It has been found that the distribution improves with shorter spanwise divisions towards the tips (given a limitation on the total number of elements to be used). All other results, including the distribution of the center of pressure, and various coefficients, have shown that this method gives results comparable to those resulting from other methods of analysis.

Calculations for oscillating swept wings and for swept wings with flaps using rectangular elements have been compared with those made by other methods. It appears that, when the rectangular elements are used, the agreement of the swept wing results with the referenced values is not as good as in the case of rectangular wings. Improvement was noticed as smaller elements were used towards the tip, but satisfactory agreement has still not been obtained at high subsonic speeds. It is believed that these results indicate a need for elements conforming to the planform such as those that have been developed in the so-called extended method. The flap moment coefficients show fair agreement with the referenced values. However, the results are limited to 18 collocation points, except in one case where 40 points were used.

Fair agreement has been obtained with other results published in the literature for two-T-tail configurations using midpoint integration for out-of-plane terms. As the number of elements is increased, however, agreement first improves and then gets worse. This appears to result from the use of mid-point integration for out-of-plane elements and indicates a need for the extended method.

The results obtained for steady rectangular wings using in-plane steady supersonic rectangular elements are good, but convergence with the referenced values seems to be slower than in the corresponding subsonic cases.

Because all of these calculations were made using a computer program which contained as subroutines all of the rectangular aerodynamic elements cited in this report, it is believed that the effectiveness of such a concept of aerodynamic elements was demonstrated. In addition, the objective of developing a method valid for subsonic and supersonic flows was partially accomplished. As is shown in the section covering the extended method, this objective has been realized conceptually.

The proposed extended method is capable of reproducing all of the in-plane calculations performed to date. It also appears to have the features necessary for better results on swept wings and out-of-plane cases (such as T-tails). It is therefore concluded that the extended method is potentially capable of handling all calculations relating to oscillating wings.

It is believed that the proposed extended method will contribute greatly to the problem of handling flutter and to other related problems in automated structural design. In particular, the following three points are of significance:

1. The computation procedure is based on the concept of aerodynamic elements. This procedure treats arbitrary panels on the aerodynamic surface which can, therefore, conform to the structural surface panels. Thus, not only can the computed forces employed act at the structural nodes, but, also, the preparation of aerodynamic input data is simplified since it is so similar to the structural input data.
2. This method applies to a broad Mach number range so that one computer program can handle subsonic and supersonic flows.
3. The calculations can be arranged so that if five matrices are computed first, then the flutter forces for the complete reduced frequency range can be calculated rapidly.

RECOMMENDATIONS

It is recommended that the proposed extended method be programmed and tested. Following this, the tasks listed below should be performed,

- (1) Adaptation of the method to the unsteady transonic ($M = 1$) case. Although this adaptation may not result in accurate air force predictions and its usefulness may thus be limited, it is needed to provide a basic linear solution capability against which more refined methods can be compared.
- (2) Investigation to determine the best method of including the Ackeret or "two-dimensional" lift effects in the supersonic case. The method used for the numerical results given in Tables 10 and 11 was selected for convenience but is too restrictive for use in the aerodynamic element concept.
- (3) Determination of optimum chordwise spacing of elements. Thus far, the Hedman (ref. 2) method of locating lift lines has been used exclusively in calculations. Again, this is too restrictive for application to the aerodynamic element concept.
- (4) Development of a set of rules for selecting aerodynamic element configurations to meet given accuracy objectives. To date, only a few variations have been made on rectangular wings and those were made mainly to observe gross effects and to demonstrate convergence.
- (5) Trial inclusion of the method in an automated design computer system. One of the goals in developing this method was to make it possible to compute aerodynamic forces at structural nodes. Therefore, an evaluation of its capability in this application and of its practical application in general would be of great interest.
- (6) Trial development of new aerodynamic elements. It is especially important to investigate arrangements which will eliminate finite vortices since it is expected that they will remove restrictions on collocation point locations.

REFERENCES

1. Haviland, J. K., "Downwash-Velocity Potential Method for Lifting Surfaces," AIAA Journal, Vol. 9, No. 11, November 1971, pp. 2268-9.
2. Hedman, S., "Vortex Lattice Method for Calculation of Quasi Steady State Loadings on Thin Elastic Wings in Subsonic Flow," Flygtekniska Forskingsanstalten (FFA), Stockholm, Sweden, Report No. 105, 1966.
3. Haviland, J. K., Yoo, Y. S., "Downwash-Velocity Potential Method for Oscillating Surfaces," AIAA Journal, Vol. 11, No. 5, May 1973, pp. 607-612.
4. Woodward, F. A., "Analysis and Design of Wing-Body Combinations at Subsonic and Supersonic Speeds," J. Aircraft, Vol. 5, No. 6, November-December 1968, pp. 528-534.
5. Rubbert, P. E., and Saaris, G. R., "Review and Evaluation of a Three-Dimensional Lifting Potential Flow Analysis Method for Arbitrary Configurations," AIAA Paper No. 72-188, presented at the AIAA 10th Aerospace Sciences Meeting, San Diego, California, January, 1972.
6. Watkins, C. E., Runyan, H. L., and Woolston, D. S., "On the Kernel Function of the Integral Equation Relating the Lift and Downwash Distributions of Oscillating Finite Wings in Subsonic Flow," NACA Report No. 1234, 1955.
7. Albano, E., and Rodden, W. P., "A Doublet-Lattice Method for Calculating Lift Distributions on Oscillating Surfaces in Subsonic Flows," AIAA Journal, Vol. 7, No. 2, February 1969, pp. 279-285.
8. Jones, W. P., "The Calculation of Aerodynamic Derivative Coefficients for Wings of any Planform in Non-Uniform Motion," Great Britain, Aeronautical Research Council R&M No. 2470, 1952.
9. Stark, V. J. E., "Calculation of Lifting Forces on Oscillating Wings," (Doctoral Thesis), The Royal Institute of Technology, Department of Aeronautics and Shipbuilding, Stockholm, Sweden.
10. Houbolt, J. C., "Some New Concepts in Oscillatory Lifting Surface Theory," U. S. Air Force, Flight Dynamics Laboratory Technical Report No. AFFDL-TR-69-2, April 1969.
11. Morino, L., and Kuo, C. C., "Unsteady Subsonic Compressible Flow around Finite Thickness Wings," AIAA Paper No. 73-313, March 1973.
12. Rodemich, E. R., and Andrew, L. V., "Unsteady Aerodynamics for Advanced Configurations: Part II-A Transonic Box Method for Planar Lifting Surfaces," U. S. Air Force, Flight Dynamics Laboratory Report No. FDL-TDR-64-152. Part II, May 1965.

13. Donato, V. W., and Huhn, Jr., C. R., "Supersonic Unsteady Aerodynamics for Wings with Trailing Edge Control Surfaces and Folded Tips," U. S. Air Force Flight Dynamics Laboratory Technical Report No. AFFDL-TR-68-30, August, 1968.
14. Watkins, C. E., and Berman, J. H., "On the Kernel Function of the Integral Equation Relating Lift and Downwash Distributions of Oscillating Wings in Supersonic Flow," NACA Report No. 1267, 1956.
15. Harder, R. L., and Rodden, W. P. "Kernel Function for Nonplanar Oscillating Surfaces in Supersonic Flow," J. of Aircraft, Vol. 8, No. 8, pp. 677-679, August 1971.
16. Landahl, M. T. and Stark, V. J. E., "Numerical Lifting Surface Theory - Problems and Progress," AIAA Journal Vol. 6, No. 11, November 1968.
17. Jones, W. P., and Moore, J. A., "Simplified Aerodynamic Theory of Oscillating Thin Surfaces in Subsonic Flow", AIAA Journal, Vol. 11, No. 9, pp. 1305-1309, September 1973.
18. Mercer, J. E., Weber, J. A., and Lesford, E. P., "Aerodynamic Influence Coefficient Method Using Singularity Splines," AIAA Paper No. 73-123, January, 1973.
19. Vivian, H. T., and Andrew, L. V., "Unsteady Aerodynamics for Advanced Configurations, Part I - Application of the Subsonic Kernel Function to Nonplanar Lifting Surfaces," U. S. Air Force, Flight Dynamics Laboratory Report No. FDL-TDR-64-152, Part I, May 1965.
20. Allen, D. J., and Sadler, D. S., "Oscillatory Aerodynamic Forces in Linearized Supersonic Flow for Arbitrary Frequencies, Planforms, and Mach Numbers," British Aeronautical Research Council, Reports and Memoranda No. 3415, January, 1963.
21. Sokolnikoff, I. S., and Redheffer, R. M. "Mathematics of Physics, and Modern Engineering," McGraw-Hill, Inc., 1966, pp. 404-406.
22. Runyan, H. L., and Woolston, D. S., "Method for Calculating the Aerodynamic Loading on an Oscillating Finite Wing in Subsonic and Sonic Flow, NACA Report No. 1322, 1957.
23. Kalman, T. P., Rodden, W. P., and Giesing, J. G., "Aerodynamic Influence Coefficients by the Doublet Lattice Method for Interfering Nonplanar Lifting Surfaces Oscillating in a Subsonic Flow-Part I," McDonnell-Douglas Corporation, Report No. DAC-67977, November 1969.
24. Stark, V. J. E., "A Subsonic Oscillating-Surface Theory for Wings with Partial-Span Controls," AIAA Paper No. 72-61, presented at the AIAA 10th Aerospace Sciences Meeting, San Diego, California, January 1972.
25. Laschka, B., "Zur Theorie der Harmonisch Schwingenden Tragenden Fläche Bei Unterschallanströmung," Zeitschrift für Flugwissenschaften, Vol. 11, No. 7, July 1963, pp. 265-292.

26. Langan, T. J., and Wang, H. T., "Evaluation of Lifting-Surface Programs for Computing the Pressure Distribution on Planar Foils in Steady Motion," Naval Ship Research and Development Center, Report No. 4021, May 1973.
27. Engineering Sciences Data, Item No. 70011 (Aeronautical Series), Engineering Sciences Data Unit, London.
28. Clevenston, S. A., Leadbetter, S. A., "Measurements of Aerodynamic Forces and Moments at Subsonic Speeds on a Simplified T-Tail Oscillating in Yaw about Fin Midchord," NACA, TN 4402, 1958.
29. Stark, V. J. E., "Aerodynamic Forces on a Combination of a Wing and a Fin Oscillating in Subsonic Flow," SAAB, Aircraft Co., Sweden, Report No. TN 54, 1964.
30. Haviland, J. K., "Development of a Supersonic Three-Dimensional Flutter Method," Report No. 00.481, Chance Vought Aircraft, June 1964.
31. Nelson, H. C., Rainey, R. A., and Watkins, C. E., "Lift and Moment Coefficients, Expanded to the Seventh Power of Frequency for Oscillating Rectangular Wings in Supersonic Flow and Applied to a Specific Flutter Problem," NACA Technical Note 3076, April 1954.
32. Heaslet, M. A., and Lomax, H., "The Use of Source-Sink and Doublet Distributions Extended to the Solutions of Boundary-Value Problems in Supersonic Flow," NACA Report No. 900, 1948.
33. Mangler, K. W., "Improper Integrals in Theoretical Aerodynamics," British Royal Aircraft Establishment Report No. Aero. 2424, June 1951.

APPENDIX A

The Computer Program

Introduction.- In order to perform the calculations on the downwash-velocity potential method, a computer program has been written in FORTRAN IV language to be used with CDC 6400 at the University of Virginia Computer Center. Its principal feature is a subroutine to calculate and store the aerodynamic influence matrix which is then inverted and used to calculate generalized forces which result from specified motions of the surfaces.

The program assumes that the user will supply data in the form of a breakdown of each surface into a large number of aerodynamic elements. To date, eight sets of subsonic compressible aerodynamic elements (all rectangular) have been formulated. For uniform size rectangular elements, the required input data can be computed by using subprograms from basic information such as the geometry of the surfaces, their planform arrangements, and the specified motions of these surfaces.

Program Description.-

Summary of Programs:

Main Program:

FLUTT

Subprograms:

DMATR and DREAD

WMAT and WREAD

ACALC and ACON3 through ACON8 and ACON11,12

CMATR and CCON5, 6 and CCON11,12

ALIST

TEST

INVER

Their roles are the following:

FLUTT:

- Reads in data controlling the desired output, controls selection of the subroutines to be used, and specifies integer words, floating

Appendix A

words, and the line counts for each type of data.

- Calculates the addresses for various matrices.
- Reads in Mach numbers and frequencies.

DMATR:

- Generates D vector for uniform size rectangular elements in each strip from the basic information.

DREAD:

- Controls reading in D vector for rectangular elements of nonuniform size.

WMAT:

- Generates W matrix from the modal displacements of each strip.

WREAD:

- Controls reading in W matrix for rectangular elements of nonuniform size.

ACALC:

- Controls retrieval of Data vector using subprogram TEST.
- Determines the conditions of symmetry for each surface.
- Calls for appropriate ACON's to be used.
- Generates A (aerodynamic) Matrix.

ACON5 through ACON8 and ACON11,12

Calculates terms in A matrix by various methods described previously.

CMATR

- Controls retrieval of Data vector by using subprogram TEST.
- Controls retrieval of A and W matrices.
- Calls for appropriate CCON's to be used.
- Calculates velocity potential discontinuity using subprogram INVER to invert A matrix.
- Computes C (flutter airforce) matrix.

Appendix A

CCON5,6 and CCON11,12

- Computes terms in C-matrix.

ALIST:

- Used in printing out various matrices.

TEST:

- Used in retrieval of Data vector for ACALC and CMATR.

INVER:

- Used in inverting A matrix.

Flow Diagram: A functional flow diagram of the computer program is pictured in Figure A-1. The aerodynamic Influence matrix calculated by ACALC is inverted and used to compute generalized forces due to specified motions of the surfaces by CMATR and the appropriate CCONs. The use of generalized forces was found to offer considerable flexibility. For example, it is possible to calculate the flutter airforce matrix or the lift slopes merely by specifying the modal displacements in the correct manner.

DATA Vector: The DATA vector contains the complete physical description of the airfoils and of the aerodynamic elements. Each block of data is designated by a "Type" number, with provisions for 15 types stored sequentially. A mixed integer and floating point format is used with the integers coming first in each line.

The first 60 words of the vector contain information required to identify the 15 types of data stored, and the 61st word represents the total number of lines. The complete vector contains the following:

Identification:

NADD(i) = First address of Type i data (i = 1,...,15).

NFIX(i) = Number of integer words per line of Type i data.

NFL(i) = Number of floating words per line of Type i data.

NL(i) = Number of lines of Type i data.

Appendix A

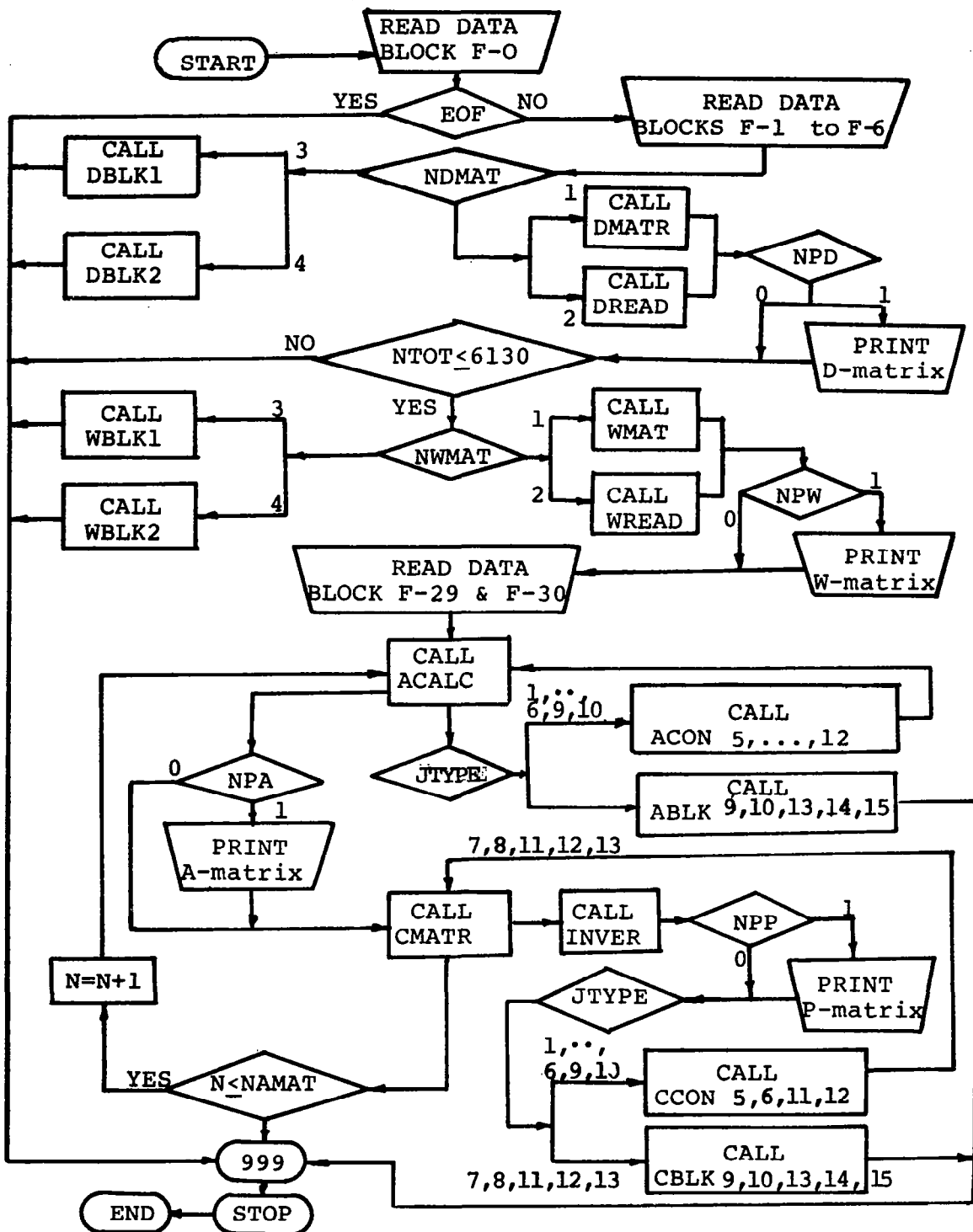


Fig. A-1 Flow Diagram

Appendix A

Type 1: Description of Airfoil Surfaces

NSURL, NSURK = Surface number

NSYMZ = $\begin{cases} 1 & \text{if surface is symmetric about z-axis} \\ -1 & \text{if surface is symmetric about z-axis, but motion is antisymmetric} \\ 0 & \text{if there is no symmetry} \end{cases}$

NSYMY = same as above, but relative to y-axis

NGEOM = number of like surfaces on which aerodynamic forces are calculated

XO = x-origin of surface

YO = y-origin of surface

ZO = z-origin of surface

COSG = $\cos g$

SING = $\sin g$

Type 2: Point Coordinates

L, K = Sending or receiving point number, l or k

NSURL, NSURK = Surface number

XL, XK = x-coordinate

SL, SK = s-coordinate

Type 5,7,11: Aerodynamic Element

L = Sending point number, l

XFOR = Most forward side, X_{FOR}

XAFT = Most rearward side, X_{AFT}

SIN = Inboard edge, S_{IN}

SOUT = Outboard edge, S_{OUT}

Types 6, 8, 12: Aerodynamic Element (Trailing edge)

L = Sending point number, l

NBOXES = Number of regions to be assumed in wake

XFOR, XAFT, SIN, SOUT as above

Element Types 5,6: Mid Point Constant Potential (MPCP)

7,8: First Order, Constant Potential (FOCP)

11,12: First Order, Zero Pressure (FOZP)

Appendix A

A Vector: In order to minimize the use of the core storage, the matrices in complex form are all stored in a one dimensional array A(I). Table A-1 shows the composition of the A vector. The matrices stored in A(I) are described as follows:

A -Matrix

The A-matrix contains the complex aerodynamic matrix $A(k, l)$, and is stored in complex form in the A vector with a blank column to facilitate matrix inversion. The general term is $A(L)$ where $L = (k - 1)(NRP + 1) + l$. The required total storage is $2NRP(NRP + 1)$.

W-Matrix

The W-matrix contains the modal values of the angle of attack, $\alpha(i, k)$, and deflection, $h(i, k)$, at each point k due to mode i stored in the complex form $\alpha(i, k)$, $h(i, k)$. W-matrix is stored in complex form in the A vector.

The general term of W-matrix is $A(NADDW + L)$ where $L = (MODE - 1)NRP + k$ and MODE takes the values 1 to $(NMODE1 + NMODE2)$. NMODE1 is the number of values of column index i in the flutter airforce matrix $C(i, j)$, and NMODE2 is the number of values of column index j in the C-matrix. If NMODE2 is equal to zero, j belongs to the same set of modes as i , and C is a square matrix as used in flutter calculations. This feature simplifies the calculation of lift derivatives and distributions. The total storage required for W-matrix is $2NRP(MODE1 + NMODE2)$.

P-Matrix

The P-matrix contains the complex matrix of potential discontinuities $P(j, k)$ and is stored in complex form in the A vector. Its general term is $A(NADDWF + J3)$ where $NADDWF = ((NRP + 1) + NMODE1 + 2NMODE2)NRP$ and $J3 = NRP(MODE-1) + k$. MODE takes the values 1 to NTEMP where $NTEMP = NMODE2$ and if $NMODE2 = 0$, $NTEMP = NMODE1$. Total storage required is $2NRP(NTEMP)$.

C-Matrix

The C-matrix contains the complex flutter airforce matrix $C(i, j)$ and is stored in complex vector form in the matrix A. Its general term is

Table A-1 Composition of A Vector

A(I)	Address					
	NADDW →	NADDW2 →	NADDW3 →	NADDWF →	NADDC →	NTOT →
Matrix	Aerodynamic Matrix A(k,P) or its Inverse	Modal Matrix w(i, k) for NMODE 1	Modal Matrix w(i, k) for NMODE 2	Same as w(i, k) for NMODE 2 except Imag. part is multi- plied by Freq. ratio (ω/v)	Potential Discont. matrix P(j, k)	Flutter Airforce matrix C(i, j)

$$NADDW = (NRP + 1) NRP$$

$$NADDW2 = NADDW + NRP \times NMODE1$$

$$NADDW3 = NADDW2 + NRP \times NMODE2$$

$$NADDWF = NADDW3 + NRP \times NMODE2$$

$$NADDC = NADDWF + NRP \times NMODE2$$

$$NTOT = NADDC + NMODE1 \times NMODE2$$

Appendix A

Appendix A

$A(NADDC + NTEMP(i-1) + j)$ where $NADDC = NADDWF + NRP*NTEMP$, and $NTEMP$, i and j take the same values as above. The total storage required is $2 NMODE1(NTEMP)$.

Symmetry: For each surface, the condition of symmetry is expressed by the two numbers $NSYMZ$ and $NSYMY$, each having three values. In each case, a nonzero value indicates structural symmetry (the sign indicates whether the downwash normal to the surface is positive or negative, respectively). Thus, there can be four conditions of structural symmetry corresponding to four values of a counter $MSYM$ as shown in Figure A-2. For each value of $MSYM$, values are assigned to the four quantities $KSYMZ$, $KSYMY$, $LSYMZ$, $LSYMY$ as shown. However, when the condition indicated is not met, the counter $MSYM$ skips a value.

To simplify computation, contributions to the A-matrix are obtained by assuming the receiving points to be rotated into the four segments in turn. The sending points remain in the principal segment. This is accomplished by altering the equations developed in Sections II and III by multiplying $\cos g$ $\sin g$, and ΔA by the following factors;

$\cos g$ by $KSYMZ$

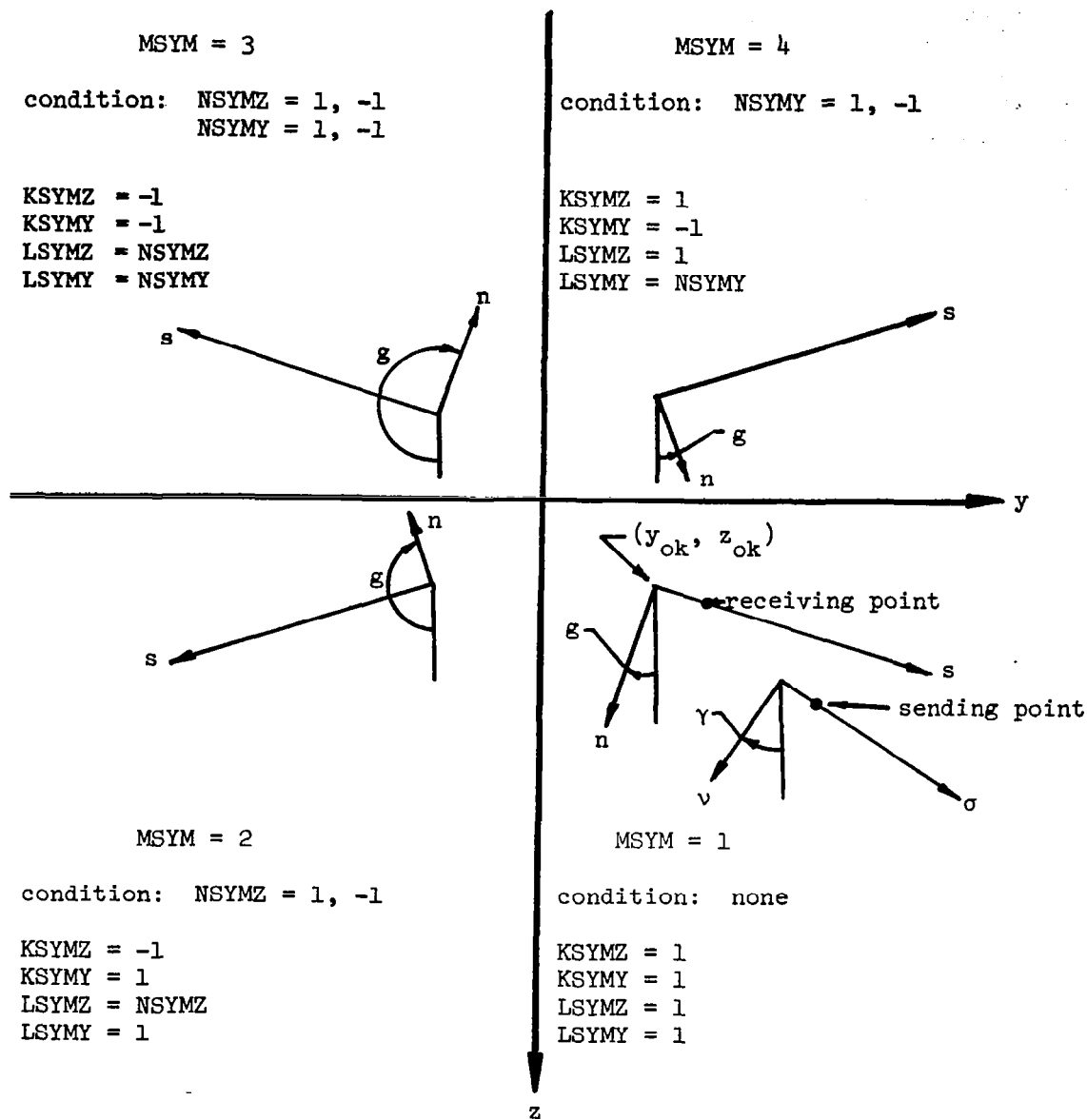
$\sin g$ by $KSYMY$

ΔA by $LSYM = LSYMZ*LSYMY*KSYMZ$

Some examples of possible airfoil combinations together with the appropriate values of $NSYMZ$ and $NSYMY$ are shown in Figure A-3. It should be noted that the symmetry conditions are supplied separately for each airfoil.

Preparation of Input Data: The input data are read by the main program FLUTT and by subprograms DMATR or DREAD, and WMAT or WREAD. The user can choose either DMATR or DREAD for input of Data vector and WMAT or WREAD for input of W matrix. For rectangular elements obtained by breaking up each surface into chordwise strips of varying width and breaking up each strip into equal size rectangular elements, one can use DMATR by supplying the coordinates of each strip and the number of elements to be contained in each strip. The W matrix for surfaces divided into such rectangular elements can be easily generated with the use of WMAT by supplying the modes of motion for each strip. To divide a surface into rectangular elements of nonuniform size, the user should calculate all the required data for D vector and then read them in by DREAD. The corresponding W matrix should also be calculated by the user and then read in by the subprogram WREAD.

Appendix A



Multiply $\cos g$ by KSYMZ; y_{ok} by KSYMZ
 $\sin g$ by KSYMY; z_{ok} by KSYMY
 ΔA by LSYM = LSYMY*LSYMZ*KSYMZ

Figure A-2. Symmetry Conditions

Appendix A

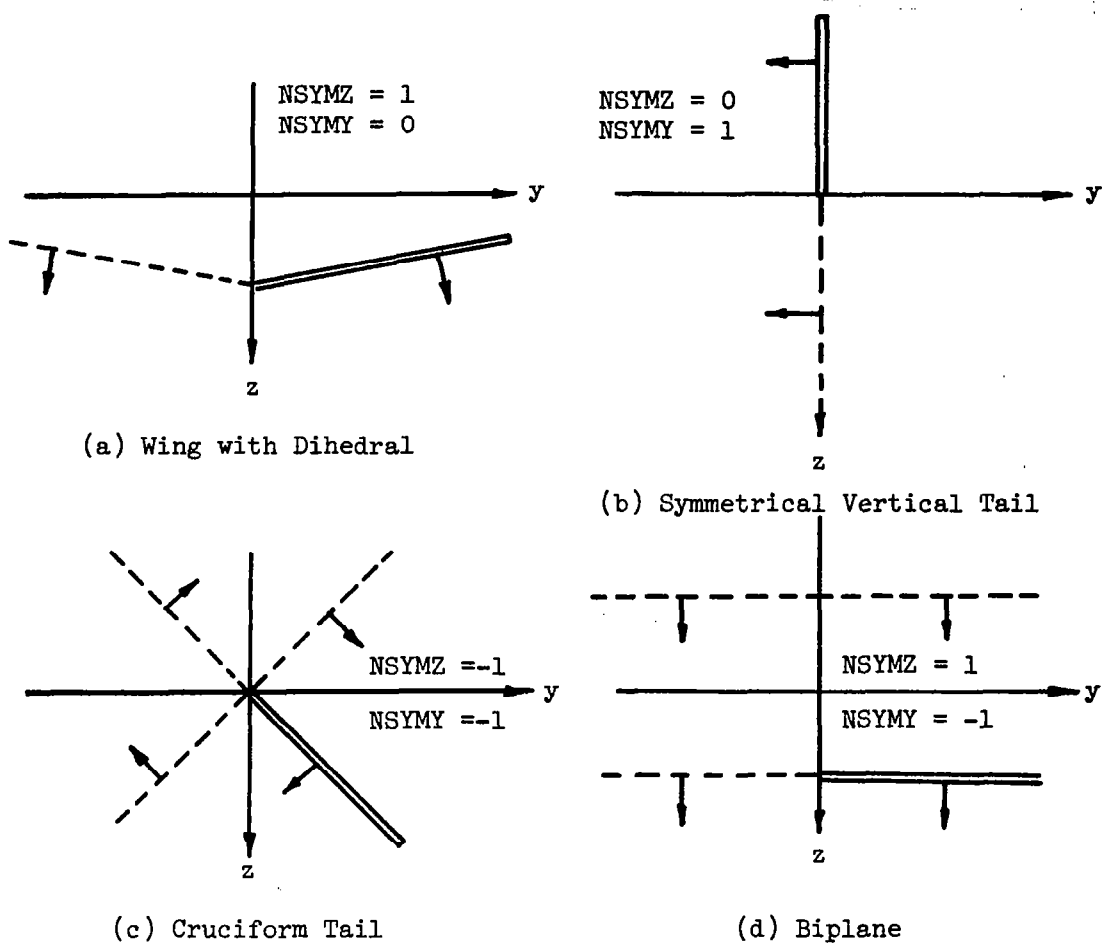


Figure A-3. Examples of Configurations

Note: Surface for which data is supplied
 Surface implied by symmetry conditions
 Direction of downwash

Appendix A

Before attempting to make use of the computer program, one should make the following selections:

- Selection of subprograms to be used: 1) Input for D vector--DMATR or DREAD; 2) Input for W matrix--WMAT or WREAD; 3) Calculation of A matrix--Select aerodynamic elements to be used.
- Desired print out of various matrices.
- Local coordinates for each surface.
- Planforms for each surface.
- Conditions of symmetry for geometry and motion of each surface.
- Numbers of collocation points and chordwise strips.
- Effective wake length.
- Number of repeated runs using same D vector and W matrix for different Mach numbers and frequency ratios.
- Mach numbers and frequency ratios.

The user should also be aware of the inherent limitations in the program as follows (as set by the DIMENSION statements):

- Number of collocation points must be ≤ 72 .
- Number of chordwise strips must be ≤ 14 .
- (Number of modes) X (Number of chordwise strips) must be ≤ 84 .
- Number of surfaces must be ≤ 4 .
- Number of repeated runs must be ≤ 10 .

Data Block F-0

Number of cards = 1; Format (1x, 79Hbbb.....b)

The above is a sample of a title card. Anything placed on this card will be printed as output at the beginning of each run.

Data Block F-1

Number of cards = 1; Format (20 I3)

This block specifies the print out of D, W, A, and P matrices.

1: print, 0: no print

Appendix A

1→3	4→6	7→9	10→12	13→15
IC	NPD	NPW	NPA	NPP

where IC = Card Identification number = 1

NPD = Print-out of D vector

NPW = Print-out of W matrix

NPA = Print-out of A matrix

NPP = Print-out of P matrix

Data Block F-2

Number of cards = 1; Format (20I3)

This block shows the number of integer words per line of Type i data.

Types not used should be equal to zero.

(i = 1, ..., 15).

1→3	4→6	37→39
IC	NFIX i	(i = 1, 2, ..., 15)	

where IC = 2

NFIX1 = 4

NFIX2 = 2

NFIX3 = 0

NFIX4 = 0

NFIX5, 7, 11, = 1 for the type i used

NFIX6, 8, 12 = 2 for the type i used

*** Data Block F-3***

Number of cards = 1; Format (20I3)

This block shows the number of floating words per line of Type i data.

Types not used should be set to zero.

1→3	4→6	37→39
IC	NFL i	(i = 1, 2, ..., 15)	

where IC = 3

NFL1 = 5

NFL2 = 2

NFL3, NFL4 = 0

NFL5, 7, 11, = 4 for the type i used

NFL6, 8, 12 = 4 for the type i used

Appendix A

*** Data Block F-4***

Number of cards = 1; Format (20I3)

This block shows the number of lines for each type of data.

1→3	4→6	37→39
<hr/>			
IC	NLI	(i = 1, 2, ..., 15)	

where IC = 4

NLI = Number of surfaces

NL2 = Number of collocation points

NL3 = 0

NL4 = 0

NL5 to NLI2: Equals the number of elements of the Type 5 to 12, respectively.

*** Data Block F-5***

Number of cards = 1; Format (20I3)

This block determines the selections of subroutines for D vector and W matrix and the number of repeated runs to be made with the same D vector and W matrix for different Mach numbers and frequency ratios.

1→3	4→6	7→9	10→12
<hr/>			
IC	NDMAT	NWMAT	NAMAT

where IC = 5

NDMAT = 1 if subprogram DMATR is used and 2 if subprogram DREAD is used.

NWMAT = 1 if subprogram WMAT is used and 2 if subprogram WREAD is used.

NAMAT = Number of runs to be made using the same D vector and W matrix for different Mach numbers and frequency ratios.

Appendix A

Data Block F-6

Number of cards = 1; Format (20I3)

This block specifies the following items;

1→3	4→6	7→9	10→12	13→15	16→18
IC	NMODE1	NMODE2	NRP	MTOT	NTE

where IC = 6

NMODE1 = Number of values of row index i in C matrix

NMODE2 = Number of values of column index j in C matrix

NRP = Number of reference points (collocation points)

MTOT = Number of chordwise strips

NTE = Number of trailing edge elements

Data Block DM-7 to Data Block DM-22 are used only when NDMAT of Block F-5
is 1.

Data Block DM-7

Number of cards = 1; Format (20I3)

1→3	4→6.....
IC	(NSUR(I), I=1, NL)

where IC = 7

(NSUR(I), I = 1, NL) = Surface number for each surface

NL = Number of surfaces

Appendix A

Data Block DM-8

Number of cards = 1; Format (20I3)

1→3	4→6
IC	(NSYMZ(I), I = 1, NL)	

where IC = 8

(NSYMZ(I), I=1, NL) = 1 if surface is symmetric about z-axis
 = -1 if surface is symmetric about z-axis, but
 motion is antisymmetric
 = 0 if there is no symmetry

Data Block DM-9

Number of cards = 1; Format (20I3)

1→3	4→6
IC	(NSYMY(I), I=1, NL)	

where IC = 9

(NSYMY(I), I = 1, NL) = same as in Block DM-8, but relative to y-axis

Data Block DM-10

Number of cards = 1; Format (20I3)

1→3	4→6
IC	(NGEOM(I), I=1, NL)	

where IC = 10

(NGEOM(I), I = 1, NL) = Number of like surfaces on which aerodynamic
 forces are calculated

Data Block DM-11

Number of cards = 1; Format (IX, I2, 4X, I3, 6F10.5)

1→3	8→10	11→20
IC	NC	(X0(I), I=1, NL)	

where IC = 11; NC = Card number in each block (i.e., for 1st card NC = 1)

(X0(I), I = 1, NL) = x-origin of surface I

Appendix A

Block DM-12***

Number of cards = 1; Format (IX, I2, 4X, I3, 6F10.5)

1→3 8→10 11→ 20
 IC NC (Y0(I), I=1, NL)

where IC = 12; NC = Card number in each block

(Y0(I), I = 1, NL) = y-origin of surface I

Block DM-13***

Number of cards = 1; Format (IX, I2, 4X, I3, 6F10.5)

1→3 8→10 11→ 20
 IC NC (Z0(I), I=1, NL)

where IC = 13; NC = Card number in the block

(Z0(I), I = 1, NL) = z-origin of surface I

Block DM-14***

Number of cards = 1; Format (IX, I2, 4X, I3, 6F10.5)

1→ 8→10 11→ 20
 IC NC (COSG(I), I=1, NL)

where IC = 14; NC = Card number

(COSG(I), I=1, NL) = cos g of the surface I

Block DM-15***

Number of cards = 1; Format (IX, I2, 4X, I3, 6F10.5)

1→ 8→10 11→ 20
 IC NC (SING(I), I=1, NL)

where IC = 15; NC = card number of the block

(SING(I), I = 1, NL) = sin g of the surface I

g = angle between local normal and z-axis, positive clockwise.

Block DM-16***

Number of cards = 1 ; Format (20I3)

4 → 6
 (NSURF (I), I=1, MTOT)

Appendix A

where IC = 16

(NSURF (I), I=1, MTOT) = Surface number of strip I

Data Block DM-17

Number of cards = 1; Format (20I3)

1→3 4 → 6
 (IC (NQT(I), I=1, MTOT)

where IC = 17

(NQT(I), I = 1, MTOT) = Number of elements in strip I

Data Block DM-18

Number of cards = 1; Format (20I3)

1→3 4 → 6
 (IC (NB(I), I = 1, MTOT)

where IC = 18

(NB(I), I=1, MTOT) = Number of elements to be assumed in the wake behind strip I

Data Block DM-19

Number of cards = MTOT/6; Format (IX, I2, 4X, I3, 6F10.5)

1→3 8→10 11 → 20
 (C NC (SFOR(I), I = 1, MTOT)

where IC = 19; NC = Card number in the block

(SFOR(I), I = 1, MTOT) = Leading edge of strip I

Data Block DM-20

Number of cards = MTOT/6; Format (IX, I2, 4X, I3, 6F10.5)

1→3 8→10 11 → 20
 (C NC (SAFT(I), I=1, MTOT)

where IC = 20; NC = Card number in the block

(SAFT(I), I = 1, MTOT) = Most rearward edge of strip I

Data Block DM-21

Number of cards = MTOT/6; Format (IX, I2, 4X, I3, 6F10.5)

1→3 8→10 11→20
 (IC NC (SIN(I), I=1, MTOT)

Appendix A

where IC = 21; NC = Card number in the block

(SIN(I), I=1, MTOT) = Inboard edge of strip I

Data Block DM-22

Number of cards = MTOT/6; Format (IX, I2, 4X, I3, 6F10.5)

1→3	8→10	11→20
IC	NC	(SOUT(I), I=1, MTOT)	

where IC = 22; NC = Card number in the block

(SOUT(I), I=1, MTOT) = Outboard edge of strip I

Data Block DR-7 to Data Block DR-10 are used only when NDMAT of Block F-5
is 2.

Data Block DR-7 and DR-8

These blocks supply type I data. Integer words are read on cards DR-7 and floating words on cards DR-8. Repeat DR-7 and DR-8 for each surface.

DR-7: Number of cards = Number of surfaces; Format (20I3)

1→3	4→6	7→9	10→12	13→15	16→18
IC	IT	NSUR	NSYMZ	NSYMY	NGEOM

where IC = 7

IT = 1

NSUR = surface number

NSYMZ = See Data Block DM-8

NSYMY = See Data Block DM-9

NGEOM = See Data Block DM-10

DR-8: Number of cards = Number of surfaces; Format (IX,I2,7X,6F10.5)

1→3	4→6	11 → 20	21 → 30	31 → 40	41 → 50	51 → 60
IC	IT	XORIG	YORIG	ZORIG	COSG	SING

where IC = 8

IT = 1

XORIG = x-origin of surface

YORIG = y-origin of surface

ZORIG = z-origin of surface

COSG = cos g

SING = sin g

Appendix A

Data Block DR-9 and DR-10

These blocks supply type 2 data. Integer words are read on cards DR-9 and floating words on cards DR-10. Repeat DR-9 and DR-10 for each collocation point.

DR-9: Number of cards = Number of collocation points;
Format (20I3)

1→3	4→6	7→9	10→12
IC	IT	PT	NSUR

where IC = 9

IT = 2

PT = Collocation point

NSUR = Surface number

DR-10: Number of cards = Number of collocation points;
Format (IX, I2, 7X, 6F10.5)

1→3	4→6	11→20	21→30
IC	IT	X	S

where IC = 10

IT = 2

X = x-coordinate of collocation point

S = s-coordinate of collocation point

Data Block DR-11 and DR-12

These blocks supply the data for the on-the-wing aerodynamic elements. Integer words are read on cards DR-11 and floating words on cards DR-12. Repeat DR-11 and DR-12 for each element.

DR-11: Number of cards = Number of elements
Format (20I3)

1→3	4→6	7→9
IC	IT	L

where IC = 11

IT = 5, 7, or 11 depending on the selection of aerodynamic elements

L = Sending point number

DR-12: Number of cards = as for DR-11; Format (IX, I2, 7X, 6F10.5)

1→3	4→6	11→20	21→30	31→40	41→50
IC	IT	XFOR	XAFT	SIN	SOUT

Appendix A

where IC = 12

IT = As in DR-11

XFOR = Most forward side of an element (X-Coord.)

XAFT = Most rearward side of an element

SIN = Inboard edge of an element (S-Coord.)

SOUT = Outboard edge of an element

Data Block DR-13 and DR-14

These blocks supply the data for trailing edge elements.
Integer words are read on cards DR-13 and floating words on cards DR-14. Repeat DR-13 and DR-14 for each element.

DR-13: Number of cards = Number of trailing edge elements;
Format (20I3)

1→3	4→6	7→9	10→12
IC	IT	L	NBOXES

where IC = 13

IT = Type of data

L = Sending point number

NBOXES = Number of regions to be assumed in the wake

DR-14: Number of cards = as for DR-13; Format (IX, I2, 7X, 6F10.5)

1→3	4→6	11 → 20	21 → 30	31→ 40	41 → 50
IC	IT	XFOR	XAFT	SIN	SOUT

where IC = 14

IT = As in DR-13

XFOR = Most forward side of a trailing edge element

XAFT = Most rearward side of wake region

SIN = Inboard edge

SOUT = Outboard edge

Data Block WM-1 to Data Block WM-6 are used only when NWMAT OF Block F-5 is 1.

Data Block WM-1

Number of cards = NMOMT/6; Format (IX, I2, 4X, I3, 6F10.5)

1→3	8→10	11 → 20
IC	NC	(H(I), I=1, NMOMT)	

Appendix A

where IC = 23; NC = Card number in the block

$(H(I), I = 1, NMOMT)$ = Deflection of strip K due to mode J

$I = ((J-1)*MTOT + K)$

J = Mode number

K = Strip number

$NMOMT = (NMODE\ 1 + NMODE\ 2)*MTOT$; [if $NMODE2 = 0$, $NMOMT = NMODE1*2*MTOT$]

Data Block WM-2

Number of cards = $NMOMT/6$; Format (IX, I2, 4X, I3, 6F10.5)

1→3	8→10	11→20
IC	NC	(ALPH(I), I=1, NMOMT)	

where IC = 24; NC = Card number in the block

$(ALPH(I), I=1, NMOMT)$ = Rotation about XROT for strip K due to mode J

See Block WM-1 for other definitions.

Data Block WM-3

Number of cards = $NMOMT/6$; Format (IX, I2, 4X, I3, 6F10.5)

1→3	8→10	11→20
IC	NC	(XROT(I), I=1, NMOMT)	

where IC = 25; NC = Card number in the block

$(XROT(I), I=1, NMOMT)$ = Axis of rotation for strip K due to mode J

See Block WM-1 for other definitions.

Data Block WM-4

Number of cards = $MTOT/6$; Format (IX, I2, 4X, I3, 6F10.5)

1→3	8→10	11→20
IC	NC	(SIN(K), K=1, MTOT)	

where IC = 26; NC = Card number in the block

$(SIN(K), K=1, MTOT)$ = Inboard edge of strip k

Data Block WM-5

Number of cards = $MTOT/6$; Format (IX, I2, 4X, I3, 6F10.5)

1→3	8→10	11→20
IC	NC	(SOUT(K), K=1, MTOT)	

Appendix A

where IC = 27; NC = Card number in the block

(SOUT(K), K=1, MTOT) = Outboard edge of strip K

Data Block WM-6

Number of cards = 1; Format (20I3)

1→3	4 → 6
IC	(NSUR(K) (K=1, MTOT)

where IC = 28; NC = Card number in the block

(NSUR(K), K=1, MTOT) = Surface number of strip K

Data Block WR-1 is used only when NWMAT OF Block F-5 is 2.

Data Block WR-1

Number of cards = NRP*NMODE*2/6; Format(IX, I2, 4X, I3, 6F10.5)

1→3	8→10	11 → 20
IC	NC	(A(I), I=1, NTOTW)

where IC = 23; NC = Card number in the block

(A(I), I=1, NTOTW) = Ith element of W matrix

NTOTW = NRP*NMODE

Data Block F-7

Number of cards = NAMAT/6; Format(IX, I2, 4X, I3, 6F10.5)

1→3	8→10	11 → 20
IC	NC	(RM(I), I=1, NAMAT)

where IC = 29; NC = Card number in the block

(RM(I), I=1, NAMAT)=Mach number for Ith repeated run

Data Block F-8

Number of cards = NAMAT/6; Format(IX, I2, 4X, I3, 6F10.5)

1→3	8→10	11 → 20
IC	NC	(FRA(I), I=1, NAMAT)

where IC = 30; NC = card number in the block

(FRA(I), I=1, NAMAT) = Frequency ratio for Ith repeated run

Appendix A

Example Problems.-

Example 1: Input data for the example in Figure A-4 is read by using subprograms DREAD and WREAD for rectangular elements of nonuniform size. In calculating A and C matrices, ACON5 and ACON6 and CCON5 and CCON6 were used. The output shows the listing of D vector, W, A, P, and C matrices.

Definitions of Modes and Aerodynamic Coefficients: The oscillating modes considered -

$$J_n(X) = \begin{cases} 1 & , n = 1 \\ X - X_{ROT} & , n = 2 \end{cases}$$

The aerodynamic coefficients considered -

$$C_{i,j} = \iint_S J_m(\underline{X}) \Delta P_n(\underline{X}) dX dy$$

	Mode	m, n	α	h	N_{RP}
$J_m(\underline{X})$ NMODE1	l=1	m=1	0	2.0	1→5
	l=2	m=2	$\frac{4}{Sc}$	$\frac{4}{S}(X-.5)$	1→5
$J_n(\underline{X})$ NMODE2	j=1	n=2	1.0	$X-.5$	1→5

S = Half Wing Area = 1.0

c = Root Chord = 1.0

ΔP_n = Pressure jump corresponding to $J_n(\underline{x})$

Example 2: The example illustrated in Figure A-5 shows how the input data for a Swept Wing with Partial-Span Flaps can be read in by using subprograms DMATR and WMAT. The A and C matrices were calculated by using ACON11 and ACON12 and CCON11, CCON12, respectively. Portions of various output listings are shown for reference.

Appendix A

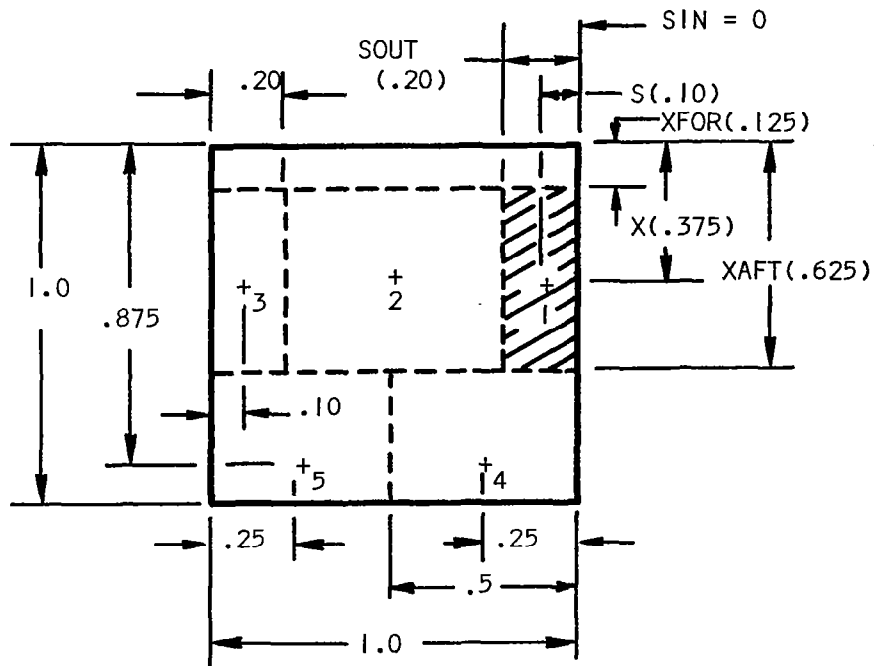


Fig. A-4 Rectangular Wing of Aspect Ratio Two,
Pitching about Midchord

Appendix A

Input for Example 1

Input															
EXAMPLE1: RECT. KING USING DREAD AND WREAD															
1	1	1	1	1											
2	4	2	0	0	1	2	-0	-0	-0	-0	-0	-0	-0	-0	-0
3	5	2	0	0	4	4	-0	-0	-0	-0	-0	-0	-0	-0	-0
4	1	5	0	0	3	2	-0	-0	-0	-0	-0	-0	-0	-0	-0
5	2	2	1												
6	2	1	5	0											
7	1	1	1	0	1										
8		1		0.00000		0.00000		0.00000		1.00000		0.00000			
9	2	1	1												
10		2		.37500		.10000									
9	2	2	1												
10		2		.37500		.50000									
9	2	3	1												
10		2		.37500		.90000									
9	2	4	1												
10		2		.87500		.25000									
9	2	5	1												
10		2		.87500		.75000									
11	5	1													
12		5		.12500		.62500		0.00000		.20000					
11	5	2													
12		5		.12500		.62500		.20000		.80000					
11	5	3													
12		5		.12500		.62500		.80000		1.00000					
13	6	4	1												
14		6		.62500		1.12500		0.00000		.50000					
13	6	5	1												
14		6		.62500		1.12500		.50000		1.00000					
23		1		0.00000		2.00000		0.00000		2.00000		0.00000		2.00000	
23		2		0.00000		2.00000		0.00000		2.00000		4.00000		-.50000	
23		3		4.00000		-.50000		4.00000		-.50000		4.00000		1.50000	
23		4		4.00000		1.50000		1.00000		-.12500		1.00000		-.12500	
23		5		1.00000		-.12500		1.00000		.37500		1.00000		.37500	
29		1		0.00000											
30		1		0.00000											

• • • • •

•

1

—

—

Cont'd Output for Example 1

WMATRIX ELEMENTS

ROW	COL	REAL	IMAGINARY
1	1	0.	2.00000000E+00
1	2	0.	2.00000000E+00
1	3	0.	2.00000000E+00
1	4	0.	2.00000000E+00
1	5	0.	2.00000000E+00
2	1	4.00000000E+00	-5.00000000E-01
2	2	4.00000000E+00	-5.00000000E-01
2	3	4.00000000E+00	-5.00000000E-01
2	4	4.00000000E+00	1.50000000E+00
2	5	4.00000000E+00	1.50000000E+00
3	1	1.00000000E+00	-1.25000000E-01
3	2	1.00000000E+00	-1.25000000E-01
3	3	1.00000000E+00	-1.25000000E-01
3	4	1.00000000E+00	3.75000000E-01
3	5	1.00000000E+00	3.75000000E-01
29	1	0.00000	
30	1	0.00000	

PART 2 - DERIVE AERODYNAMIC MATRIX

A MATRIX 1 NRPE 5 MACH NOE 0.00000 FRA= 0.00000

ROW	COL	REAL	IMAGINARY
1	1	2.54264435E+00	0.
1	2	-1.20611763E+00	0.
1	3	-2.31479812E-02	0.
1	4	-3.24884234E-01	0.
1	5	-6.53705959E-02	0.
1	6	0.	0.
2	1	-1.52650845E-01	0.
2	2	1.62966875E+00	0.
2	3	-1.19814250E-01	0.
2	4	-1.95477195E-01	0.
2	5	-1.73197113E-01	0.
2	6	0.	0.
3	1	-2.31479812E-02	0.
3	2	-1.04753637E+00	0.
3	3	3.42694250E+00	0.
3	4	-5.30789816E-02	0.
3	5	-2.08162491E-01	0.
3	6	0.	0.
4	1	-1.29919653E-01	0.
4	2	-2.37126394E-01	0.
4	3	-1.93063241E-02	0.
4	4	1.57137243E+00	0.

Cont'd Output for Example 1

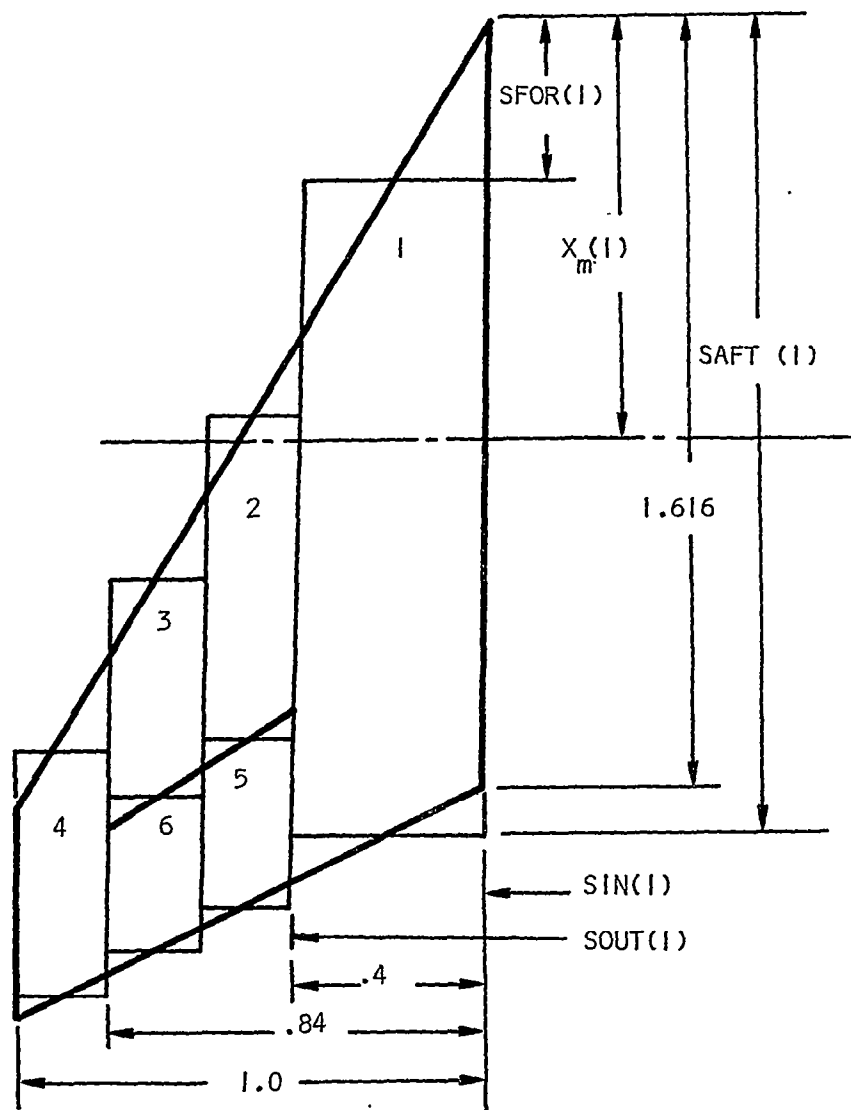
4	5	-2.51088980E-01	0.
4	6	0.	0.
5	1	-2.37347138E-02	0.
5	2	-2.08863271E-01	0.
5	3	-8.81988782E-02	0.
5	4	-2.51088980E-01	0.
5	5	1.79448833E+00	0.
5	6	0.	0.

PART 3-DERIVE CMATRIX

LISTING OF POTENTIAL DISCONTINUITIES			
ROW	COL	REAL	IMAGINARY
1	1	1.01059101E+00	0.
1	2	9.69483211E-01	0.
1	3	8.62725712E-01	0.
1	4	1.01138540E+00	0.
1	5	8.57518178E-01	0.

CMATRIX FOR L= 1			
MACH NO.= 0.00000 FRA= 0.00000			
ROW	COL	REAL	IMAGINARY
1	1	1.86890357E+00	0.
2	1	-1.36537685E+00	0.

Appendix A



Control Surface Chord = $.712 \times \text{half local chord}$

Wing Aspect Ratio = 2

Wing Taper Ratio = $.2378$

Leading Edge Sweep Angle = 60°

Fig. A-5 Chordwise Strip Arrangement for a Swept Wing
Partial-Span Flaps

Appendix A

Definitions of Modes and Aerodynamic Coefficients:

The oscillating modes considered:

$$J_n(\underline{X}) = \begin{cases} 1 & \text{For Wing, } n=1 \\ X-X_m & \text{For Wing, } n=2 \\ 1 & \text{For Control Surface, } n=3 \\ X-X_c & \text{For Control Surface, } n=4 \end{cases}$$

The aerodynamic coefficients considered:

$$C_{i,j} = \frac{1}{2s} \iint_S J_m(\underline{X}) \Delta P_n(\underline{X}) dxdy$$

where ΔP_n = pressure jump corresponding to $J_n(\underline{x})$

s = half span

S = half wing area

	Mode	m, n	H(I)	Strips	ALPH(I)	Strips	XROT(I)	Strips
$J_m(\underline{X})$ NMODE1	i=1	m=1	$\frac{2}{S}$	1→6	0	1→6	0	1→6 7
	i=2	m=2	0	1→6	$\frac{2}{S}$	1→6	.808	1→6
	i=3	m=3	0 $\frac{2}{S}$	1→4 5→6	0	1→6	0	1→6
	i=4	m=4	0	1→6	0 $\frac{2}{S}$	1→4 5→6	0 1.5153 1.7201	1→4 5 6
$J_n(\underline{X})$ NMODE2	j=1	n=2	0	1→6	.732	1→6	.808	1→6
	j=2	n=3	0 1.0	1→4 5→6	0	1→6	0	1→6
	j=3	n=4	0	1→6	0 1.0	1→4 5→6	0 1.5153 1.7201	1→4 5 6

Appendix A

Input for Example 2

EXAMPLE 2: SWEEP WING WITH CONTROL SURFACE, NRP=14

1	1	1	0	1															
2	4	2	-0	-0	-0	-0	-0	-0	-0	-0	1	2	-0	-0	-0				
3	5	2	-0	-0	-0	-0	-0	-0	-0	-0	4	4	-0	-0	-0				
4	2	14	-0	-0	-0	-0	-0	-0	-0	-0	10	4	-0	-0	-0				
5	1	1	5																
6	4	3	14	6	4														
7	1	2																	
8	1	1																	
9	0	0																	
10	1	1																	
11		1	-0.00000	-0.00000															
12		1	-0.00000	-0.00000															
13		1	-0.00000	-0.00000															
14		1	1.00000	1.00000															
15		1	-0.00000	-0.00000															
16	1	1	1	1	2	2													
17	3	2	2	3	2	2													
18	16	0	0	16	11	11													
19		1	.34640	.86600	1.21240	1.55880	1.51540	1.72010											
20		1	1.71360	1.51540	1.72010	2.05490	1.85990	1.95750											
21		1	0.00000	.40000	.62000	.84000	.40000	.62000											
22		1	.40000	.62000	.84000	1.00000	.62000	.84000											
23		1	2.00000	2.00000	2.00000	2.00000	2.00000	2.00000											
23		2	-0.00000	-0.00000	-0.00000	-0.00000	-0.00000	-0.00000											
23		3	-0.00000	-0.00000	-0.00000	-0.00000	-0.00000	-0.00000											
23		4	-0.00000	-0.00000	-0.00000	-0.00000	-0.00000	-0.00000											
23		5	-0.00000	-0.00000	-0.00000	-0.00000	-0.00000	-0.00000											
23		6	-0.00000	-0.00000	-0.00000	-0.00000	-0.00000	1.00000	1.00000										
23		7	-0.00000	-0.00000	-0.00000	-0.00000	-0.00000	-0.00000	-0.00000										
24		1	-0.00000	-0.00000	-0.00000	-0.00000	-0.00000	-0.00000	-0.00000										
24		2	2.00000	2.00000	2.00000	2.00000	2.00000	2.00000	2.00000										
24		3	-0.00000	-0.00000	-0.00000	-0.00000	-0.00000	-0.00000	-0.00000										
24		4	-0.00000	-0.00000	-0.00000	-0.00000	-0.00000	2.00000	2.00000										
24		5	.73200	.73200	.73200	.73200	.73200	.73200	.73200										
24		6	-0.00000	-0.00000	-0.00000	-0.00000	-0.00000	-0.00000	-0.00000										
24		7	-0.00000	-0.00000	-0.00000	-0.00000	-0.00000	1.00000	1.00000										
25		1	-0.00000	-0.00000	-0.00000	-0.00000	-0.00000	-0.00000	-0.00000										
25		2	.80800	.80800	.80800	.80800	.80800	.80800	.80800										
25		3	-0.00000	-0.00000	-0.00000	-0.00000	-0.00000	-0.00000	-0.00000										
25		4	-0.00000	-0.00000	-0.00000	-0.00000	-0.00000	1.51530	1.72010										
25		5	.80800	.80800	.80800	.80800	.80800	.80800	.80800										
25		6	-0.00000	-0.00000	-0.00000	-0.00000	-0.00000	-0.00000	-0.00000										
25		7	-0.00000	-0.00000	-0.00000	-0.00000	-0.00000	1.51530	1.72010										
26		1	0.00000	.40000	.62000	.84000	.40000	.62000	.84000										
27		1	.40000	.62000	.84000	1.00000	.62000	.84000											
28	1	1	1	1	2	2													
29		1	0.00000	.50000	.70000	.80000	.90000												
30		1	1.00000	1.00000	1.00000	1.00000	1.00000	1.00000											

Appendix A

Output for Example 2

PROGRAM FOR UNSTEADY AIR FORCES USING DOWNWASH-VELOCITY POTENTIAL METHOD

BY J.K. HAVILAND AND Y.S. YOO - UNIV OF VA

PART 1 - READ IN W AND DATA MATRICES DATA MATRIX ELEMENTS

62	4	5	2	80	2	2	14	136	-0	-0	-0
136	-0	-0	-0	136	-0	-0	-0	136	-0	-0	-0
136	-0	-0	-0	136	-0	-0	-0	136	-0	-0	-0
136	-0	-0	-0	136	1	4	10	186	2	4	4
210	-0	-0	-0	210	-0	-0	-0	210	-0	-0	-0
210											
1	1	1	0	1							
1	-0.00000000	-0.00000000	-0.00000000	1.00000000	-0.00000000						
1	2	1	0	1							
1	-0.00000000	-0.00000000	-0.00000000	1.00000000	-0.00000000						
2	1	1									
2	.68820000	.20000000									
2	2	1									
2	1.14393333	.20000000									
2	3	1									
2	1.10952500	.51000000									
2	4	1									
2	1.43422500	.51000000									
2	5	1									
2	1.40278750	.73000000									
2	6	1									
2	1.65663750	.73000000									
2	7	1									
2	1.68282500	.92000000									
2	8	1									
2	1.84819167	.92000000									
2	9	2									
2	1.64458750	.51000000									
2	10	2									
2	1.80912500	.73000000									
2	11	1									
2	1.59966667	.20000000									
2	12	1									
2	2.01355833	.92000000									
2	13	2									
2	1.98908750	.51000000									
2	14	2									
2	2.04652500	.73000000									
11	1										
11	.46033333	.91606667	0.00000000	.40000000							
11	2										
11	.91606667	1.37180000	0.00000000	.40000000							

Appendix A

Cont'd Output for Example 2

WMATRIX ELEMENTS			
ROW	COL	REAL	IMAGINARY
1	1	-0.	2.00000000E+00
1	2	-0.	2.00000000E+00
1	3	-0.	2.00000000E+00
1	4	-0.	2.00000000E+00
1	5	-0.	2.00000000E+00
1	6	-0.	2.00000000E+00
1	7	-0.	2.00000000E+00
1	8	-0.	2.00000000E+00
1	9	-0.	2.00000000E+00
1	10	-0.	2.00000000E+00
1	11	-0.	2.00000000E+00
1	12	-0.	2.00000000E+00
1	13	-0.	2.00000000E+00
1	14	-0.	2.00000000E+00
2	1	2.00000000E+00	-2.39600000E-01
2	2	2.00000000E+00	6.71866667E-01
2	3	2.00000000E+00	6.03050000E-01
2	4	2.00000000E+00	1.25245000E+00
2	5	2.00000000E+00	1.18957500E+00
2	6	2.00000000E+00	1.69727500E+00
2	7	2.00000000E+00	1.74965000E+00
2	8	2.00000000E+00	2.08038333E+00
2	9	2.00000000E+00	1.67317500E+00
2	10	2.00000000E+00	2.00225000E+00
2	11	2.00000000E+00	1.58333333E+00
2	12	2.00000000E+00	2.41111667E+00
2	13	2.00000000E+00	2.36217500E+00
2	14	2.00000000E+00	2.47705000E+00
3	1	-0.	0.
3	2	-0.	0.
3	3	-0.	0.
3	4	-0.	0.
3	5	-0.	0.
3	6	-0.	0.
3	7	-0.	0.
3	8	-0.	0.
3	9	-0.	2.00000000E+00
3	10	-0.	2.00000000E+00
3	11	-0.	0.
3	12	-0.	0.
3	13	-0.	2.00000000E+00
3	14	-0.	2.00000000E+00
4	1	-0.	0.
4	2	-0.	0.
4	3	-0.	0.
4	4	-0.	0.
4	5	-0.	0.
4	6	-0.	0.

Appendix A

Cont'd for Example 2

PART 2 - DERIVE AERODYNAMIC MATRIX

A MATRIX		1 NRP= 14	MACH NO= .70000	FRA= 1.00000
ROW	COL	REAL	IMAGINARY	
1	1	1.47645344E+00	7.40374286E-03	
1	2	-2.30407783E-01	9.50228066E-02	
1	3	-4.92222006E-02	2.38331129E-02	
1	4	-8.88720944E-03	1.29734819E-02	
1	5	-5.91692197E-03	9.19569541E-03	
1	6	-7.72368777E-04	5.73546826E-03	
1	7	-2.04522320E-05	2.46429225E-03	
1	8	5.61022988E-04	1.81960463E-03	
1	9	-9.91527271E-04	4.87913843E-03	
1	10	3.61765554E-04	2.18064490E-03	
1	11	-1.24052829E-04	3.34679343E-02	
1	12	3.22993542E-03	3.31610288E-04	
1	13	4.02740113E-03	4.02313751E-03	
1	14	5.36009830E-03	7.69676263E-04	
1	15	0.	0.	
2	1	-2.04411530E-01	-4.33756905E-02	
2	2	1.47645344E+00	7.40374286E-03	
2	3	-2.96346732E-01	2.10531821E-03	
2	4	-1.01923316E-01	2.55039169E-02	
2	5	-3.68973917E-02	1.24130106E-02	
2	6	-1.34087399E-02	1.04745443E-02	
2	7	-4.03207363E-03	4.14043549E-03	
2	8	-2.02912877E-03	3.61443247E-03	
2	9	-1.51234926E-02	1.05108725E-02	
2	10	-3.33496549E-03	4.45918174E-03	
2	11	-2.15677709E-01	1.25451330E-01	
2	12	3.26458742E-03	5.51131065E-03	
2	13	-3.70683910E-03	1.66086156E-02	
2	14	4.38441613E-03	1.09612281E-02	
2	15	0.	0.	
3	1	-1.46780441E-01	-2.72107623E-02	
3	2	-1.06648139E+00	6.61679208E-03	
3	3	3.20433063E+00	2.25398425E-03	
3	4	-1.65627950E-01	3.78511216E-02	
3	5	-8.92789699E-02	2.40201301E-02	
3	6	-1.52776211E-02	1.18819624E-02	
3	7	-4.77809758E-03	4.74043228E-03	
3	8	-2.04304184E-03	3.73013038E-03	
3	9	-1.30731458E-02	9.95308345E-03	
3	10	-3.08981740E-03	4.42260538E-03	
3	11	-9.07982028E-02	8.15845866E-02	
3	12	3.20195257E-03	5.04209210E-03	
3	13	-1.84017549E-03	1.41290677E-02	
3	14	4.58966359E-03	9.57498621E-03	
3	15	0.	0.	
4	1	-3.88413133E-02	-1.53173113E-02	

Appendix A

Cont'd for Example 2

PART 3-DERIVE CMATRIX

LISTING OF POTENTIAL DISCONTINUITIES			
ROW	COL	REAL	IMAGINARY
1	1	7.19240047E-01	-1.96046962E-01
1	2	1.12190693E+00	6.19647631E-02
1	3	7.82588972E-01	4.45566363E-02
1	4	1.11157379E+00	2.77268333E-01
1	5	7.49497603E-01	1.90192592E-01
1	6	9.29313913E-01	3.40077119E-01
1	7	5.99494642E-01	2.43762016E-01
1	8	6.58601669E-01	3.10765401E-01
1	9	1.17338193E+00	3.57908726E-01
1	10	9.74568491E-01	4.05036350E-01
1	11	1.32432438E+00	3.45992226E-01
1	12	6.74430936E-01	3.17596219E-01
1	13	1.21778906E+00	2.89990190E-01
1	14	1.00525883E+00	3.73063626E-01
2	1	2.28537254E-02	-1.00678125E-02
2	2	6.94409307E-02	1.85305132E-02
2	3	4.68362780E-02	1.23600268E-02
2	4	8.94395525E-02	9.72468758E-02
2	5	5.83969759E-02	5.76615346E-02
2	6	8.08251905E-02	2.00663205E-01
2	7	5.21469123E-02	1.11077066E-01
2	8	5.64875102E-02	1.93862280E-01
2	9	9.92489587E-02	4.33071999E-01
2	10	7.97854832E-02	4.95524806E-01
2	11	1.12070872E-01	1.21716905E-01
2	12	6.84566594E-02	2.20200364E-01
2	13	1.26839334E-01	5.48240810E-01
2	14	1.15338995E-01	5.66342821E-01
3	1	-3.31905867E-03	-2.68749724E-02
3	2	4.05511239E-02	-6.60891619E-02
3	3	2.71556190E-02	-4.47067358E-02
3	4	1.26424457E-01	-6.43118486E-02
3	5	7.66394524E-02	-4.34688242E-02
3	6	2.27806481E-01	-2.61098239E-02
3	7	1.28759268E-01	-2.07230550E-02
3	8	2.13937738E-01	2.25854757E-03
3	9	4.66146099E-01	-7.67512014E-03
3	10	5.23098757E-01	3.74847134E-02
3	11	1.59097132E-01	-7.80808271E-02
3	12	2.44860925E-01	7.19108775E-03
-3	13	5.92013163E-01	1.00081713E-01
3	14	6.07729750E-01	8.19817326E-02

Appendix A

Cont'd for Example 2

CMATRIX FOR N= 1			
MACH NO.=		FRA=	
.70000		1.00000	
ROW	COL	REAL	IMAGINARY
1	1	1.93944033E+00	2.42293213E+00
1	2	-3.84698368E-02	7.71292667E-01
1	3	7.67700013E-01	3.13311215E-01
2	1	2.23415548E-01	1.32273833E+00
2	2	-1.27653711E-01	5.68402451E-01
2	3	5.33188544E-01	3.47877202E-01
3	1	8.43453971E-01	6.39851554E-01
3	2	-6.05133618E-02	5.13395599E-01
3	3	4.95997098E-01	2.54582146E-01
4	1	2.00508664E-02	5.95289405E-02
4	2	-1.89865173E-02	3.38392790E-02
4	3	2.73564388E-02	4.14206999E-02

Appendix A

Listing of Program FLUTT PI

```

PROGRAM FLUTT (INPUT,OUTPUT,TAPE5=INPUT,TAPE6=OUTPUT)
DIMENSION DATA(800 ),RM(10),FRA(10),NVECT(5),VECT(5)
REAL NKL
COMPLEX A(6130)
EQUIVALENCE(NDATA,DATA)
COMMON/BLOCKA/NDATA(800 ),A,NRP,RM,FRA,DERS,OC,ALSQ,SGAL
COMMON/BLOCKB/XKOL,SKOL,LSYM,NPLANE,N,NKL
COMMON/BLOCKC/NVECT,VECT
CALL FTNBIN(0,0,0)
C *****
C * PROGRAM FOR UNSTEADY AIR FORCES USING *
C * DOWNWASH-VELOCITY POTENTIAL METHOD *
C * BY J.K. HAVILAND AND Y.S. YOO - UNIV OF VA *
C *****
2 DO 3 J=1,6130
3 A(J)=(0.,0.)
DO 4 J=1,61
4 NDATA(J)=0
READ (5,700)
IF(EOF,5) 999,5
5 READ(5,800) IC,NPD,NPW,NPA,NPP
IF(IC,NE.1) GO TO 999
WRITE(6,820)
WRITE (6,700)
WRITE(6,800) IC,NPD,NPW,NPA,NPP
READ(5,800) IC,(NDATA(J),J=2,58,4)
WRITE(6,800) IC,(NDATA(J),J=2,58,4)
IF(IC,NE.2) GO TO 999
READ(5,800) IC,(NDATA(J),J=3,59,4)
WRITE(6,800) IC,(NDATA(J),J=3,59,4)
IF(IC,NE.3) GO TO 999
READ(5,800) IC,(NDATA(J),J=4,60,4)
WRITE(6,800) IC,(NDATA(J),J=4,60,4)
IF(IC,NE.4) GO TO 999
READ(5,800) IC,NDMAT,NWMAT,NAMAT
WRITE(6,800) IC,NDMAT,NWMAT,NAMAT
IF(IC,NE.5) GO TO 999
READ(5,800) IC,NMODE1,NMODE2,NRP,MTOT,NTE
WRITE(6,800) IC,NMODE1,NMODE2,NRP,MTOT,NTE
IF(IC,NE.6) GO TO 999
NDATA(1)=62
DO 25 J=1,15
25 NDATA(4*J+1)=(NDATA(4*J-2)+NDATA(4*J-1))*NDATA(4*J)+
1 NDATA(4*J-3)
IF(NDATA(61).LE.800 ) GO TO 30
WRITE(6,105)

```

Appendix A
Cont'd for Program FLUTT

```

105 FORMAT(2X*LINE COUNT EXCEEDS STORAGE FOR DATA MATRIX*)
    GO TO 999
    30 IF (NPD .EQ.0) GO TO 35
        WRITE (6,106) (NDATA(K),K=1,61)
106 FORMAT(1X* DATA MATRIX ELEMENTS*/(4X,4I4,4X,4I4,4X,4I4))
    35 GO TO (110,120,130,140),NDMAT
110 CALL DMATR(MTOT,NPD,NTE)
    GO TO 500
120 CALL DREAD (NPD)
    GO TO 500
130 CALL DBLK1
    GO TO 951
140 CALL DBLK2
    GO TO 951
500 NMODF=NMODE1+NMODE2
    NTOTW=NRP*NMODE
    N1=NRP+1
    NADDW=N1*NRP
    NSIZE1=NRP*NMODE1
    NADDW2=NADDW+NSIZE1
    IF(NMODE2.NE.0) GO TO 510
    NTEMP=NMODE1
    NSIZE2=NSIZE1
    GO TO 520
510 NTEMP=NMODE2
    NSIZE2=NRP*NMODE2
520 NADDW3=NADDW2+NSIZE2
    NADDWF=NADDW3+NSIZE2
    NCSIZE=NMODE1*NTEMP
    NADDC=NADDWF+NSIZE2
    NTOT=NADDC+NCSIZE
    IF(NTOT.LT.11000) GO TO 10
    WRITE(6,830) NTOT
    GO TO 999
    10 GO TO (210,220,230,240),NWMAT
210 CALL WMAT(NMODE,MTOT,NADDW,NTOTW)
    GO TO 310
220 CALL WREAD(NMODE,NADDW,NTOTW)
    GO TO 310
230 CALL WBLK1
    GO TO 953
240 CALL WBLK2
    GO TO 953
310 IF(NPW.EQ.0) GO TO 45
    WRITE(6,840)
    CALL ALIST (A,NADDW,NMODE,NRP)
    45 READ(5,810) IC,NC,(RM(I),I=1,NAMAT)
    WRITE(6,810) IC,NC,(RM(I),I=1,NAMAT)
    IF(IC.NE.29) GO TO 999
    READ(5,810) IC,NC,(FRA(I),I=1,NAMAT)
    WRITE(6,810) IC,NC,(FRA(I),I=1,NAMAT)

```

Appendix A

Cont'd for Program FLUTT

```

      IF(IC.NE.30) GO TO 999
      DO 940 N=1,NAMAT
      WRITE(6,850)
      WRITE(6,860) N,NRP,RM(N),FRA(N)
      DO 50 J=1,NADDW
      CALL ACALC
C 50 A(J)=(0.,0.)
      CALL ACALC(MTOT)
      IF(NPA.NE.0) CALL ALIST(A,0,NRP,N1)
      CALL CMATR(N1,NTOTW,NADDW,NMODE1,NMODE2,NTMP,NSIZE1,
1NSIZE2,NCSIZE,NADDC,NPP,NADDW2,NADDW3,NADDWF)
      700 FORMAT (1X,79H
1
800 FORMAT(1X,I2,20I3)
810 FORMAT(1X,I2,4X,I3,6F10.5)
820 FORMAT(2X//1X*PROGRAM FOR UNSTEADY AIR FORCES USING*/
12X* DOWNWASH-VELOCITY POTENTIAL METHOD*//
21X*BY J.K. HAVILAND AND Y.S. YOO - UNIV OF VA*//
830 FORMAT(1X*STORAGE CAPACITY FOR TOTAL A MATRIX IS*,I6)
840 FORMAT(1X//* WMATRIX ELEMENTS*//)
850 FORMAT(2X//1X* PART 2 - DERIVE AERODYNAMIC MATRIX*//)
860 FORMAT(1X*A MATRIX*,I3,* NRP=*,I3,* MACH NO=*,F8.5,*
1FRA=*,F8.5)
940 CONTINUE
950 CONTINUE
951 CONTINUE
953 CONTINUE
      GO TO 2
999 CONTINUE
      STOP
      END.

```

```

      SUBROUTINE DMATR(MTOT,NPD,NTE)
      DIMENSION DATA(800 ),XO(4),YO(4),ZO(4),COSG(4),SING(4),
1DELX(14)
      DIMENSION RM(10),FRA(10)
      COMPLEX A(6130)
      DIMENSION NSUR(4),NSYMZ(4),NSYMY(4),NGEOM(4)
      DIMENSION SFOR(14),SAFT(14),SIN(14),SOUT(14),DELS(14)
      DIMENSION NB(14),NQT(14),NSURF(14)
      EQUIVALENCE (NDATA,DATA)
      COMMON/BLOCKA/NDATA(800 ),A,NRP,RM,FRA,DERS,OC,ALSO,SGAL
      DO 950 J=1,15
      NADD=NDATA(4*J-3)
      NFIX=NDATA(4*J-2)
      NFI=NDATA(4*J-1)
      NL=NDATA(4*J)
      IF(NL.EQ.0) GO TO 950
      GOTO(110,115,120,120,120,120,120,120,120,120,120,
1120,120,120),J

```

Appendix A

Cont'd for Program FLUTT

```

110 READ(5,800) IC,(NSUR(I),I=1,NL)
    WRITE(6,800) IC,(NSUR(I),I=1,NL)
    IF(IC.NE. 7) STOP
    READ(5,800) IC,(NSYMZ(I),I=1,NL)
    WRITE(6,800) IC,(NSYMZ(I),I=1,NL)
    IF(IC.NE. 8) STOP
    READ(5,800) IC,(NSYMY(I),I=1,NL)
    WRITE(6,800) IC,(NSYMY(I),I=1,NL)
    IF(IC.NE. 9) STOP
    READ(5,800) IC,(NGEOM(I),I=1,NL)
    WRITE(6,800) IC,(NGEOM(I),I=1,NL)
    IF(IC.NE.10) STOP
    READ(5,810) IC,NC,(XO(I),I=1,NL)
    WRITE(6,810) IC,NC,(XO(I),I=1,NL)
    IF(IC.NE.11) STOP
    READ(5,810) IC,NC,(YO(I),I=1,NL)
    WRITE(6,810) IC,NC,(YO(I),I=1,NL)
    IF(IC.NE.12) STOP
    READ(5,810) IC,NC,(ZO(I),I=1,NL)
    WRITE(6,810) IC,NC,(ZO(I),I=1,NL)
    IF(IC.NE.13) STOP
    READ(5,810) IC,NC,(COSG(I),I=1,NL)
    WRITE(6,810) IC,NC,(COSG(I),I=1,NL)
    IF(IC.NE.14) STOP
    READ(5,810) IC,NC,(SING(I),I=1,NL)
    WRITE(6,810) IC,NC,(SING(I),I=1,NL)
    IF(IC.NE.15) STOP
    GO TO 500
115 READ(5,800) IC,(NSURF(I),I=1,MTOT)
    WRITE(6,800) IC,(NSURF(I),I=1,MTOT)
    IF(IC.NE.16) STOP
    READ(5,800) IC,(NQT(I),I=1,MTOT)
    WRITE(6,800) IC,(NQT(I),I=1,MTOT)
    IF(IC.NE.17) STOP
    READ(5,800) IC,(NB(I),I=1,MTOT)
    WRITE(6,800) IC,(NB(I),I=1,MTOT)
    IF(IC.NE.18) STOP
    ND=0
    DO 10 I1=1,MTOT,6
        I2=I1+5
        IF(I2.GT.MTOT) I2=MTOT
        READ(5,810) IC,NC,(SFOR(I),I=I1,I2)
        WRITE(6,810) IC,NC,(SFOR(I),I=I1,I2)
        ND=ND+1
10 IF(IC.NE.19,OR,NC.NE.ND) STOP
    ND=0
    DO 20 I1=1,MTOT,6
        I2=I1+5
        IF(I2.GT.MTOT) I2=MTOT
        READ(5,810) IC,NC,(SAFT(I),I=I1,I2)
        WRITE(6,810) IC,NC,(SAFT(I),I=I1,I2)

```

Appendix A
Cont'd for Program FLUTT

```

ND=ND+1
20 IF(IC.NE.20.OR.NC.NE.ND) STOP
ND=0
DO 30 I1=1,MTOT,6
  I2=I1+5
  IF(I2.GT.MTOT) I2=MTOT
  READ(5,810) IC,NC,(SIN(I),I=I1,I2)
  WRITE(6,810) IC,NC,(SIN(I),I=I1,I2)
  ND=ND+1
30 IF(IC.NE.21.OR.NC.NE.ND) STOP
ND=0
DO 40 I1=1,MTOT,6
  I2=I1+5
  IF(I2.GT.MTOT) I2=MTOT
  READ(5,810) IC,NC,(SOUT(I),I=I1,I2)
  WRITE(6,810) IC,NC,(SOUT(I),I=I1,I2)
  ND=ND+1
40 IF(IC.NE.22.OR.NC.NE.ND) STOP
  DERS=SOUT(1)-SIN(1)
  IF(IC.NE.22) STOP
120 GO TO 500
500 DO 940 NLINE=1,NL
  K1=NADD+(NFI*+NFL)*(NLINE-1)
  K3=K1+NFI*
  K2=K3-1
  K4=K2+NFL
  GO TO(210,220,230,240,250,260,250,260,250,260,
1330,340,350),J
210 NDATA(K1)=NSUR(NLINE)
  NDATA(K1+1)=NSYMZ(NLINE)
  NDATA(K1+2)=NSYMY(NLINE)
  NDATA(K2)=NGEOM(NLINE)
  DATA(K3)=XO(NLINE)
  DATA(K3+1)=YO(NLINE)
  DATA(K3+2)=ZO(NLINE)
  DATA(K3+3)=COSG(NLINE)
  DATA(K4)=SING(NLINE)
  GO TO 32
220 LINE=0
DO 930 M=1,MTOT
  NQ=NQT(M)
  DO 920 IQ=1,NQ
    IF(IQ.LT.NQ.OR.NB(M).LT.1) GO TO 222
    IF(NLINE.LE.(NRP+NTE)) GO TO 930
    LINE=NLINE
    NTB=0
    DO 4 MTEST=1,MTOT
      IF(NB(MTEST).GE.1) NTB=NTB+1
      IF(NTB.EQ.(NLINE-NRP+NTE))M=MTEST
      IF(NTB.EQ.(NLINE-NRP+NTE))GO TO 224
4 CONTINUE

```


Appendix A
Cont'd For Program FLUTT

```

222 LINE=LINE+1
   IF(LINE.NE.NLINE) GO TO 920
224 DELX(M)=(SAFT(M)-SFOR(M))/NQT(M)
   DELS(M)=SOUT(M)-SIN(M)
   ITYPE=J-1
   GO TO(420,430,440,450,460,450,460,450,460,
1450,460,530,540,550),ITYPE
230 GO TO 220
240 GO TO 260
250 GO TO 220
260 NLINE=NRP-NTE+NLINE
   GO TO 220
330 GO TO 950
340 GO TO 950
350 GO TO 220
420 NDATA(K1)=LINE
   NDATA(K2)=NSURF(M)
   DATA(K3)=SFOR(M)+(.75+(IQ-1))*DELX(M)
   DATA(K4)=SIN(M)+DELS(M)*.5
   GO TO 32
430 GO TO 450
440 GO TO 460
450 NDATA(K1)=LINE
   XF=SFOR(M)+DELX(M)*.25
   DATA(K3)=XF+(IQ-1)*DELX(M)
   DATA(K3+1)=DATA(K3)+DELX(M)
   DATA(K3+2)=SIN(M)
   DATA(K4)=SOUT(M)
   IF(IQ.EQ.NQ.AND.NB(M).LE.1) GO TO 452
   GO TO 453
452 DO 6 MT=1,MTOT
   IF(SIN(MT).LT.DATA(K4).AND.SOUT(MT).GT.DATA(K3+2)
1.AND.MT.GT.M) GO TO 5
   GO TO 6
5 DATA(K3+1)=SFOR(MT)+(SAFT(MT)-SFOR(MT))/(NQT(MT)*4)
   GO TO 453
6 CONTINUE
453 GO TO 32
460 NDATA(K1)=LINE
   NDATA(K2)=NB(M)
   DATA(K3)=SAFT(M)-DELX(M)*.75
   DATA(K3+1)=DATA(K3)+DELX(M)*NDATA(K2)
   DATA(K3+2)=SIN(M)
   DATA(K4)=SOUT(M)
   NLINE=NLINE-NRP+NTE
   GO TO 32
530 GO TO 950
540 GO TO 950
550 GO TO 450
32 IF(NPD.NE.0) WRITE(6,107) J,(NDATA(K),K=K1,K2)
107 FORMAT(3X,7I4)

```

Appendix A
Cont'd for Program FLUTT

```
      IF(NPD.NE.0) WRITE(6,109) J , (DATA(K),K=K3,K4)
109  FORMAT(2X,I3,5F13.8)
800  FORMAT(1X,I2,20I3)
810  FORMAT(1X,I2,4X,I3,6F10.5)
      GO TO 940
920  CONTINUE
930  CONTINUE
940  CONTINUE
950  CONTINUE
      RETURN
      END
```

```
      SUBROUTINE DREAD(NPD)
      DIMENSION DATA(800 ),RM(10),FRA(10)
      COMPLEX A(6130)
      EQUIVALENCE(NDATA,DATA)
      COMMON/BLOCKA/NDATA(800 ),A,NRP,RM,FRA,DEFS,OC,ALSQ,SQAL
35  DO 5 J=62,800
5   NDATA(J)=0
      ND1=6
      ND2=7
      DO 50 J=1,15
      NADD=NDATA(4*J-3)
      NFIX=NDATA(4*J-2)
      NFL=NDATA(4*J-1)
      NL=NDATA(4*J)
      IF(NL.EQ.0) GO TO 50
      ND1=ND1+1
      ND2=ND2+1
      DO 40 NLINE=1,NL
      K1=NADD+(NFIX+NFL)*(NLINE-1)
      K3=K1+NFIX
      K2=K3-1
      K4=K2+NFL
      READ(5,800) IC,IT,(NDATA(K),K=K1,K2)
      IF(IC.EQ.(ND1 ).AND.IT.EQ.J) GO TO 37
      WRITE(6,108) J,IT
108  FORMAT(1X*TYPE*,I3,*CARD OUT OF ORDER READ FIXED*,I3)
      GO TO 999
37  IF(NPD.NE.0) WRITE(6,800) IC,IT,(NDATA(K),K=K1,K2)
      READ(5,810) IC,IT,(DATA(K),K=K3,K4)
      DEFS=DATA(K4)-DATA(K3+2)
      IF(IC.EQ.(ND2 ).AND.IT.EQ.J) GO TO 38
      WRITE(6,110) J,IT
110  FORMAT(1X*TYPE*,I3,*CARD OUT OF ORDER READ FLOAT*,I3)
      GO TO 999
38  IF(NPD.NE.0) WRITE(6,810) IC,IT,(DATA(K),K=K3,K4)
40  CONTINUE
      ND1=ND1+1
      ND2=ND2+1
```

Appendix A

Cont'd

```

30 CONTINUE
800 FORMAT (1X,I2,20I3)
810 FORMAT(1X,I2,4X,I3,6F10.5)
999 CONTINUE
    RETURN
    END

```

```

SUBROUTINE WMAT(NMODE,MTOT,NADOW,NTOTW)
DIMENSION DATA(800 ), NSUR(14),SIN(14),SOUT(14),XROT(84)
DIMENSION RM(10),FRA(10),H(84),ALPH(84)
COMPLEX A(6130)
EQUIVALENCE(NDATA,DATA)
COMMON/BLUCKA/NDATA(800 ),A,NRP,RM,FRA,DERS,OC,ALSQ,SQL
DO 5 J=1,NTOTW
5 A(NADCW+J)=(0)
NMOMT=NMODE*MTOT
ND=0
DO 23 I1=1,NMOMT,6
I2=I1+5
IF(I2.GT,NMOMT) I2=NMOMT
READ(5,810) IC,NC,(H(I),I=I1,I2)
WRITE(6,810) IC,NC,(H (I),I=I1,I2)
ND=ND+1
23 IF(IC,NE.23.OR.NC,NE.ND) STOP
ND=0
DO 24 I1=1,NMOMT,6
I2=I1+5
IF(I2.GT,NMOMT) I2=NMOMT
READ(5,810) IC,NC,(ALPH(I),I=I1,I2)
WRITE(6,810) IC,NC,(ALPH(I),I=I1,I2)
ND=ND+1
24 IF(IC,NE.24.OR.NC,NE.ND) STOP
ND=0
DO 25 I1=1,NMOMT,6
I2=I1+5
IF(I2.GT,NMOMT) I2=NMOMT
READ(5,810) IC,NC,(XROT(I),I=I1,I2)
WRITE(6,810) IC,NC,(XROT(I),I=I1,I2)
ND=ND+1
25 IF(IC,NE.25.OR.NC,NE.ND) STOP
ND=0
DO 26 I1=1,MTOT,6
I2=I1+5
IF(I2.GT,MTOT) I2=MTOT
READ(5,810) IC,NC,(SIN(I),I=I1,I2)
WRITE(6,810) IC,NC,(SIN (I),I=I1,I2)
ND=ND+1
26 IF(IC,NE.26.OR.NC,NE.ND) STOP
ND=0

```

Appendix A

Cont'd

```

DO 27 I1=1,MTOT,6
  I2=I1+5
  IF(I2.GT.MTOT) I2=MTOT
  READ(5,810) IC,NC,(SOUT(I),I=I1,I2)
  WRITE(6,810) IC,NC,(SOUT(I),I=I1,I2)
  ND=ND+1
27 IF(IC.NE.27.OR.NC.NE.ND) STOP
  READ(5,800) IC,(NSUR(I),I=1,MTOT)
  WRITE(6,800) IC,(NSUR(I),I=1,MTOT)
  IF(IC.NE.28) STOP
800 FORMAT(1X,I2,20I3)
810 FORMAT(1X,I2,4X,I3,6F10,5)
DO 40 MODE=1,NMODE
DO 40 LIN2=1,NRP
DO 40 M=1,MTOT
  NADD2=NDATA(5)+4*(LIN2-1)
  IF(NSUR(M).NE.NDATA(NADD2+1)) GO TO 40
  X= DATA(NADD2+2)
  S1=DATA(NADD2+3)
  IF(SIN(M).GT.S1.OR.(SOUT(M).LT.S1)) GO TO 40
  N=MTOT*(MODE-1)+M
  J=NRP*(MODE-1)+LIN2+NADDW
  A(J)=CMPLX((ALPH(N)), (H(N)+(X-XROT(N))*ALPH(N)))
40 CONTINUE
999 CONTINUE
  RETURN
  END

```

```

SUBROUTINE WREAD(NMODE,NADDW,NTOTW)
  COMPLEX A(6130)
  DIMENSION DATA(800),RM(10),FRA(10)
  EQUIVALENCE(NDATA,DATA)
  COMMON/BLOCKA/NDATA(800),A,NRP,RM,FRA,DERS,OC,ALSO,SQAL
  DO 5 J=1,NTOTW
5  A(NADDW+J)=(0)
  J=NRP*NMODE+NADDW
  ND=0
  IW=NADDW+1
  DO 10 I1=IW,J,3
  I2=I1+2
  IF(I2.GT.J) I2=J
  READ(5,810) IC,NC,(A(I),I=I1,I2)
  WRITE(6,810) IC,NC,(A(I),I=I1,I2)
  ND=ND+1
  IF(IC.NE.23.OR.NC.NE.ND) STOP
10 CONTINUE
810 FORMAT(1X,I2,4X,I3,6F10,5)
  RETURN
  END

```

Appendix A

Cont'd

```

SUBROUTINE ACALC
  DIMENSION DATA(800 ),RM(10),FRA(10),NVECT(5),VECT(5)
  REAL NKL,NLK,NKLNK
  COMPLEX A(6130),AK,AA
  EQUIVALENCE(NDATA,DATA)
  COMMON/BLOCKA/NDATA(800 ),A,NRP,RM,FRA,DERS,OC,ALSQ,SQAL
  COMMON/BLOCKB/XKOL,SKOL,LSYM,NPLANE,N,NKL
  COMMON/BLOCKC/NVECT,VECT
  ALSQ=1.0-RM(N)*RM(N)
  SQAL=SQRT(ABS(ALSQ))
  OC=RM(N)*FRA(N)
  NL1=NDATA(4)
  NL2=NDATA(8)
  DO 900 LIN1K=1,NL1
    NADD1K=NDATA(1)+9*(LIN1K-1)
    NSURK=NDATA(NADD1K)
    XK=DATA(NADD1K+4)
    YK=DATA(NADD1K+5)
    ZK=DATA(NADD1K+6)
    COSGK=DATA(NADD1K+7)
    SINGK=DATA(NADD1K+8)
    DO 900 LIN2K=1,NL2
      NADD2=NDATA(5)+4*(LIN2K-1)
      IF (NDATA(NADD2+1).NE.NSURK) GO TO 900
      K=NDATA(NADD2)
      XK=DATA(NADD2+2)
      SK=DATA(NADD2+3)
      DO 898 LIN1L=1 , NL1
        NADD1L=NDATA(1)+9*(LIN1L-1)
        NSURL=NDATA(NADD1L)
        NSYMZ=NDATA(NADD1L+1)
        NSYMY=NDATA(NADD1L+2)
        NGEOM=NDATA(NADD1L+3)
        XOL=DATA(NADD1L+4)
        YOL=DATA(NADD1L+5)
        ZOL=DATA(NADD1L+6)
        COSGL=DATA(NADD1L+7)
        SINGL=DATA(NADD1L+8)
        DO 897 MSYM=1,4
          GO TO (105,110,115,120),MSYM
105      KSYMZ=KSYMY=LSYMZ=LSYMY=1
          GO TO 130
110      IF(NSYMZ.NE.0) GO TO 111
          MSYM=3
          GO TO 897
111      KSYMZ=-1
          LSYMZ=NSYMZ
          GO TO 130
115      IF(NSYMY.EQ.0) GO TO 898
116      KSYMY=-1
          LSYMY=NSYMY

```

Appendix A
Cont'd

```

GO TO 130
120 KSYMZ=LSYMZ=1
GO TO 116
130 LSYM=LSYMY*LSYMZ*KSYMZ
NPLANE=KSYMZ*KSYMY
IF(NSURL.NE.NSURK)NPLANE=0
IF((ABS(SINGL)*(1-KSYMZ)+ABS(COSGL)*(1-KSYMY)).NE.0)
1NPLANE=0
XKOL=XK+XOK-XOL
DELZ=ZOK*KSYMY-ZOL
DELY=YOK*KSYMZ-YOL
T1KL=COSGK*COSGL*KSYMZ+SINGK*SINGL*KSYMY
SKOL=DELZ*SINGL+DELY*COSGL+SK*T1KL
SINGKL=SINGK*COSGL*KSYMY-COSGK*SINGL*KSYMZ
NKL=DELZ*COSGL-DELY*SINGL+SK*SINGKL
DO 897 LIN2L=1,NL2
NADD2=NDATA(5)+4*(LIN2L-1)
IF(NDATA(NADD2+1).NE.NSURL) GO TO 897
L=NDATA(NADD2)
XL=DATA(NADD2+2)
SL=DATA(NADD2+3)
IF (NPLANE.NE.0) GO TO 153
NLK=-SL*SINGKL-DELZ*COSGK*KSYMZ+DELY*SINGK*KSYMY
NKLNLK=NKL*NLK
153 DO 897 NTYPE=3,15
CALL TEST(NTYPE,L,NL,NADDJ)
IF(NL.EQ.0) GO TO 897
IF(NDATA(NADDJ).NE.L) GO TO 897
JTYPE=NTYPE-2
GO TO(230,240,250,260,270,280,290,300,310,320,330,340
1,350),JTYPE
230 CALL ACON3(T1KL,AA ,NKLNLK,AK,XL,SL,L,K,NADDJ)
GO TO 896
240 CALL ACON4(T1KL,AA ,NKLNLK,AK,XL,SL,L,K,NADDJ)
GO TO 896
250 CALL ACON5(T1KL,AA ,NKLNLK,AK,XL,SL,L,K,NADDJ)
GO TO 896
260 CALL ACON6(T1KL,AA ,NKLNLK,AK,XL,SL,L,K,NADDJ)
GO TO 896
270 CALL ACON7(T1KL,AA ,NKLNLK,AK,XL,SL,L,K,NADDJ)
GO TO 896
280 CALL ACON8(T1KL,AA ,NKLNLK,AK,XL,SL,L,K,NADDJ)
GO TO 896
290 CALL ABLK9
GO TO 897
300 CALL ABLK10
GO TO 897
310 CALL ACON11 (T1KL,AA ,NKLNLK,AK,XL,SL,L,K,NADDJ)
GO TO 896
320 CALL ACON12 (T1KL,AA ,NKLNLK,AK,XL,SL,L,K,NADDJ)

```

Appendix A
Cont'd

```

      GO TO 896
330  CALL ABLK13
      GO TO 897
340  CALL ABLK14
      GO TO 897
350  CALL ACON15 (T1KL,AA ,NKLNK,AK,XL,SL,L,K,NADDJ)
896  CONTINUE
      NADD=(L+(K-1)*(NRP+1))
      A(NADD)=A(NADD)+AA
897  CONTINUE
898  CONTINUE
900  CONTINUE
      RETURN
      END

```

```

SUBROUTINE ACON5 (T1KL,AA ,NKLNK,AK,XL,SL,L,K,NADDJ)
DIMENSION DATA(800 ),RM(10),FRA(10),VECT(5),NVECT(5)
REAL NKL,NLK,NKLNK
COMPLEX A(6130),AK,AA
EQUIVALENCE(NDATA,DATA)
COMMON/BLOCKA/NDATA(800 ),A,NRP,RM,FRA,DEFS,OC,ALSQ,SGAL
COMMON/BLOCKB/XK0L,SK0L,LSYM,NPLANE,N,NKL
COMMON/BLOCKC/NVECT,VECT
R(X,S)=(XK0L-X)**2+ALSQ*((SK0L-S)**2+NKL**2)
AA=0
IF(NDATA(NADDJ).EQ.L) GO TO 100
GO TO 894
100  XFOR=VECT(1)
      XFORW=XFOR
      XLSTAR=XL
      XAFT=VECT(2)
      SIN=VECT(3)
      SOUT=VECT(4)
      ALP=((XAFT-XFOR)*(SOUT-SIN))/12.566371
      DELX=0
      NBOXES=1
      GO TO 267
ENTRY ACON6
AA=0
IF(NDATA(NADDJ).EQ.L) GO TO 200
GO TO 894
200  NBOXES=NVECT(2)
      XFORW=VECT(2)
      XAFTW=VECT(3)
      DELX=(XAFTW-XFORW)/NBOXES
      XFOR=XFORW-DELX
      XLSTAR=XFORW-.5*DELX
      XAFT=XFORW
      SIN=VECT(4)

```

Appendix A

Cont'd

```

SOUT=VECT(5)
ALP=DELX*(SOUT-SIN)/12.566371
267 DO 894 NBOX=1,NBOXES
XFOR=XFOR+DELX
XLSTAR=XLSTAR+DELX
XAFT=XAFT+DELX
RKLSQ=R(XLSTAR,SL)
RKL=SQRT(RKLSQ)
RKLCU=RKLSQ*RKL
IF(NPLANE.NE.0) GO TO 440
IF(L.EQ.K) GO TO 450
AK=-ALSQ*ALP/RKLCU
GO TO 450
440 AK=FUNK(XAFT,SOUT)-FUNK(XAFT,SIN)-FUNK(XFOR,SOUT)+FUNK
1(XFOR,SIN)
AK=AK*(1./12.566371)
450 IF(OC.NE.0) AK=AK*(1+(0.,1.)*OC*RKL/ALSQ)
AK=AK*T1KL
IF(L.EQ.K) GO TO 500
IF(NPLANE.EQ.0) AK=AK+NKLNLK*ALP*(-3.*ALSQ**2/RKLSQ
1-3.*(0.,1.)*OC*ALSQ/RKL+OC**2)/RKLCU
500 AK=AK*LSYM
IF (OC.EQ.0) GO TO 495
XFUN=FRA(N)*(XL-XLSTAR+(RM(N)**2/ALSQ)*(XKOL-XLSTAR)-
1 (RM(N)/ALSQ)*RKL)
AK=AK*CEXP((0.,1.)*XFUN)
495 AA=AA+AK
894 CONTINUE
RETURN
END

```

```

SUBROUTINE ACON7 (T1KL,AA ,NKLNLK,AK,XL,SL,L,K,NADDJ)
DIMENSION DATA(800 ),RM(10),FRA(10),VECT(5),NVECT(5)
REAL NKL,NLK,NKLNLK
COMPLEX A(6130),AK,AA
EQUIVALENCE(NDATA,DATA)
COMMON/BLOCKA/NDATA(800 ),A,NRP,RM,FRA,DERS,OC,ALSQ,SGAL
COMMON/BLOCKB/XKOL,SKOL,LSYM,NPLANE,N,NKL
COMMON/BLOCKC/NVECT,VECT
R(X,S)=(XKOL-X)**2+ALSQ*((SKOL-S)**2+NKL**2)
AA=0
IF(NDATA(NADDJ).EQ.L) GO TO 100
GO TO 894
100. XFOR=VECT(1)
XFORW=XFOR
XLSTAR=XL
XAFT=VECT(2)
SIN=VECT(3)
SOUT=VECT(4)

```


Appendix A

Cont'd

```

ALP=((XAFT-XFOR)*(SOUT-SIN))/12.566371
DELX=0
NBOXES=1
GO TO 267
ENTRY ACON8
AA=0
IF(NDATA(NADDJ).EQ.L) GO TO 200
GO TO 894
200 NBOXES=NVECT(2)
XFORW=VECT(2)
XAFTW=VECT(3)
DELX=(XAFTW-XFORW)/NBOXES
XFOR=XFORW-DELX
XLSTAR=XFORW-.5*DELX
XAFT=XFORW
SIN=VECT(4)
SOUT=VECT(5)
ALP=DELX*(SOUT-SIN)/12.566371
267 DO 894 NBOX=1,NBOXES
  XFOR=XFOR+DELX
  XLSTAR=XLSTAR+DELX
  XAFT=XAFT+DELX
  RKLSQ=R(XLSTAR,SL)
  RKL=SQRT(RKLSQ)
  RKLCU=RKLSQ*RKL
  IF(NPLANE.NE.0) GO TO 420
  AK=-ALSQ*ALP/RKLCU
  AKU=-OC*ALP/RKLSQ
  AK=(AK+(0.,1.)*AKU)*T1KL+NKLNK*ALP*(-3.*ALSQ**2/RKLSQ
1 -3.*(0.,1.)*OC*ALSQ/RKL+OC**2)/RKLCU
420 IF(NPLANE.EQ.0) GO TO 425
  IF(NPLANE.NE.0) AK=FUNK(XAFT,SOUT)-FUNK(XAFT,SIN)-FUNK
1(XFOR,SOUT)+FUNK(XFOR,SIN)
  AK=AK*(1./12.566371)
  AKU=FUNKU(XAFT,SOUT)-FUNKU(XAFT,SIN)-FUNKU(XFOR,SOUT)
1+FUNKU(XFOR,SIN)
  AKU=AKU*(OC*RM(N)/(12.566371*SQAL))
  AKU=AKU+(OC/ALSQ)*(RM(N)*(XLSTAR-XKOL)+RKL)*AK
  AK=(AK+(0.,1.)*AKU)*T1KL
425 XFUN=FRA(N)*(XL-XLSTAR+(RM(N)**2/ALSQ)*(XKOL-XLSTAR)-
1 (RM(N)/ALSQ)*RKL)
  AK=AK*LSYM*CEXP((0.,1.)*XFUN)
  AA=AA+AK
894 CONTINUE
RETURN
END

```

Appendix A

Cont'd

```

SUBROUTINE ACON11(T1KL,AA ,NKLNLK,AK,XL,SL,L,K,NADDJ)
DIMENSION DATA(800 ),RM(10),FRA(10),NVECT(5),VECT(5)
REAL NKL,NLK,NKLNLK
COMPLEX A(6130),AK,AA
EQUIVALENCE(NDATA,DATA)
COMMON/BLOCKA/NDATA(800 ),A,NRP,RM,FRA,DERS,OC,ALSQ,SQAL
COMMON/BLOCKB/XKOL,SKOL,LSYM,NPLANE,N,NKL
COMMON/BLOCKC/NVECT,VECT
R(X,S)=(XKOL-X)**2+ALSQ*((SKOL-S)**2+NKL**2)
AA=0
IF(NDATA(NADDJ).EQ.L) GO TO 100
GO TO 894
100 XFOR=VECT(1)
XFORW=XFOR
XLSTAR=XL
XAFT=VECT(2)
SIN=VECT(3)
SOUT=VECT(4)
ALP=((XAFT-XFOR)*(SOUT-SIN))/12.566371
DELX=0
NBOXES=1
GO TO 267
ENTRY ACON12
AA=0
IF(NDATA(NADDJ).EQ.L) GO TO 200
GO TO 894
200 NBOXES=NVECT(2)
XFORW=VECT(2)
XAFTW=VECT(3)
DELX=(XAFTW-XFORW)/NBOXES
XFUR=XFORW-DELX
XLSTAR=XFORW-.5*DELX
XAFT=XFORW
SIN=VECT(4)
SOUT=VECT(5)
ALP=DELX*(SOUT-SIN)/12.566371
267 DO 894 NBOX=1,NBOXES
XFOR=XFOR+DELX
XLSTAR=XLSTAR+DELX
XAFT=XAFT+DELX
RKLSQ=R(XLSTAR,SL)
RKL=SQRT(RKLSQ)
RKLCU=RKLSQ*RKL
AK=(1./12.56637)* (FUNK(XAFT,SOUT)-FUNK(XAFT,SIN)-FUNK
1(XFOR,SOUT)+FUNK(XFOR,SIN))
AKU=(FUNKU(XAFT,SOUT)-FUNKU(XAFT,SIN)-FUNKU(XFOR,SOUT)
1+FUNKU(XFOR,SIN))*(FRA(N)/(12.566371*SQAL))
AKU=AKU+ (RKL*RM(N)+XLSTAR-XKOL)*AK*(FRA(N)/ALSQ)
AK=(AK+(0.,1.)*AKU)*T1KL
IF(NPLANE.NE.0) GO TO 425

```

Appendix A
Cont'd

```

      IF(L,EQ,K) GO TO 425
      AK= AK +NKLNLK*ALP*(-3,*ALSQ**2/RKLSQ
1 -3,*(0.,1.)*OC*ALSQ/RKL+OC**2)/RKLCU
425 XFUN=FRA(N)*(XL-XLSTAR+(RM(N)**2/ALSQ)
      1*(XKOL-XLSTAR)-(RM(N)/ALSQ)*RKL)
      AK=AK*LSYM*CEXP((0.,1.)* XFUN)
      AA=AA+AK
894 CONTINUE
      RETURN
      END

```

```

FUNCTION FUNK(X,S)
REAL NKL,NLK,NKLNLK
DIMENSION DATA(800 ),RM(10),FRA(10),NVECT(5),VECT(5)
COMPLEX A(6130)
EQUIVALENCE(NDATA,DATA)
COMMON/BLOCKA/NDATA(800 ),A,NRP,RM,FRA,DERS,OC,ALSQ,SQAL
COMMON/BLOCKB/XKOL,SKOL,LSYM,NPLANE,N,NKL
R(X,S)=(XKOL-X)**2+ALSQ*((SKOL-S)**2+NKL**2)
IF(NPLANE.NE.0) GO TO 10
IF(ABS(NKL/DERS).GT..0001) GO TO 5
GO TO 10
5 FUNK=(1./NKL)*ATAN2(NKL*SQRT(R(X,S)),((XKOL-X)*(SKOL-S)))
RETURN
10 CONTINUE
IF(ABS((XKOL-X)/DERS).LT..0001) GO TO 20
IF(ABS((SKOL-S)/DERS).LT..0001) GO TO 20
FUNK=SQRT(R(X,S))/((XKOL-X)*(SKOL-S))
GO TO 30
20 FUNK=0
30 CONTINUE
RETURN
END

```

```

FUNCTION FUNKU(X,S)
DIMENSION DATA(800 ),RM(10),FRA(10),NVECT(5),VECT(5)
COMPLEX A(6130)
EQUIVALENCE(NDATA,DATA)
REAL NKL,NLK,NKLNLK
COMMON/BLOCKA/NDATA(800 ),A,NRP,RM,FRA,DERS,OC,ALSQ,SQAL
COMMON/BLOCKB/XKOL,SKOL,LSYM,NPLANE,N,NKL
R(X,S)=(XKOL-X)**2+ALSQ*((SKOL-S)**2+NKL**2)
IF(ABS(NKL/DERS).GT..0001) GO TO 10
IF(RM(N).GT.1.) GO TO 10
IF((ABS((XKOL-X)/DERS).LT..0001).AND.(SKOL.LE.S))GOTO20
10 IF(RM(N).GT.1.) GO TO 12
FUNKU=ALOG(SQAL*(SKOL-S)+SQRT(R(X,S)))

```

Appendix A

Cont'd

```

GO TO 30
12 IF(((XKOL-X)/DERS).LT..0001) GO TO 20
   FUNKU=ASIN((SKOL-S)*SQAL/(XKOL-X))
   GO TO 30
20 FUNKU=0
30 CONTINUE
   RETURN
   END

SUBROUTINE CMATR(N1,NTOTW,NADDW,NMODE1,NMODE2,NTEMP,
1NSIZE1,NSIZE2,NCSIZE,NADDC,NPP,NADDW2,NADDW3,NADDWF)
  DIMENSION DATA(800 ),RM(10),FRA(10),NVECT(5),VECT(5)
  REAL NKL,NLK,NKLNK
  COMPLEX A(6130),CK
  EQUIVALENCE(NDATA,DATA)
  COMMON/BLOCKA/NDATA(800 ),A,NRP,RM,FRA,DERS,OC,ALSQ,SQAL
  COMMON/BLOCKB/XKOL,SKOL,LSYM,NPLANE,N,NKL
  COMMON/BLOCKC/NVECT,VECT
  WRITE(6,115)
115 FORMAT(1X//1X*PART 3-DERIVE CMATRIX*//)
  NL1=NDATA(4)
  NL2=NDATA(8)
  IF (NMODE2.NE.0) GO TO 80
  DO 85 J=1,NSIZE1
85  A(NADDW2+J)=A(NADDW+J)
80  DO 90 J=1,NSIZE2
90  A(NADDW3+J)=CMPLX(REAL(A(NADDW2+J)),FRA(N)*AIMAG(A
1(NADDW2+J)))
  DO 95 J=1,NSIZE2
95  A(NADDWF+J)=(0.,0.)
  CALL INVER(A,NRP)
  DO 200 MODE=1,NTEMP
  DO 200 LM=1,NRP
  DO 200 KM=1,NRP
  J1=N1*(LM-1)+KM
  J2=NRP*(MODE-1)+KM
  J3=NRP*(MODE-1)+LM
200 A(NADDWF+J3)=A(NADDWF+J3)+A(J1)*A(NADDW3+J2)
  IF(NPP .EQ.0) GO TO 217
  WRITE(6,117)
117  FORMAT(2X*LISTING OF POTENTIAL DISCONTINUITIES*)
  CALL ALIST(A,NADDWF,NTEMP,NRP)
217 CONTINUE
  DO 219 J=1,NCSIZE
219 A(NADDC+J)=(0.,0.)
  DO 600 J=1,NTEMP
  DO 600 I=1,NMODE1
  DO 600 L =1,NRP

```

Appendix A
Cont'd

```
DO 600 NTYPE=3,15
CALL TEST(NTYPE,L,NL,NADDJ)
IF(NL.EQ.0) GO TO 600
IF(NDATA(NADDJ).NE.L) GO TO 600
J1=NADDW+NRP*(I-1)+L
J2=NADDWF+NRP*(J-1)+L
J3=NADDC+NTEMP*(I-1)+J
DO 335 LIN=1,NL2
NADD2=NDATA(5)+4*(LIN -1)
IF (NDATA(NADD2).EQ.L ) GO TO 355
335 CONTINUE
GO TO 600
355 XL=DATA(NADD2+2)
NSURF=NDATA(NADD2+1)
DO 445 LIN1=1,NL1
NADD1L=NDATA(1)+9*(LIN1-1)
NSURL=NDATA(NADD1L)
IF(NSURF.EQ.NSURL) GO TO 455
445 CONTINUE
GO TO 600
455 NGEOM=NDATA(NADD1L+3)
JTYPE=NTYPE-2
GO TO(230,240,250,260,270,280,290,300,310,320,330,340,
1350),JTYPE
230 CALLCCON11(J1,J2,J3,NGEOM,XL,L,NADDJ,CK)
GO TO 500
240 CALLCCON12(J1,J2,J3,NGEOM,XL,L,NADDJ,CK)
GO TO 500
250 CALL CCON5(J1,J2,J3,NGEOM,XL,L,NADDJ,CK)
GO TO 500
260 CALL CCON6(J1,J2,J3,NGEOM,XL,L,NADDJ,CK)
GO TO 500
270 GO TO 250
280 GO TO 260
290 CALL CBLK9
GO TO 600
300 CALL CBLK9
GO TO 600
310 CALLCCON11(J1,J2,J3,NGEOM,XL,L,NADDJ,CK)
GO TO 500
320 CALLCCON12(J1,J2,J3,NGEOM,XL,L,NADDJ,CK)
GO TO 500
330 CALL CBLK13
GO TO 600
340 CALL CBLK14
GO TO 600
350 CALL CBLK15
GO TO 600
500 IF(NDATA(NADDJ).NE.L) GO TO 600
A(J3)=A(J3)+CK
```

Appendix A

Cont'd

```

600 CONTINUE
    WRITE(6,800) N, RM(N), FRA(N)
800 FORMAT(1X//1X*CMATRIX FOR N=*, I5/
    11X*MACH NO.=*, F9.5,*   FRA=*, F9.5/)
    CALL ALIST(A, NADDC, NMODE1, NTEMP)
999 CONTINUE
    RETURN
    END

```

```

SUBROUTINE CCON5(J1,J2,J3,NGEOM,XL,L,NADDJ,CK)
DIMENSION DATA(800 ), RM(10), FRA(10), VECT(5), NVECT(5)
REAL NKL,NLK,NKLNK
COMPLEX A(6130), CK
EQUIVALENCE(NDATA, DATA)
COMMON/BLOCKA/NDATA(800 ), A, NRP, RM, FRA, DERS, OC, ALSQ, SQAL
COMMON/BLOCKB/XKOL, SKOL, LSYM, NPLANE, N, NKL
COMMON/BLOCKC/NVECT, VECT
IF(NDATA(NADDJ).NE.L) GO TO 290
XFOR=VECT(1)
XAFT=VECT(2)
SIN=VECT(3)
SOUT=VECT(4)
ALP=(XAFT-XFOR)*(SOUT-SIN)
CK=-(ALP*(REAL(A(J1))-(0.,1.)*FRA(N)*AIMAG(A(J1)))*A(J2))
1 *NGEOM
290 CONTINUE
    RETURN
    ENTRY CCON6
    IF(NDATA(NADDJ).NE. L) GO TO 390
    XFOR=VECT(2)
    XAFT=VECT(3)
    SIN=VECT(4)
    SOUT=VECT(5)
    NBOXES=NVECT(2)
    DX=XFOR-XL
    DELX=DX+(XAFT-XFOR)*.5/NBOXES
    CK=
    ((SOUT-SIN)*(DX*REAL(A(J1))
    1+AIMAG(A(J1)))*A(J2)*CEXP(-(0.,1.)*FRA(N)*DELX))*NGEOM
390 CONTINUE
    RETURN
    END

```

Appendix A

```

SUBROUTINE CCON11(J1,J2,J3,NGEOM,XL,L,NADDJ,CK)
DIMENSION DATA(800 ),RM(10),FRA(10),NVECT(5),VECT(5)
REAL NKL,NLK,NKLNK
COMPLEX A(6130),CK
EQUIVALENCE(NDATA,DATA)
COMMON/BLOCKA/NDATA(800 ),A,NRP,RM,FRA,DERS,OC,ALSQ,SQL
COMMON/BLOCKB/XKOL,SKOL,LSYM,NPLANE,N,NKL
COMMON/BLOCKC/NVECT,VECT
IF(NDATA(NADDJ).NE.L) GO TO 290
XFOR=VECT(1)
XAFT=VECT(2)
SIN=VECT(3)
SOUT=VECT(4)
CK=(SOUT-SIN)*((AIMAG(A(J1)))+(XFOR-XL)*REAL(A(J1)))*
1CEXP(-(0.,1.)*FRA(N)*(XFOR-XL))-(AIMAG(A(J1))+(XAFT-XL)
2*REAL(A(J1)))*CEXP(-(0.,1.)*FRA(N)*(XAFT-XL))*A(J2)*NGEOM
290 CONTINUE
RETURN
ENTRY CCON12
IF(NDATA(NADDJ).NE. L) GO TO 390
XFOR=VECT(2)
SIN=VECT(4)
SOUT=VECT(5)
CK=(SOUT-SIN)*((AIMAG(A(J1)))+(XFOR-XL)*REAL(A(J1)))*
1NGEOM*CEXP(-(0.,1.)*FRA(N)*(XFOR-XL))*A(J2)
390 CONTINUE
RETURN
END

```

```

SUBROUTINE ALIST (A,NADD,NROWS,NCOLS)
COMPLEX A(6130)
WRITE (6,201)
DO 200 J=1,NROWS
DO 200 K=1,NCOLS
IS=NADD+(J-1)*NCOLS+K
WRITE(6,202) J,K,A(IS)
201 FORMAT(X*ROW*3X*COL*2X*REAL*14X*IMAGINARY*)
202 FORMAT(X2I4,2E18.8)
200 CONTINUE
RETURN
END

```

Appendix A

```
SUBROUTINE TEST(NTYPE,L,NL,NADDJ)
  DIMENSION DATA(800 ),RM(10),FRA(10),NVECT(5),VECT(5)
  COMPLEX A(6130)
  -----
  EQUIVALENCE(NDATA,DATA)
  COMMON/BLOCKA/NDATA(800 ),A,NRP,RM,FRA,DEFS,OC,ALSQ,SQAL
  COMMON/BLOCKC/NVECT,VECT
  NADD=NDATA(4*NTYPE-3)
  NFIX=NDATA(4*NTYPE-2)
  NFL=NDATA(4*NTYPE-1)
  -----
  NL=NDATA(4*NTYPE)
  IF(NL.EQ.0) GO TO 897
  DO 159 LIN=1,NL
    NADDJ=NADD+(LIN-1)*(NFIX+NFL)
    IF(NDATA(NADDJ).NE.L) GO TO 159
    DO 157 J=1,5
      -----
      NVECT(J)=0
157  VECT(J)=0
      DO 158 J=1,NFIX
158  NVECT(J)=NDATA(NADDJ+J-1)
      NFL=NFL+NFIX-1
      DO 156 J=1,NFL
156  VECT(J)=DATA(NADDJ+J)
      GO TO 897
159  CONTINUE
897  RETURN
  END
  -----
```


Appendix A

```

SUBROUTINE INVER (A,N)
COMPLEX PIVOT,A(6130)
N1=N+1
DO 1 I=1,N
DO 1 J=1,N
1 A(I*N1-N1+N+2-J)=A(I*N1-N1+N+1-J)
J=1
I=0
2 I=I+1
J1=J+1
ID=0
NN=0
3 IF(REAL(A(I*N1-N1+J1))) 5,4,5
4 IF(AIMAG(A(I*N1-N1+J1))) 5,6,5
5 IF(ID) 6,10,6
6 IF(I-N) 8,7,8
7 I=0
8 I=I+1
NN=NN+1
IF(N-NN) 20,20,3
10 ID=J
DO 101 LA=1,N
101 A(LA*N1-N1+J)=(0.,0.)
A(I*N1-N1+J)=(1.0,0.0)
PIVOT=A(I*N1-N1+J1)
DO 11 M=1,N1
11 A(I*N1-N1+M)=A(I*N1-N1+M)/PIVOT
DO 17 LA=1,N
IF(I-LA)12,12,15
12 KK=LA+1
IF(N-KK) 18,13,13
13 PIVOT=A(KK*N1-N1+J1)
DO 14 M=1,N1
14 A(KK*N1-N1+M)=A(KK*N1-N1+M)-PIVOT*A(I*N1-N1+M)
GO TO 17
15 PIVOT=A(LA*N1-N1+J1)
DO 16 M=1,N1
16 A(LA*N1-N1+M)=A(LA*N1-N1+M)-PIVOT*A(I*N1-N1+M)
17 CONTINUE
18 IF(N-J) 20,20,19
19 J=J1
GO TO 2
20 RETURN
END

```

APPENDIX B

List of Integral Formulas

$$1. \int \frac{dx}{(ax^2 + c)^{3/2}} = \frac{x}{c\sqrt{ax^2 + c}}$$

$$2. \int \frac{dx}{x^2\sqrt{ax^2 + c}} = \frac{-\sqrt{ax^2 + c}}{cx}$$

$$3. \int \frac{x \, dx}{(ax^2 + c)^{3/2}} = -\frac{1}{a\sqrt{ax^2 + c}}$$

$$4. \int \frac{dx}{\sqrt{ax^2 + c}} = \frac{1}{\sqrt{a}} \log (x\sqrt{a} + \sqrt{ax^2 + c}), \quad a > 0$$

$$5. \int \frac{dx}{(x^2 + b^2)\sqrt{x^2 + a^2}} = \frac{1}{b\sqrt{a^2 - b^2}} \tan^{-1} \frac{b\sqrt{x^2 + a^2}}{x\sqrt{a^2 - b^2}}$$

$$6. \int \frac{dx}{x\sqrt{ax^2 + b}} = \frac{1}{\sqrt{b}} \log \left\{ \frac{\sqrt{ax^2 + b} - \sqrt{b}}{x} \right\}, \quad b > c$$

APPENDIX C

Subroutines For Steady Supersonic Calculations

```

SUBROUTINE ACON3 (T1KL,AA,NKLNLK,AK,XL,SL,L,K,NADDJ)
DIMENSION DATA( 800),RM(10),FRA(10),NVECT(5),VECT(5)
REAL NKL,NLK,NKLNLK
COMPLEX A(6130),AK,AA
EQUIVALENCE(NDATA,DATA)
COMMON/BLOCKA/NDATA(800 ),A,NRP,RM,FRA,DERS,OC,ALSQ,SQAL
COMMON/BLOCKB/XK0L,SK0L,LSYM,NPLANE,N,NKL
COMMON/BLOCKC/NVECT,VECT
R(X,S)=(XK0L-X)**2+ALSQ*((SK0L-S)**2+NKL**2)
AA=0
AKS=0
IF(NDATA(NADDJ).EQ.L) GO TO 100
GO TO 894
100 XFOR=VECT(1)
XAFT=VECT(2)
SIN=VECT(3)
SOUT=VECT(4)
NBOXES=1
GO TO 267
ENTRY ACON4
AA=0
AKS=0
IF(NDATA(NADDJ).EQ.L) GO TO 200
GO TO 894
200 NBOXES=NVECT(2)
XFOR=VECT(2)
XAFT=VECT(3)
SIN=VECT(4)
SOUT=VECT(5)
267 DO 894 NBOX=1,NBOXES
500 IF(XL.GT.XK0L) GO TO 894
IF(L.EQ.K.AND.SK0L.EQ.SL) GO TO 278
IF(SL.EQ.SK0L.AND.XK0L.EQ.XAFT) GO TO 279
277 AK=(1./12.56637)*(FUNS(XAFT,SOUT)-FUNS(XAFT,SIN)-FUNS
1(XFOR,SOUT)+FUNS(XFOR,SIN))
AK=(2.*AK+AKS)*LSYM*T1KL
GO TO 884
278 AKS=SQAL/(2.*(XAFT-XFOR))
AK=AKS*T1KL*LSYM
GO TO 884
279 AKS=-SQAL/(2.*(XAFT-XFOR))
GO TO 277
884 AA=AA+AK
894 CONTINUE
RETURN
END

```

Appendix C

Cont'd Subroutines for Steady Supersonic Calculations

```

FUNCTION FUNS(X,S)
REAL NKL,NLK,NKLNLK
DIMENSION DATA(800 ),RM(10),FRA(10),NVECT(5),VECT(5)
COMPLEX A( 6130)
EQUIVALENCE(NDATA,DATA)
COMMON/BLOCKA/NDATA( 800),A,NRP,RM,FRA,DERS,OC,ALSQ,SQAL
COMMON/BLOCKB/XK0L,SK0L,LSYM,NPLANE,N,NKL
R(X,S)=(XK0L-X)**2+ALSQ*((SK0L-S)**2+NKL**2)
IF(NPLANE.NE.0) GO TO 10
RETURN
10 CONTINUE
IF(ABS((XK0L-X)/DERS).LT..0001) GO TO 20
IF(ABS((SK0L-S)/DERS).LT..0001) GO TO 20
ARG=R(X,S)
IF(-SQAL*ABS(S-SK0L).LE.(X-XK0L)) GO TO 20
IF(ARG.GT.-.000001 .AND. ARG.LT.0) ARG=0
FUNS=SQRT(ARG)/((XK0L-X)*(SK0L-S))
GO TO 30
20 FUNS=0
30 CONTINUE
RETURN
END

```

Modifications in DMATR for Steady Supersonic Calculations: The method for breaking up a surface into rectangular elements in the case of steady supersonic calculation is slightly different from that used in subsonic case, and is shown in Fig. 36. The modifications required in subroutine DMATR are as follows:

Subsonic

DATA(K3)=SFOR(M)+(.75+(IQ-1))*
DELX(M)

XF=SFOR(M)+DELX(M)*.25

DATA(K3)=SAFT(M)-DELX(M)*.75

Supersonic

DATA(K3)=SFOR(M)+
(.50+(IQ-1)*DELX(M)

XF=SFOR(M)+DELX(M)*.50

DATA(K3)=SAFT(M)-DELX(M)*.50

The DMATR program listed in Appendix A is in the subsonic form.